SOUTHAMPTON OCEANOGRAPHY CENTRE

INTERNAL DOCUMENT No. 39

Evaluation of profiling ALACE float performance

S Bacon[1], L Centurioni[2] & W J Gould[1]

1998

Southampton Oceanography Centre
University of Southampton
Waterfront Campus
European Way
Southampton
Hants SO14 3ZH UK
Tel: +44 (0)1703 596441
Fax: +44 (0)1703 596204
Email: S.Bacon@soc.soton.ac.uk

[1]James Rennell Division for Ocean Circulation
[2]School of Ocean and Earth Science

DOCUMENT DATA SHEET

AUTHOR

BACON, S, CENTURIONI, L & GOULD, W J

PUBLICATION DATE

1998

TITLE

Evaluation of profiling ALACE float performance.

REFERENCE

Southampton Oceanography Centre Internal Document, No. 39, 72pp. (Unpublished manuscript)

ABSTRACT

This report describes trajectories and profiles obtained to date from seven profiling ALACE floats deployed in the Irminger Basin in the North Atlantic subpolar gyre in October 1996. One expired soon after launch, two others expired in January 1998; the remaining four are still working and are approaching their median expected life of 50 cycles (2 years). All the floats were deployed to run at a nominal depth of 1500 dbar. Their running depths have all shoaled at about 50 dbar per year, which is attributed to mass loss due to corrosion. The most significant result of this study is that comparison data show that the salinity derived from the floats' sensors is stable and accurate to ±0.005 after offset correction. Comparison data are from WOCE cruises in the area, including the launch cruise and five others, the latest in October 1997. Float salinities were calibrated by comparison with ship CTDs which occurred within 100 km and 50 days of float profiles. Indirect evidence (stability of theta / S relationships) suggest that three of the four floats' sensors continue to be stable through to August 1998 (the latest data examined in this study); one may be failing.

KEYWORDS

ALACE, ARGOS NAVIGATION, AUTONOMOUS PROFILING FLOATS, CONDUCTIVITY SENSORS, CTD PROFILERS, FLOATS, INTERCOMPARISONS, IRMINGER BASIN, NORTH ATLANTIC, SALINITY

ISSUING ORGANISATION

Southampton Oceanography Centre
University of Southampton
Waterfront Campus
European Way
Southampton SO14 3ZH
UK **Telephone 01703 596116**

Director: Professor John Shepherd

Not generally distributed - please refer to author

CONTENTS

LIST OF TABLES

LIST OF FIGURES

1. INTRODUCTION

The Autonomous LAgrangian Circulation Explorer, or ALACE float was intended as a subsurface float that was independent of acoustic tracking networks. Its location is obtained when on the surface via System Argos satellites; it gets to the surface and back to its 'cruising' depth again by changing its buoyancy. It was soon realised that this vehicle made a useful platform for other measurements, which led to the addition of temperature and then conductivity probes to make profiles during the ascent to the surface; these floats were called PALACE (Profiling ALACE).

Energy is the fundamental constraint on the operational lifetime of ALACE-type floats. To resolve usefully the low-frequency velocities of intermediate (ca. 1000 m) oceanic depths, it was decided that they required endurance of a couple of years. The float changes buoyancy by pumping hydraulic fluid from an internal reservoir to an external bladder to increase volume and so decrease density, which causes the float to ascend. The process is reversed for descent. Also, the float spends about a day on the surface transmitting data via Argos. The hydraulic pump and the data transmissions are the floats' main power consumers. As presently configured, they are expected to carry sufficient energy for 50 cycles, so they should last for one year on weekly cycling, four years on monthly cycling, etc. Information relating to the mechanics and electronics can be found in Davis, Webb, Regier and Dufour (1992). There is a quantity of useful information in the 'grey' literature also, particularly Sherman (1993) and Davis (1998) in this context; see Appendix 1, which contains the results of a search on the WOCE literature web site for ALACE–related documents.

As a U. K. contribution to the World Ocean Circulation Experiment (WOCE), seven PALACE floats were purchased from Webb Research Corporation (WRC) of Falmouth, MA, U. S. A. in 1996. Of these, four were conductivity-temperature-depth (CTD) profilers (S/N 77-80) and three temperature-depth (TD) profilers (S/N 81-83). Following previous U. K. interest in the area (e.g., RRS *Charles Darwin* cruise 62: Gould, 1992, Read and Gould, 1992, Bacon, 1997), it was decided to deploy these floats in the Irminger Basin of the North Atlantic, part of the sub-polar gyre. This was done by one of us (SB) in the late autumn of 1996 on RRS *Discovery* cruise 223 (Leach and Pollard, 1998). Deployment times and locations are included in Tables 1. Float 81 expired soon after launch due to damage caused by foul weather during the launch process. Two more expired (79 and 82) early in 1998, leaving four operational at the time of writing. A supplement to this report will be written on expiry of the last float, as a final summary.

In this report, we describe in detail the setup of these floats, their trajectories to date and the measurements they have made both at cruising depth and while profiling. By way of a conclusion, we offer an evaluation of float and sensor performance.

2. OPERATION

We were interested in circulation at or near the 'level of no motion' in the Irminger Basin, meaning the middle of the Labrador Sea Water (LSW) layer at about 1500 dbar. Using measurements from *Darwin* 62, we decided that local conditions were adequately approximated by temperature T = 3.21°C, salinity S = 34.88 resulting in density at 1500 db of ρ = 1034.674 kg m^{-3}. All floats were ballasted by WRC accordingly.

We wished to try to locate the floats in the least oceanographically active part of the Irminger Basin, which meant avoiding the basin boundaries: the western boundary off Greenland, the eastern boundary of the Reykjanes Ridge, and the northern boundary at Denmark Strait. In this meteorologically rather data-poor area, we hoped that the annual upper ocean heat flux cycle might be estimated via the T and S profiles of the floats. We were also interested, even with this relatively small number of floats, in attempting to identify broad patterns in the circulation of the LSW level of the basin. We opted for a 14-day cycle from which some floats should survive through two full years (based on energy considerations).

2.1 Float cycling

To summarise the complete float cycle, beginning at the initiation of ascent from cruising depth: the pump is run for 15 minutes to inflate partially the external bladder. The float ascends at 10–15 cm s^{-1}, so it should reach the surface in about 4 hours. The float is programmed to wait for 6 hours to ensure the surface is reached, after which time the pump runs for a further 99 minutes. These measures ensure that (a) a reasonable minimum of work against pressure is done by the pump while at depth, and (b) the antenna is well clear of the surface on arrival there. 24 hours are then spent on the surface obtaining position fixes from and transmitting data to Argos satellites. Then the float descends back to cruising depth by emptying the external bladder back into the interior reservoir. Following Davis *et al.* (1992), the time to drop from the surface to cruising depth is about 7 hours. The floats are programmed to restart measurements 14.2 hours after initiation of descent, so that of the whole 14-day (336 hour) cycle, the remaining 289.9 hours are spent at depth, after which time, the cycle begins again.

2.2 Argos Navigation

2.2.1 Trajectories

He we give an overview of the floats' trajectories on the large scale, and consider also the surface fixes. In figures 2.1 to 2.7, we show the float trajectories where each period on the surface ('cycle' or 'event') is represented by one average position. Event number 0 is the float launch time / position. Three CTD floats were launched on the section westgoing along 60°N, at the

end of *Discovery* station 12995 (78), 12996 (77) and 12998 (80). These positions spanned the western half of the basin. On the section going southeast from Cape Farewell, the last CTD float (79) was launched after station 13002, then 82 and 83 (TD floats) were launched without a CTD station for comparison (during a SeaSoar run). These positions spanned the eastern half of the basin, taking the centre line of the basin as a northeast to southwest axis. Finally, the last TD float, 81, was launched after station 13003, on the eastern flank of the Reykjanes Ridge, outside the Irminger Basin.

Circulation in the Irminger Basin is believed to be generally cyclonic at all depths. The dominant features are: the surface Western Boundary Current (WBC) flowing south down the east coast of Greenland, comprising the East Greenland Current (EGC), a fresh, cold current of polar origin, and the Irminger Current, a salty recirculating component of the North Atlantic Current; the deep Iceland–Scotland Overflow waters (ISOW, also referred to as Charlie–Gibbs Fracture Zone waters in the western basins) heading north up the western flank of the Reykjanes Ridge, across the Denmark Strait, and south down the continental slope off east Greenland; and the Deep Western Boundary Current, made from the Denmark Strait Overflow, overlain by ISOW. In the middle between surface and deep flows lies the Labrador Sea Water (LSW), the vicinity of which is usually a good guess for a level of no motion in geostrophic calculations. Part of the scientific interest of the float missions lies in the description of the actual patterns of motion of the LSW layer, which cannot be stationary, as shown by flux balance and tracer considerations, and other current meter and float measurements which we will not detail here.

We see (figs. 2.1–2.7) that the Irminger Basin interior flow is sluggish and eddy–filled. Floats 77–80 and 82 all made their way northwards with much quasi-random motion superimposed. Floats 77–79 crossed the basin westwards at about 62°N and were entrained into the WBC. Floats 77 and 78 have since then been making rapid progress in the boundary flow around Greenland and are at present over half way round the Labrador Sea. Float 79 expired in February 1998 while southbound in the EGC; it was probably damaged or destroyed by ice. We are quite amazed by the survival of float 77, however. It operated normally until early November 1997; then on the mid-November transmission (event 28), the deep pressure data (see 2.3 below) showed that the float had grounded in depths of 100 m and less; on fig. 2.1, the float track crosses to the inshore side of the 1500 m isobath. It had moved into deeper water by event 29, recording about 1000 m between events, but still grounded. On event 30 it was back in deep water. There was no data from event 31, but on event 32 it had grounded again, in about 1000 m water depth. This was the last apparent grounding. This is not the whole story. At the beginning of January 1998 (event 31), only one transmission containing one position fix was received. Events 32 and 33 covered only 8 and 12 hours of transmission. Event 34 was fine, but then there were 2 entire cycles with no transmissions at all received. Event 35 was a half-hearted resumption, providing four fixes over 15 hours; all subsequent events were fine. Given the location (northern Labrador

Sea) and the season, it is likely that the surface difficulties were caused by ice; and given the troubles the float would appear to have had both at the surface and at the bottom, we are surprised and delighted by its survival.

Float 83 has performed in a dull but potentially very useful manner. It has remained quite close to its launch position, give or take a degree or two (fig. 2.7). We hope to use this float as a pseudo–profiling–mooring to estimate the annual upper ocean heat flux cycle in its vicinity.

As previously mentioned, float 81 expired soon after launch (after 3 cycles), so it will not be considered further in this report.

2.2.2 Displacements and velocities

At this stage, we have only made the simplest calculation of float displacements and velocities by taking the first and last valid position fix from each surface cycle and calculating differences within and between cycles to give net figures, without any allowance being made for rise and fall time, which affects the values at depth. Resulting statistics are presented in Tables 2.1 (Deep) and 2.2 (Surface). As can be seen from the float trajectories, there is short-term (~monthly) random noise due to eddying motions, and long-term tendencies due to the 'mean' circulation, so that all mean values are much less than associated standard deviations. For the deep data, $|ve|$, $|vn| < 2$ cm/s, and $sd(ve)$, $sd(vn) < 6$ cm/s. Net displacements are of the order of 50 km. For the surface data, $|ve|$, $|vn| < 6$ cm/s, except float 82, which is a little higher; $sd(ve)$, $sd(vn) < 23$ cm/s. Net displacements are about 15 km. With surface speeds approximately 0.75 km/hr (21 cm/s), a time for rise and fall of about 6 hours total, and assuming the surface speed to apply throughout the water column (obviously an over-estimate), we have a maximum deep displacement error of 4.5 km, or ~10% of the deep displacements. This error estimate can be refined by considering more sensible velocity profiles, and by seeing whether it might actually be a bias, through correlation of surface and deep directions of motion.

2.3 Submerged Measurements

While at depth, the floats measure temperature and pressure every 2.8 hours. These measurements are averaged into first-half (first week at depth) and second-half (second week at depth) mean values, so two values each of submerged temperature and pressure are returned for each cycle. Some other diagnostic quantities are also returned for each cycle: both float types return average and minimum values of surface pressure, voltages at the processor and pump, and an error flag. Additionally, the CTD floats return two check resistances for the FSI conductivity cell, and the TD floats return surface and pump temperatures, and transmitter voltage. In this section we will only inspect the deep pressure time series, as measures of float behaviour. The

deep pressure time series are shown in figures 2.8–2.13, which for later reference also include the deep temperature time series. Three general issues stand out from these data; we note first the behaviour of float 77.

2.3.1 Float 77

The second panel in figure 2.8 shows the full surface-to-operational-depth range for this float. This shows the occasions when the float appeared to run aground around cycles 27–32, when on two occasions the float spent its submerged time around 1000 dbar, and on one occasion was at 100 dbar or less.

2.3.2 Target depth

It is evident that the target depth was missed in several cases, sometimes by a large amount. Approximate initial float depths are summarised in Table 2.3. Three floats (77, 79, 80) went too deep by 90–150 dbar. No explanation is available for this. We show the depth of the target density surface on the 60°N section during the deployment cruise in figure 2.14, from which it can be seen that the intended depth of the target density of 1500 dbar was closely approached in 1996, when it lay at 1496–1497 dbar. Environmental factors can be ruled out therefore.

2.3.3 Shoaling

The submerged depths of all six floats have changed in similar ways to date. For about the first six months (12 cycles) they remained at fairly constant depths, after which they began to rise. In some floats the rate of rise has slowed recently (77, 83). The change in mean submerged depth over the whole deployment period to date is included in Table 2.3, where it is also expressed as a velocity (dbar per month). Net rise rates are of 3–4 dbar per month, but periods of more rapid rise can be seen in figs. 2.8–2.13. WRC suggest that this is caused by mass loss due to corrosion. If so, a rise rate of 3 dbar per month corresponds to a rate of mass loss of about 0.3 grams per month, given constant float volume and local density gradient of 5×10^{-3} kg m^{-4}.

2.3.4 First to second week differences

The floats' pressure sensors record a consistent mean increase of about 2.5 dbar from the first to the second submerged week of each cycle. The time series of pressure differences, calculated as second week minus first week mean submerged pressure for each cycle, are shown in figures 2.8–2.13, and the statistics of the apparent drop are included in Table 2.3. Three possible explanations present themselves (there may be other candidates): (1) pressure sensor hysteresis; (2) plastic deformation of the float hull (creep); and (3) temperature-dependent pressure sensor response.

Explanation (1) seems to be the least likely because any hysteresis would have to be of large magnitude in a short time to produce a measurable bias over a week at depth, assuming symmetrical behaviour over rise and fall parts of the cycle, which occur over a few hours.

Explanation (2) is possible We noted that all floats remain at roughly constant depth for the first six months or so after deployment. The inferred net rise rate, presumed due to mass loss by corrosion of about 4 dbar per month, is very similar to this fall rate, equivalent to 5 dbar per month; ie creep and corrosion happen to be nicely balanced initially. This explanation requires corrosion to be removing mass from the moment of deployment at a rate which must double after six months to enable the long-term shoaling to exceed the cumulative effect of creep. It is simpler to assume that the cause is a reversible process, however, and that the floats are not appreciably corroding to begin with, so that the first-to-second-week bias is the result of a reversible or elastic process, such as (1) or (3).

Explanation (3) we believe to be the most plausible. As an illustration of the kind of effect which can pertain, figure 2.15 shows the measured thermal response of a pressure transducer (John Smithers, pers. comm., 1998) obtained by plunging the transducer, initially at an ambient temperature of 24.5°C, into water at 0°C. The transducer was in a stainless steel CTD pressure case, fitted behind the pressure port directly onto the case. Over the course of an hour, the measured pressure drops by over 20 dbar. It is in the right sense, ie, a drop. One can imagine that the differently insulated floats might extend the time constant such that the observed bias results. so perhaps this bias is the result of the floats sinking from 'warm' surface water into LSW at about 3°C. Measurements would be required to confirm the above speculation, but such a thermal effect should have an associated seasonal cycle. The pressure difference time series in figures 2.8–2.13 provide some such evidence. Considering float 80 (fig. 2.11.2), we see summer pressure differences are maxima of ~4 dbar, winter differences are minima of ~0–1 dbar. All the floats except 82 appear to have such a cycle, albeit underlying some noise.

2.4 Profile Measurements

In this section we outline the method of temperature and conductivity profile generation. The float rises to the surface at 10–15 cm s^{-1}; while so doing, it measures P, T and C (pressure, temperature and conductivity) every 2.5 s. When at the surface, the processor averages the measured profiles into pre-set template depth bins to reduce the quantity of data to be transmitted. This limitation is imposed by the Argos message regime. In our case, the depth template with variable depth increments was approximately (increments in parentheses): 5 (10) 195 dbar, 207 (20) 527 dbar, 555 (50) 1455 dbar, although the actual values varied very slightly from these because the template is applied to pressure counts as output by the pressure sensor which is only converted to dbar on reception of data by application of a calibration coefficient

determined by WRC before deployment. This value is no more than 1% different from 1 count = 1 dbar. 56 depth bins result.

Data resolution is a function of message restrictions. Temperature is transmitted with resolution ca. 0.01°C, conductivity with equivalent salinity resolution ca. 0.008. The following section describes the results of our attempts to calibrate the salinities derived from the floats' conductivity sensors.

3. CONDUCTIVITY SENSOR CALIBRATION

3.1 Float / CTD comparisons

The availability of a large quantity of high-resolution, high-quality WOCE hydrographic data from the subpolar gyre over 1996-1997 makes possible an evaluation of the performance of the conductivity sensor of each float. There are two approaches to comparing the float data with the hydrographic data: (1) we can compare float salinity profiles with individual or small groups of ship CTD profiles which are closely adjacent to the float data in time and space, and: (2) we can take a statistical approach by using 'background' θ / S distributions. Version 1 is more accurate, because one is attempting to compare independent measures of the same water mass, whereas in version 2, the background θ / S distribution contains much spread (greater range of S for given θ) due to eddy noise, seasonal / interannual variability, and systematic variations with position in the Irminger Basin.

Data from six cruises were used; see Table 3.1 for details. The first is the launch cruise itself in October 1996, the last presently available the *Knorr* cruise in October 1997. Relevant station positions from each cruise are shown in figures 3.1–3.6.

We compared all float tracks with all cruise tracks to look for crossovers and close approaches. We decided to restrict comparisons to stations that occurred within 50 days and 100 km of float profiles. The time constraint ensured that the measurements had been made in the same season; the distance constraint, equivalent to about ±1° in position, was rather arbitrary but ensured our comparisons were not subject to biases resulting from systematic variations of salinity with position. The results of the comparisons are summarised in Tables 3.2, in which are also shown the CTD station / float profile pairs used below.

The next stage in the analysis was the visual comparison of float and ship θ / S profiles, in the groups suggested by Tables 3.2. First we confirmed that there was reasonable similarity between float and ship data, and that the difference between the two sets could be explained by an offset in float salinities. Offsets were crudely estimated to be up to 0.03 in salinity. Then we sub-selected the ship data by rejecting profiles with noticeably different θ / S relationships.

The last stage in the analysis was the determination of the offsets. Simply taking the mean salinity difference between ship and float profiles is not right because of the high variability in the upper few hundred metres. We wanted to match relatively stable water masses and we decided to reproduce computationally the estimation of the offset by overlaying two θ / S profiles and sliding one horizontally (ie at constant θ) until the profiles lined up. To do this computationally meant that much of the processing was directed at removing or avoiding θ / S inversions, both on the small scale (a few dbar in pressure and ~0.005 in salinity) and the large scale (hundreds of dbar, 0.05 in salinity). This was done as follows. We put the float and ship profiles for each matching group on a coarse grid of ΔP = 100 dbar, one grid each for ship and float profiles. Where a grid file contained more than one profile, the grid was horizontally averaged to a single mean profile. This averaged out small scale inversions. The top half of the grid files were cut off leaving data between about 700 and 1500 dbar, in which depth range the θ / S relationships are monotonic; this removed the large-scale inversions. The grid files were then regridded using potential temperature instead of pressure as independent variable, with grid spacing $\Delta\theta$ = 0.1°C. Now the float and ship grid files were merged using potential temperature as the common independent variable, with float salinity (sal.F) and ship CTD salinity (sal.C) as dependent variables. It was then simple to solve sal.C = sal.F + Offset. The float profile / CTD station matched groups and the calculated offsets are given in Table 3.3. Different values of ΔP and $\Delta\theta$ were tried but found to alter the salinity offset only in the fourth decimal place, which is not significant.

The calibrated data are presented in section 4 below, and the remarks above relating to water masses are put into context there. We proceed with some observations and conclusions pertinent to this part of the analysis.

We were fortunate in having so much ship data in the same region as the floats. Even so, it only amounts in practice to a 2-point check on each float: one point at launch in Autumn 1996, and a group of points not very widely separated in time around Summer 1997. No ship data from 1998 are presently available.

We now consider the offsets float by float. Float 77 has effectively 5 calibration points with a mean offset of +0.016 and sd 0.005. Float 78 has only 2 points; they average to –0.024 (sd 0.005). Float 79 has 3 points, mean –0.031, sd 0.003. Ignoring the first (launch) calibration point, float 80 has 4 points, mean –0.012, sd 0.004. The first and most pleasing results that stand out are the consistency of the errors. All sd's are 0.004–0.005 in salinity, so ±1 sd is surprisingly close to the float salinity profile resolution of 0.008. Furthermore, there is no evidence of trends in offset (with the exception of the start of float 80's record) over the year spanning the calibration exercise. Both of these inferences are highly encouraging. Before

inspecting the data more closely, we proceed with a further consistency check, described in 3.2 below.

3.2 Float / float comparisons

One can apply the matching technique described above to float / float intercomparison. Float comparison statistics are given in Tables 3.4, and computed float – float salinity offsets are presented in Table 3.5. According to the float – ship CTD comparison, the difference in offset between float 77 and 78 should be 0.016–(–0.024) = 0.040, compared with the direct estimation of 0.051 from Table 3.5, the difference in offsets being 0.011. Similarly the difference between 78 and 79 should be 0.007, compared with 0.012 estimated directly, the difference here being 0.005. The other three float – float comparisons involve float 80, which exhibits a puzzling ambiguity in offset as noted above. Considering the comparison with float 79, the difference in offset from the ship CTD data is –0.031–(–0.012) = –0.019, compared with –0.029 estimated directly. Similarly, comparing float 77 with float 80 cycle 3, the offset should be 0.016–(–0.012) = 0.028, compared with 0.032 estimated directly. All the foregoing are consistent with a salinity measurement error of sd = 0.005. We now compare float 80 cycle 1 with float 77, using 77's mean offset of 0.016 and 80's offset estimated at 0.013 from the launch cruise, which gives a relative offset of 0.016–0.013 = 0.003. The direct estimate gives 0.011, a difference of 0.008, also within the stated error. Thus it appear that out of all four floats, we can only identify one short period of drift, at the start of float 80's mission, when the sensor slipped by about 0.025 in salinity at some time during the first 2 cycles, but was probably stable thereafter.

4. FLOAT DATA: DISCUSSION

In this section, we present the float and some ship data in various forms, and offer some comments thereon. We apply the mean offsets derived above from the data in Table 3.3 to the floats' salinity data. The offset for float 80 excludes the anomalous first offset. All section 4 float plots pertain to the four CTD floats, except figures 4.9 and 4.10, which show contoured time series of T for the two TD floats 82 and 83. θ / S relationships are shown in figures 4.1–4.4, which show plots for all data and for deep data for each float; time series contour plots of S, θ and σ_0 are shown in figures 4.5–4.8; and deep S, θ and σ_0 time series are shown in figures 4.11–4.14. These latter are interpolated values from a common depth for all floats (1400 dbar). Figures 4.15–4.17 show ship data from summer 1997 (*Discovery* 230), and figure 4.18 is a form of summary, showing mean salinity binned on θ for both float and ship data.

The data quality appears high, once the salinity offsets have been applied. There is little obviously bad data, none of which have yet been edited. There is a spike in salinity to be seen in fig. 4.1.2 (float 77) at about S = 34.89, θ = 2.8°C. More seriously, we wonder whether the conductivity sensor of float 80 has just lately begun to fail (figs. 4.8.1 and 4.14); in the last few cycles presented here (42-44), salinity at 1400 dbar has dropped below 34.8 when the typical range at this depth is more like 34.85–34.87. This is reminiscent of the sensor failure reported by Freeland (1997), when salinities went markedly fresh. More puzzlingly, the density at 1400 dbar starts dropping around cycle 20, but this is due to warming; the salinities are stable. The rate of density decrease increases about cycle 35, but this is not unambiguously due to salinity; there are two fresh events at about cycles 35 and 39, but there are strong warm events after them. It is not easy to identify the extent of any problem. It is possible that our sensor is adjusting to a different but usable equilibrium; we will inspect later data with interest. One other point of interest in float 80's conductivities is the peculiar offset right at the start of its mission, mentioned in section 3 above. We can see from figure 4.14 that anomalously low salinity appears at cycles 1 and 2, after which the sensor appears stable, which is good evidence for extent of the problem at the start of the mission. We still need to look more closely at float 77's salinities after its grounding. We have not yet looked in any detail at ship CTD data in the Labrador Sea, which is needed to confirm the θ and S behaviour when the float settles down again after about cycle 33.

All θ / S plots overlie quite nicely, meaning in the deeper data within the computed ±0.005 error in salinity, and more generally within appropriate ranges for the shallower data. Generally, the cold, fresh extremum which represents the core of the LSW layer is at about S = 34.84, θ = 2.8°C; immediately above and below are more saline water masses, all ultimately of Atlantic origin, whether locally recirculated in the Irminger Current (above LSW) from the North Atlantic Current, or rather more distantly related, as in the overflows (below LSW). The wide range of θ and S in the upper waters reflects the Polar origin of cold, fresh waters at one extreme and the Atlantic origin of warm, salty waters at the other. The data range used for calculating float salinity offsets is seen in the waters immediately above the LSW extremum. Figure 4.18 shows mean θ / S relationships for the deep waters for each float and for *Discovery* 230 data in the Irminger basin, the latter divided into three segments: stations between Cape Farewell and mid-basin, stations south-east from mid-basin, and stations from the north-west section. Salinity values are binned by θ in 0.05°C bins. Stations were treated like float data, and were truncated at 1500 dbar. The data are all satisfactorily clustered, but some oddities remain to be explained. All θ / S curves have about the same slope, but the stations generally lie fresh of the floats. This may be due to mixing of more saline waters in the western boundary regime above and below the LSW layer into that layer, so that the floats which go west appear more saline at the deepest levels. Also, float 80, which has remained on the mid-basin axis, appears to have avoided the saline influence of the Irminger Current, in which all the other floats have spent some time.

This illustrates the difficulty of bulk θ / S analysis when comparing fixed, approximately area-weighted, section data with quasi-Lagrangian measurements. More analysis is required to rationalise these small differences.

In general scientific terms, there is a wealth of information even in these few floats. We can see the upper ocean thermal annual cycle; there are many eddy-like signatures; deep mixing appears in the two winters so far (see for example float 78 around cycles 11 and 37); float 83 seems to show an annual cycle at depth, with cold water rising up shallower than 1400 dbar in the winter; the general circulation at the 'level of no motion' in the Irminger Basin is to some extent elucidated; we have some information about random eddy velocities, mean propagation velocities, and boundary currents.

5. SUMMARY

Seven floats were launched at the end of October 1996. At the time of writing (October 1998), four are still functioning, and are thus approaching their median lifetime of 50 cycles. The main result of this study is to find that float salinities, calibrated by reference to CTD measurements from research vessels, are accurate to ±0.005, a range very close to the salinity resolution of the floats of 0.008. The calibration applies to the first year of float operation; there appear to be no significant changes, considering internal evidence (θ / S stability), over subsequent data, with exception of one float whose conductivity sensor may be failing. When satellite technology permits transmission of longer messages, salinity resolution should be increased. A second report will be produced in due course as a final summary after all these floats have expired.

Finally, the material of this report may be relevant to the Argo programme, intended as a global array of profiling floats. Until such time as conductivity sensors are developed which report accurately and without offsets, a global float array will require data quality control on the lines employed herein. Ship CTD data, penetrating into relatively stable intermediate / deep waters, will be needed for float salinity calibration if the best is to be obtained from float salinity profiles. Cruises of opportunity should largely suffice, because when float density is sufficiently high, other floats away from the vicinity of a cruise can be cross-calibrated by inter-float comparison.

ACKNOWLEDGEMENTS

The authors are most grateful to all WOCE principal scientists who allowed early use of their North Atlantic data for this report; these are Ruth Curry (*Knorr* 154), Mike McCartney (*Knorr* 147), Fritz Schott (*Meteor* 39 leg 4) and Lynne Talley (*Knorr* 151). We also thank Raymond Pollard who was principal scientist of *Discovery* 223 leg 2, when the floats were launched, for his cooperation and assistance, and for subsequent use of the cruise data. Howard Freeland was generous with advice at the start of the project. Clayton Jones, who assembled the floats at SOC prior to the launch cruise, and Dan Webb, of Webb Research Corporation, have also provided help along the way.

REFERENCES

Bacon, S., 1997: Circulation and fluxes in the North Atlantic between Greenland and Ireland. *J. Phys. Oceanogr.*, **27** (7) 1420-1435.

Bacon, S., 1998: Two hydrographic sections across the boundaries of the subpolar gyre, 'FOUREX'. SOC Cruise Report No. 16, 104 pp.

Davis, R. E., 1998: Autonomous floats in WOCE. *Int. WOCE Newsl.*, No. 30, 3-6.

Davis, R. E., D. C. Webb, L. A. Regier and J. Dufour, 1992: The Autonomous Lagrangian Circulation Explorer (ALACE). *J. Atmos. Oceanic Tech.*, **9** (3) 264-285.

Freeland, H. 1997: Calibration of the conductivity cells on P-ALACE floats. US WOCE Implementation Report, No. 9, 37-38.

Gould, W. J., 1992: *RRS Charles Darwin Cruise 62 1 August - 4 September 1991. CONVEX - WOCE Control Volume AR12.* IOSDL Cruise Report, No. 230, Wormley, 60 pp.

Leach, H. and R. T. Pollard, 1998: *RRS Discovery Cruise 223 28 September – 19 November 1996. Vivaldi '96.* SOC Cruise Report, No. 17, Southampton, 104 pp.

Read, J. F. and W. J. Gould, 1992: Cooling and freshening of the subpolar North Atlantic Ocean since the 1960s. *Nature* **360** 55-57.

Sherman, J., 1993: Profiling ALACE instruments. Scripps Institution of Oceanography, 28 pp. Unpublished manuscript.

APPENDIX 1: WOCE BIBLIOGRAPHY SEARCH RESULTS

A search on subject 'ALACE' on the WOCE bibliography resulted in the list below. The bibliography and related search routines can be found here: http://www.cms.udel.edu/woce/woce_bib.html.

Subject: ALACE; number of entries: 22

Anonymous, 1996: U.S. Indian Ocean field program nears completion. US WOCE Implementation Report, No. 8, 3-6.

Anonymous, 1992: WOCE Subsurface Float DAC. *Int. WOCE Newsl.*, No. 13, 20-22.

Baker, D. J., 1991: Oceans, climate change and a global ocean observing system. WMO Bulletin, **40** (2) 93-100.

Baker, D. J., 1991: Towards a global ocean observing system. *Oceanus*, **34** (1) 76-83.

Davis, R., 1990: ALACE explores Antarctic Circumpolar Current. *Int. WOCE Newsl.*, No.10, p.5.

Davis, R., 1991: ALACE float ready for WOCE field work. *WOCE Notes*, **13** (3) 1-3.

Davis, R., 1995: ALACE tracks subsurface ocean currents with Argos. Argos Newsl., No. 49, 5,7.

Davis, R. E., 1995: Early ALACE results from the Pacific. *Int. WOCE Newsl.*, No. 18, 22-26.

Davis, R. E., 1996: ALACEs return data on mean circulation in the western South Pacific. US WOCE Implementation Report, No. 8, 7-10.

Davis, R. E., 1998: Autonomous floats in WOCE. *Int. WOCE Newsl.*, No. 30, 3-6.

Davis, R. E., 1998: The mid-depth circulation in the tropical and subtropical Pacific from ALACE floats. US WOCE Implementation Report, No. 10, 18-21.

Davis, R. E., P. D.Killworth and J. R. Blundell, 1996: Comparison of ALACE and FRAM results in the South Atlantic. *J. Geophys. Res.*, **101** (C1) 855-884.

Davis, R. E., D. C. Webb, L. A. Regier and J. Dufour, 1992: The Autonomous Lagrangian Circulation Explorer (ALACE). *J. Atmos. Oceanic Tech.*, **9** (3) 264-285.

Freeland, H. 1997: Calibration of the conductivity cells on P-ALACE floats. US WOCE Implementation Report, No. 9, 37-38.

Gould, J. and J. Church, 1996: Oceans and climate. *Physics World*, December 1996, 33-37.

John, G. C., J. L. Bullister, R. A. Feely and B. A. Taft, 1995: Researchers complete WHP P18 observations. *WOCE Notes*, 7 (1) 6-10.

Killworth, P. and J. Blundell, 1996: Comparison of ALACE floats and FRAM in the South Atlantic. Understanding ocean circulation. pp. 24-25 in UK WOCE: the first six years, (ed. R. T. Pollard and D. Smythe-Wright). Southampton: Southampton Oceanography Centre, 32 pp.

Matthews, R., 1992: Oceans of information. (ALACE probe) Times, 26 Aug 1992, p.6.

McCartney, M. S. and M. O'Neil Baringer, 1993: Notes on the S. Pacific hydrographic section near 32S – WHP P6. *WOCE Notes*, **5** (2) 1,4-10.

Pingree, R. D., 1995: The droguing of meddy pinball and seeding with ALACE floats. *J. Mar. Biol. Assoc. UK*, **75** (1) 235-252.

Riser, S. C., 1995: Pacific RAFOS floats measure mid-depth flow. *WOCE Notes*, 7 (3) 1,3-6.

Riser, S. C., 1998: An examination of North Atlantic circulation using PALACE floats. . US WOCE Implementation Report, No. 10, 22-25.

Toole, J. M., 1995: ALACE results help determine thermocline depth variability. *WOCE Notes*, 7 (2) 7-10.

Zenk, W. and C. Schmid, 1998: WOCE floats in the South Atlantic. *Int. WOCE Newsl.*, No. 30, 39-43.

Table 1.1: Float 77 launch (event 0) and mean surface dates (yymmdd) and positions.

Event	Date	Lat	Lon
0	961027	059 59.916 N	038 24.282 W
1	961110	059 21.183 N	038 20.732 W
2	961124	059 46.920 N	039 2.958 W
3	961208	060 26.930 N	037 54.043 W
4	961222	060 4.907 N	039 35.776 W
5	970105	061 11.777 N	037 33.154 W
6	970119	061 44.649 N	036 8.079 W
7	970202	061 45.447 N	037 20.633 W
8	970216	061 45.999 N	037 21.834 W
9	970302	061 57.924 N	036 51.285 W
10	970316	060 54.519 N	037 27.456 W
11	970330	061 0.660 N	037 54.496 W
12	970413	061 27.607 N	037 52.097 W
13	970427	062 9.737 N	037 4.883 W
14	970511	061 55.707 N	038 14.010 W
15	970525	061 30.864 N	038 51.300 W
16	970608	060 54.700 N	039 46.043 W
17	970622	060 24.054 N	040 16.311 W
18	970706	060 31.137 N	040 25.266 W
19	970720	060 4.570 N	040 50.243 W
20	970803	059 19.524 N	041 17.124 W
21	970817	059 32.444 N	041 18.581 W
22	970831	059 21.752 N	040 28.398 W
23	970914	059 3.429 N	041 43.017 W
24	970928	058 10.660 N	045 12.803 W
25	971012	058 48.234 N	045 12.319 W
26	971026	060 2.463 N	048 29.025 W
27	971109	061 21.050 N	050 8.277 W
28	971123	061 55.658 N	050 41.368 W
29	971207	061 56.479 N	050 53.175 W
30	971221	062 9.056 N	050 52.536 W
31	980105	062 9.540 N	050 48.360 W
32	980118	062 21.828 N	051 3.738 W
33	980201	062 58.424 N	052 45.772 W
34	980215	062 52.570 N	054 6.167 W
35	980329	061 51.150 N	057 20.955 W
36	980412	060 59.457 N	057 54.483 W
37	980426	059 56.845 N	058 8.735 W
38	980510	059 26.454 N	058 26.700 W
39	980524	059 17.403 N	057 48.818 W
40	980607	058 56.773 N	059 1.671 W
41	980621	058 41.871 N	059 2.316 W
42	980705	058 45.096 N	058 54.708 W

Table 1.2: Float 78 launch (event 0) and mean surface dates (yymmdd) and positions.

Event	Date	Lat	Lon
0	961027	060 0.372 N	036 37.062 W
1	961110	059 43.191 N	037 4.077 W
2	961124	060 25.428 N	037 58.959 W
3	961208	059 25.566 N	036 55.779 W
4	961222	059 30.878 N	035 28.652 W
5	970105	059 53.640 N	035 2.388 W
6	970119	060 30.597 N	033 39.196 W
7	970202	060 48.886 N	033 0.388 W
8	970216	060 56.051 N	032 44.915 W
9	970302	061 5.157 N	032 28.512 W
10	970316	061 30.857 N	032 18.453 W
11	970330	061 25.926 N	031 39.789 W
12	970413	061 20.949 N	032 17.659 W
13	970427	061 3.329 N	032 58.023 W
14	970511	061 20.423 N	033 0.529 W
15	970525	062 6.149 N	032 42.149 W
16	970608	061 47.368 N	033 41.271 W
17	970622	062 14.664 N	035 28.224 W
18	970706	061 46.806 N	036 24.744 W
19	970720	061 25.765 N	035 36.297 W
20	970803	062 33.072 N	035 42.951 W
21	970817	062 23.149 N	038 9.286 W
22	970831	062 8.024 N	037 39.193 W
23	970914	062 25.877 N	038 7.597 W
24	970928	061 56.691 N	037 46.652 W
25	971012	062 11.238 N	037 4.875 W
26	971026	062 2.686 N	037 36.680 W
27	971109	061 58.874 N	037 6.391 W
28	971123	062 33.821 N	037 52.074 W
29	971207	062 41.233 N	038 30.351 W
30	971221	061 39.729 N	038 19.686 W
31	980104	061 39.414 N	038 5.299 W
32	980118	061 35.871 N	037 48.761 W
33	980201	061 33.582 N	040 8.457 W
34	980215	060 57.687 N	040 48.237 W
35	980301	060 52.520 N	040 22.570 W
36	980315	059 20.947 N	041 18.491 W
37	980329	059 20.478 N	039 37.716 W
38	980412	059 44.166 N	040 37.418 W
39	980426	059 17.413 N	041 56.193 W
40	980510	058 56.432 N	044 3.676 W
41	980524	060 11.557 N	048 10.590 W
42	980608	060 48.506 N	050 0.163 W
43	980621	061 17.666 N	053 36.009 W
44	980706	060 35.003 N	055 25.383 W

Table 1.3: Float 79 launch (event 0) and mean surface dates (yymmdd) and positions.

Event	Date	Lat	Lon
0	961029	058 1.698 N	040 25.518 W
1	961112	057 55.734 N	041 14.599 W
2	961126	057 39.507 N	040 56.487 W
3	961210	057 7.920 N	040 58.097 W
4	961224	057 7.632 N	041 37.341 W
5	970107	057 28.999 N	041 40.854 W
6	970121	057 50.859 N	040 44.255 W
7	970204	057 53.550 N	040 38.685 W
8	970218	058 14.664 N	040 6.060 W
9	970304	058 8.933 N	039 15.420 W
10	970318	058 12.210 N	038 58.326 W
11	970401	058 44.227 N	038 22.917 W
12	970415	058 24.954 N	040 26.432 W
13	970429	059 1.834 N	038 32.100 W
14	970513	059 14.691 N	037 45.960 W
15	970527	059 7.535 N	036 44.043 W
16	970610	059 37.644 N	035 20.403 W
17	970624	060 14.877 N	037 32.488 W
18	970708	060 32.327 N	037 31.604 W
19	970722	060 51.586 N	037 6.451 W
20	970805	061 16.140 N	035 58.349 W
21	970819	062 9.806 N	033 56.551 W
22	970902	061 7.143 N	035 24.483 W
23	970916	061 34.437 N	037 26.548 W
24	970930	061 51.514 N	035 2.680 W
25	971014	062 23.961 N	034 37.587 W
26	971028	062 39.663 N	034 3.190 W
27	971111	062 29.094 N	032 25.602 W
28	971125	062 14.163 N	035 1.151 W
29	971209	062 41.069 N	036 23.331 W
30	971223	062 11.831 N	038 14.357 W
31	980106	062 45.483 N	038 23.659 W
32	980120	062 14.511 N	039 50.397 W
33	980203	061 13.380 N	040 46.980 W

Table 1.4: Float 80 launch (event 0) and mean surface dates (yymmdd) and positions.

Event	Date	Lat	Lon
0	961028	059 58.956 N	040 30.480 W
1	961110	060 10.367 N	039 5.460 W
2	961124	059 56.553 N	041 3.366 W
3	961208	060 0.707 N	038 49.721 W
4	961222	060 43.364 N	040 19.383 W
5	970105	060 43.697 N	040 13.653 W
6	970119	060 19.426 N	039 59.129 W
7	970203	059 35.268 N	040 18.426 W
8	970217	059 5.388 N	041 23.442 W
9	970303	058 55.260 N	040 11.346 W
10	970317	058 36.342 N	037 24.912 W
11	970331	058 43.533 N	037 11.163 W
12	970414	058 20.013 N	037 32.708 W
13	970428	058 16.407 N	037 36.810 W
14	970512	058 4.314 N	037 59.214 W
15	970526	058 35.835 N	039 37.452 W
16	970609	057 53.801 N	042 7.688 W
17	970623	058 4.009 N	042 48.259 W
18	970707	058 24.015 N	040 50.464 W
19	970721	057 49.061 N	040 31.674 W
20	970804	058 29.873 N	039 27.716 W
21	970818	058 55.427 N	040 8.883 W
22	970901	058 52.398 N	039 19.359 W
23	970915	059 32.445 N	038 24.966 W
24	970929	058 45.431 N	037 52.017 W
25	971013	058 37.560 N	037 3.231 W
26	971027	058 55.314 N	037 23.229 W
27	971110	059 32.316 N	037 15.036 W
28	971124	059 35.772 N	036 46.173 W
29	971208	059 10.634 N	036 29.300 W
30	971222	059 36.576 N	036 4.413 W
31	980105	060 10.905 N	035 15.108 W
32	980119	060 20.927 N	035 44.924 W
33	980202	060 17.355 N	035 5.745 W
34	980216	060 27.897 N	035 35.973 W
35	980302	061 10.977 N	036 15.319 W
36	980316	061 0.557 N	034 4.287 W
37	980330	061 22.178 N	032 40.923 W
38	980413	061 25.153 N	032 20.627 W
39	980427	062 1.824 N	031 56.871 W
40	980511	062 23.886 N	031 47.677 W
41	980525	062 28.450 N	032 12.320 W
42	980608	061 51.528 N	033 6.444 W
43	980622	061 34.530 N	033 3.037 W
44	980706	061 19.833 N	033 2.817 W

Table 1.5: Float 81 launch (event 0) and mean surface dates (yymmdd) and positions.

Event	Date	Lat	Lon
0	961031	054 5.472 N	033 22.818 W
1	961114	054 8.950 N	032 5.865 W
2	961128	054 45.732 N	031 13.884 W
3	961212	055 31.920 N	030 58.195 W

Table 1.6: Float 82 launch (event 0) and mean surface dates (yymmdd) and positions.

Event	Date	Lat	Lon
0	961030	056 58.494 N	038 19.950 W
1	961112	056 13.594 N	037 32.415 W
2	961126	056 53.620 N	036 36.773 W
3	961211	057 5.183 N	037 9.787 W
4	961224	057 19.364 N	037 42.354 W
5	970108	057 19.008 N	037 34.791 W
6	970122	057 10.825 N	038 15.850 W
7	970205	057 12.051 N	038 29.059 W
8	970219	057 12.582 N	037 25.327 W
9	970305	057 48.733 N	036 20.880 W
10	970319	057 49.578 N	034 30.582 W
11	970402	058 11.564 N	034 28.964 W
12	970416	057 52.926 N	034 25.282 W
13	970430	058 7.397 N	034 13.129 W
14	970514	058 28.197 N	033 41.178 W
15	970528	059 0.969 N	032 50.697 W
16	970611	059 59.255 N	032 3.733 W
17	970625	060 45.024 N	032 40.806 W
18	970709	060 33.994 N	033 59.069 W
19	970723	060 29.175 N	034 2.295 W
20	970806	060 47.597 N	033 35.270 W
21	970820	060 28.646 N	034 10.571 W
22	970903	059 57.676 N	033 56.192 W
23	970917	060 0.060 N	033 45.648 W
24	971001	060 6.735 N	034 23.979 W
25	971015	059 40.689 N	034 16.344 W
26	971029	059 29.559 N	033 59.103 W
27	971112	058 52.020 N	033 54.303 W
28	971126	058 37.206 N	033 23.597 W
29	971210	058 55.433 N	033 6.897 W
30	971224	059 14.466 N	033 36.150 W
31	980106	059 16.740 N	034 2.100 W

Table 1.7: Float 83 launch (event 0) and mean surface dates (yymmdd) and positions.

Event	Date	Lat	Lon
0	961030	055 54.090 N	036 24.132 W
1	961113	056 0.607 N	036 50.270 W
2	961127	055 41.125 N	037 1.038 W
3	961211	055 30.160 N	037 4.140 W
4	961225	055 42.300 N	036 57.275 W
5	970108	055 58.100 N	038 46.600 W
6	970122	055 45.432 N	039 19.528 W
7	970205	055 33.070 N	038 14.523 W
8	970219	055 41.293 N	037 39.999 W
9	970305	055 14.276 N	037 10.481 W
10	970319	055 26.719 N	037 0.435 W
11	970402	055 10.057 N	036 51.513 W
12	970416	054 39.840 N	037 1.380 W
13	970430	054 0.413 N	036 57.176 W
14	970514	053 49.244 N	038 4.240 W
15	970528	053 41.598 N	037 47.058 W
16	970611	053 43.296 N	037 13.864 W
17	970625	054 14.300 N	036 32.656 W
18	970709	054 12.709 N	036 11.269 W
19	970723	053 59.354 N	036 21.946 W
20	970806	053 46.736 N	036 48.446 W
21	970820	053 41.080 N	037 1.224 W
22	970903	053 43.368 N	037 14.396 W
23	970917	053 48.488 N	037 20.372 W
24	971001	054 0.844 N	037 21.184 W
25	971015	053 51.527 N	037 58.076 W
26	971029	053 43.748 N	037 20.972 W
27	971112	053 42.448 N	037 12.360 W
28	971126	054 7.507 N	037 28.493 W
29	971210	054 16.031 N	037 58.849 W
30	971224	054 28.461 N	038 24.342 W
31	980107	054 14.988 N	038 42.448 W
32	980121	054 13.800 N	038 57.630 W
33	980205	054 37.761 N	038 41.813 W
34	980219	054 39.192 N	038 15.876 W
35	980305	054 11.633 N	038 46.338 W
36	980319	054 44.441 N	039 3.158 W
37	980402	054 4.865 N	038 40.745 W
38	980416	054 19.586 N	039 5.228 W
39	980430	054 12.210 N	038 37.879 W
40	980514	053 47.936 N	038 21.576 W
41	980528	053 47.140 N	038 52.970 W
42	980611	053 36.101 N	038 33.581 W
43	980625	053 24.400 N	037 45.080 W
44	980709	053 17.451 N	036 20.884 W

Tables 2.1 and 2.2: Float navigation statistics. The mean and standard deviation (sd) of east and north components of velocity (vn, ve), net distance travelled (dist) and duration (time) for each float (first column). Statistics in Table 2.1 (Deep) are derived from values calculated from pairs of cycles using the last satellite surface position fix for each cycle and the first surface fix of the subsequent cycle. Statistics in Table 2.2 (Surface) are derived from individual cycles using the first and last fix for each cycle.

Table 2.1: Deep

	ve (cm/s)		**vn** (cm/s)		**dist** (km)		**time** (hours)	
	mean	sd	mean	sd	mean	sd	mean	sd
77	-1.87	5.02	-0.18	5.27	72.8	51.9	315.9*	3.5*
78	-1.84	5.51	-0.14	4.99	70.9	48.8	314.6	1.8
79	-0.13	5.79	1.28	3.98	69.9	38.9	315.4	2.2
80	0.63	5.15	0.30	4.02	63.0	38.3	314.8	2.0
82	0.23	2.84	0.24	3.43	45.2	20.9	313.6	1.0
83	-0.24	2.95	-0.61	2.59	38.8	22.5	315.1	2.3

Table 2.2: Surface

	ve (cm/s)		**vn** (cm/s)		**dist** (km)		**time** (hours)	
	mean	sd	mean	sd	mean	sd	mean	sd
77	-5.29	15.72	0.95	15.52	13.7	8.6	20.4	3.3
78	-3.08	22.28	3.73	17.46	16.9	15.0	22.0	1.9
79	4.46	21.47	0.23	14.39	16.7	9.4	21.1	2.0
80	3.35	16.57	-0.04	13.43	14.2	21.8	21.8	2.1
82	8.41	20.58	6.96	19.55	20.2	14.1	22.9	0.7
83	3.88	15.63	0.72	12.36	13.5	7.4	21.5	2.0

Table 2.3: Float depths and depth change statistics. Depth change and rise rate refer to latest data for surviving floats, or to depth on last reported cycle for expired floats. Rise rate is net over this period. Mean diff. & diff (sd) are the mean difference and standard deviation of difference about the mean between second and first week submerged pressure measurements.

Float	77	78	79	80	82	83
Initial Depth (dbar)	1650	1530	1600	1590	1515	1510
Depth Change (dbar)	80	65	70	45	65	85
Rise rate (dbar/mon)	4.0	3.2	4.7	2.2	4.6	4.2
Mean diff. (dbar)	2.5	2.6	2.5	1.9	2.9	2.4
Diff. (sd, dbar)	2.0	1.5	1.3	1.3	1.5	1.5

Table 3.1: Cruises used in float salinity profile evaluation.

Cruise	Principal Scientist	Dates
Discovery 223 leg 2	Raymond Pollard, SOC	Oct 1996
Knorr 147	Mike McCartney, WHOI	Nov 1996
Knorr 151	Lynne Talley, Scripps	Jun 1997
Meteor 39 leg 4	Fritz Schott, IfM Kiel	Jul 1997
Discovery 230	Sheldon Bacon, SOC	Aug 1997
Knorr 154	Ruth Curry, WHOI	Oct 1997

Tables 3.2: The following tables show all comparisons made between floats 77–80 and the six cruises identified in Table 3.1. In each table, float number and cruise number are given in the top left box. Float cycle number is shown in the left hand column; cruise station number in the top row. Where a box shows 'xxx', no match is reported; where a box shows two numbers, the upper number is time in days (float minus ship); where the lower of the two figures is 'x', the time separation is too large, so no distance calculation was made; where the figures are in italic script, this indicates a float / CTD pair selected for analysis, as being within (or nearly within) 100 km and 50 days of each other.

Table 3.2.1: Float 77 and *Discovery* 230

230 77	82	83	84	85	86	87	94	95	96	97
6	xxx	xxx	xxx	xxx	xxx	xxx	-229 x	-229 x	-230 x	-230 x
7	xxx	xxx	xxx	xxx	xxx	xxx	-215 x	-215 x	-216 x	-216 x
8	xxx	xxx	xxx	xxx	xxx	xxx	-201 x	-201 x	-202 x	-202 x
9	xxx	xxx	xxx	xxx	xxx	xxx	-197 x	-197 x	-198 x	-198 x
13	xxx	xxx	xxx	xxx	xxx	xxx	-131 x	-131 x	-132 x	-132 x
14	xxx	xxx	xxx	xxx	xxx	xxx	-117 x	-117 x	-118 x	-118 x
20	*-27* *109.6*	*-27* *78.3*	*-27* *64.4*	*-28* *57.1*	*-28* *56.6*	*-28* *66.7*	xxx	xxx	xxx	xxx
21	-13 130.9	*-13* *98.9*	*-13* *83.1*	*-14* *73.0*	*-14* *67.3*	*-14* *70.2*	xxx	xxx	xxx	xxx
22	1 113.3	*1* *96.6*	*1* *94.1*	*0* *94.8*	*0* *100.6*	*0* *114.0*	xxx	xxx	xxx	xxx
23	*15* *85.4*	*15* *47.0*	*15* *26.2*	*14* *16.3*	*14* *24.7*	*14* *46.7*	xxx	xxx	xxx	xxx

Table 3.2.2: Float 77 and *Knorr* 147

147 77	53
23	307 x

Table 3.2.3: Float 77 and *Knorr* 151

151 77	98	99	100	101	102	103
20	*44* *97.9*	*45* *88.8*	*45* *84.4*	*45* *77.0*	*45* *63.1*	*45* *71.3*
21	*58* *88.9*	*59* *81.9*	*59* *78.9*	*59* *74.2*	*59* *71.6*	*59* *88.5*
22	72 x	73 x	73 x	73 x	73 x	73 x
23	86 x	87 x	87 x	87 x	87 x	87 x

Table 3.2.4: Float 77 and *Meteor* 39 leg 4

394 77	31	32	33	98	99	100	101	102	103
26	94 x	94 x	94 x	xxx	xxx	xxx	xxx	xxx	xxx
19	xxx	xxx	xxx	-19 149.6	-19 122.4	*-19* *102.5*	*-19* *88.8*	*-20* *84.2*	*-20* *87.8*
20	xxx	xxx	xxx	*-5* *86.5*	*-5* *52.9*	*-5* *22.3*	*-5* *9.34*	*-6* *39.2*	*-6* *60.3*
21	xxx	xxx	xxx	*9* *104.4*	*9* *71.3*	*9* *42.3*	*9* *19.9*	*8* *29.0*	*8* *47.5*
22	xxx	xxx	xxx	*23* *62.6*	*23* *39.3*	*23* *38.7*	*23* *56.9*	*22* *83.1*	*22* *102.7*
23	xxx	xxx	xxx	*37* *90.1*	*37* *61.4*	*37* *40.7*	*37* *38.1*	*36* *55.7*	*36* *72.8*

Table 3.2.5: Float 78 and *Discovery* 230

230 78	83	84	85	86	87	88
36	198 x	198 x	199 x	199 x	199 x	199 x
39	240 x	240 x	241 x	241 x	241 x	241 x

Table 3.2.6: Float 78 and *Knorr* 147

147 78	52	53	54	55	56	77	78
15	xxx	xxx	xxx	xxx	xxx	190 x	190 x
36	489 x	489 x	488 x	488 x	488 x	xxx	xxx
39	528 x	528 x	527 x	527 x	527 x	xxx	xxx
40	542 x	542 x	541 x	541 x	541 x	xxx	xxx

Table 3.2.7: Float 78 and *Knorr* 151

151 78	84	85	101	102	103	104
15	*-21* *65.2*	*-22* *63.0*	xxx	xxx	xxx	xxx
36	xxx	xxx	270 x	270 x	270 x	270 x
39	xxx	xxx	312 x	312 x	312 x	312 x
40	xxx	xxx	326 x	326 x	326 x	326 x

Table 3.2.8: Float 78 and *Meteor* 39 leg 4

394 78	31	32	33	34	35	99	100	101	102
36	xxx	xxx	xxx	xxx	xxx	220 x	220 x	220 x	219 x
37	xxx	xxx	xxx	xxx	xxx	234 x	234 x	234 x	233 x
38	xxx	xxx	xxx	xxx	xxx	246 x	246 x	246 x	245 x
39	xxx	xxx	xxx	xxx	xxx	258 x	258 x	258 x	257 x
40	xxx	xxx	xxx	295 x	294 x	xxx	xxx	xxx	xxx
41	310 x	310 x	310 x	xxx	xxx	xxx	xxx	xxx	xxx

Table 3.2.9: Float 78 and *Knorr* 154

154 78	75	76	77	78
10	-227 x	-227 x	-227 x	-228 x
11	-213 x	-213 x	-213 x	-214 x
12	-199 x	-199 x	-199 x	-200 x
15	-157 x	-157 x	-157 x	-158 x

Table 3.2.10: Float 79 and *Discovery* 230

230 79	78	79	80	81	82	83
1	-291 x	-291 x	-291 x	-291 x	-292 x	-292 x
2	-277 x	-277 x	-277 x	-277 x	-278 x	-278 x
3	-263 x	-263 x	-263 x	-263 x	-264 x	-264 x
5	-249 x	-249 x	-249 x	-249 x	-250 x	-250 x
6	-235 x	-235 x	-235 x	-235 x	-236 x	-236 x
7	-221 x	-221 x	-221 x	-221 x	-222 x	-222 x
8	-207 x	-207 x	-207 x	-207 x	-208 x	-208 x
9	-193 x	-193 x	-193 x	-193 x	-194 x	-194 x
10	-179 x	-179 x	-179 x	-179 x	-180 x	-180 x
12	-151 x	-151 x	-151 x	-151 x	-152 x	-152 x

Table 3.2.11: Float 79 and *Knorr* 147

147 79	47	48	49	50	74	75	76	77	78
1	1 126.4	*0* *73.0*	*0* *24.3*	*0* *45.7*	xxx	xxx	xxx	xxx	xxx
2	*15* *104.9*	*14* *52.6*	*14* *24.7*	*14* *68.0*	xxx	xxx	xxx	xxx	xxx
3	*29* *62.2*	*28* *57.1*	*28* *82.3*	28 131.7	xxx	xxx	xxx	xxx	xxx
4	*43* *109.9*	*42* *87.9*	*42* *97.6*	42 132.2	xxx	xxx	xxx	xxx	xxx
5	57 114.8	*56* *77.0*	*56* *68.8*	*56* *98.7*	xxx	xxx	xxx	xxx	xxx
6	71 x	70 x	70 x	70 x	xxx	xxx	xxx	xxx	xxx
7	85 x	84 x	84 x	84 x	xxx	xxx	xxx	xxx	xxx
8	99 x	98 x	98 x	98 x	xxx	xxx	xxx	xxx	xxx
9	113 x	112 x	112 x	112 x	xxx	xxx	xxx	xxx	xxx
10	127 x	126 x	126 x	126 x	xxx	xxx	xxx	xxx	xxx
12	155 x	154 x	154 x	154 x	xxx	xxx	xxx	xxx	xxx
26	xxx	xxx	xxx	xxx	346 x	346 x	346 x	346 x	346 x
27	xxx	xxx	xxx	xxx	360 x	360 x	360 x	360 x	360 x

Table 3.2.12: Float 79 and *Knorr* 151

151 79	84	85	86	87	104	105	106	107	108
1	xxx	xxx	xxx	xxx	-250 x	-250 x	-251 x	-251 x	-251 x
2	xxx	xxx	xxx	xxx	-236 x	-236 x	-237 x	-237 x	-237 x
3	xxx	xxx	xxx	xxx	-222 x	-222 x	-223 x	-223 x	-223 x
4	xxx	xxx	xxx	xxx	-208 x	-208 x	-209 x	-209 x	-209 x
5	xxx	xxx	xxx	xxx	-194 x	-194 x	-195 x	-195 x	-195 x
6	xxx	xxx	xxx	xxx	-180 x	-180 x	-181 x	-181 x	-181 x
7	xxx	xxx	xxx	xxx	-166 x	-166 x	-167 x	-167 x	-167 x
8	xxx	xxx	xxx	xxx	-152 x	-152 x	-153 x	-153 x	-153 x
9	xxx	xxx	xxx	xxx	-138 x	-138 x	-139 x	-139 x	-139 x
10	xxx	xxx	xxx	xxx	-124 x	-124 x	-125 x	-125 x	-125 x
12	xxx	xxx	xxx	xxx	-96 x	-96 x	-97 x	-97 x	-97 x
26	135 x	134 x	134 x	134 x	xxx	xxx	xxx	xxx	xxx
27	149 x	150 x	150 x	150 x	xxx	xxx	xxx	xxx	xxx

Table 3.2.13: Float 79 and *Knorr* 39 leg 4

394 79	95	96	97	98	99	100
1	-270 x	-270 x	-271 x	-271 x	-271 x	-271 x
2	-256 x	-256 x	-257 x	-257 x	-257 x	-257 x
6	-200 x	-200 x	-201 x	-201 x	-201 x	-201 x
7	-186 x	-186 x	-187 x	-187 x	-187 x	-187 x
8	-172 x	-172 x	-173 x	-173 x	-173 x	-173 x
9	-158 x	-158 x	-159 x	-159 x	-159 x	-159 x
10	-144 x	-144 x	-145 x	-145 x	-145 x	-145 x
11	-130 x	-130 x	-131 x	-131 x	-131 x	-131 x
12	-116 x	-116 x	-117 x	-117 x	-117 x	-117 x
13	-102 x	-102 x	-103 x	-103 x	-103 x	-103 x

Table 3.2.14: Float 79 and *Knorr* 154

154 79	73	74	75	76	77
21	-70 x	-70 x	-70 x	-70 x	-70 x
25	-14 129.0	*-14* *103.1*	*-14* *105.6*	-14 131.7	-14 175.4
26	0 114.2	*0* *73.7*	*0* *65.1*	*0* *94.7*	0 143.7
27	14 168.5	14 112.6	*14* *55.9*	*14* *11.4*	*14* *58.5*

Table 3.2.15: Float 80 and *Discovery* 230

230 80	79	80	81	82	83	84	85	86	94	95
8	-195 x	-195 x	-195 x	-196 x	-196 x	-196 x	-197 x	-197 x	xxx	xxx
9	-181 x	-181 x	-181 x	-182 x	-182 x	-182 x	-183 x	-183 x	xxx	xxx
14	-125 x	-125 x	-125 x	-126 x	-126 x	-126 x	-127 x	-127 x	xxx	xxx
15	-111 x	-111 x	-111 x	-112 x	-112 x	-112 x	-113 x	-113 x	xxx	xxx
16	-97 x	-97 x	-97 x	-98 x	-98 x	-98 x	-99 x	-99 x	xxx	xxx
17	-83 x	-83 x	-83 x	-84 x	-84 x	-84 x	-85 x	-85 x	xxx	xxx
18	-69 x	-69 x	-69 x	-70 x	-70 x	-70 x	-71 x	-71 x	xxx	xxx
19	*-55* *80.0*	*-55* *24.3*	*-55* *32.3*	*-56* *76.7*	-56 116.3	-56 140.6	-57 158.9	-57 178.7	xxx	xxx
20	-41 131.8	*-41* *92.4*	*-41* *77.9*	*-42* *89.8*	-42 115.5	-42 135.0	-43 149.8	-43 167.2	xxx	xxx
21	-27 186.4	-27 138.0	*-27* *99.7*	*-28* *80.6*	*-28* *83.2*	*-28* *94.1*	*-29* *104.0*	-29 118.0	xxx	xxx
22	-13 181.1	-13 142.0	-13 118.5	-14 113.4	-14 124.0	-14 136.4	-15 146.5	-15 160.0	xxx	xxx
35	xxx	xxx	xxx	xxx	xxx	xxx	xxx	xxx	181 x	181 x

Table 3.2.16: Float 80 and *Knorr* 147

147 80	47	48	49	50	51	52	53	54	55	77	78
8	97 x	97 x	97 x	97 x	96 x	96 x	96 x	95 x	95 x	xxx	xxx
9	111 x	111 x	111 x	111 x	110 x	110 x	110 x	109 x	109 x	xxx	xxx
14	181 x	181 x	181 x	181 x	180 x	180 x	180 x	179 x	179 x	xxx	xxx
15	195 x	195 x	195 x	195 x	194 x	194 x	194 x	193 x	193 x	xxx	xxx
16	209 x	209 x	209 x	209 x	208 x	208 x	208 x	207 x	207 x	xxx	xxx
17	223 x	223 x	223 x	223 x	222 x	222 x	222 x	221 x	221 x	xxx	xxx
18	237 x	237 x	237 x	237 x	236 x	236 x	236 x	235 x	235 x	xxx	xxx
19	251 x	251 x	251 x	251 x	250 x	250 x	250 x	249 x	249 x	xxx	xxx
20	265 x	265 x	265 x	265 x	264 x	264 x	264 x	263 x	263 x	xxx	xxx
21	279 x	279 x	279 x	279 x	278 x	278 x	278 x	277 x	277 x	xxx	xxx
22	293 x	293 x	293 x	293 x	292 x	292 x	292 x	291 x	291 x	xxx	xxx
40	xxx	xxx	xxx	xxx	xxx	xxx	xxx	xxx	xxx	541 x	541 x
41	xxx	xxx	xxx	xxx	xxx	xxx	xxx	xxx	xxx	555 x	555 x

Table 3.2.17: Float 80 and *Knorr* 151

151 80	101	102	103	104	105	106	107	108	83	84	85
8	-124 x	-124 x	-124 x	-124 x	-124 x	-125 x	-125 x	-125 x	xxx	xxx	xxx
9	-110 x	-110 x	-110 x	-110 x	-110 x	-111 x	-111 x	-111 x	xxx	xxx	xxx
14	-40 318.7	-40 287.1	-40 256.3	-40 224.1	-40 203.5	-41 177.1	-41 163.0	-41 167.3	xxx	xxx	xxx
15	-26 204.9	-26 174.0	-26 145.9	-26 122.2	-26 115.1	-27 121.0	-27 145.7	-27 185.6	xxx	xxx	xxx
16	-12 178.0	-12 141.4	*-12* *106.0*	*-12* *69.6*	*-12* *55.3*	*-13* *80.1*	*-13* *126.8*	-13 180.0	xxx	xxx	xxx
17	2 161.4	2 129.4	*2* *102.2*	*2* *83.6*	*2* *86.5*	1 120.8	1 167.4	1 219.7	xxx	xxx	xxx
18	16 157.4	16 119.1	*16* *80.4*	*16* *38.6*	*16* *28.6*	*15* *69.8*	15 120.8	15 176.1	xxx	xxx	xxx
19	30 225.2	30 186.6	30 147.0	*30* *100.1*	*30* *65.6*	*29* *24.5*	*29* *54.3*	*29* *108.1*	xxx	xxx	xxx
20	44 209.0	44 176.6	44 146.4	44 119.1	*44* *108.4*	43 110.2	43 135.5	43 173.5	xxx	xxx	xxx
21	58 154.8	58 127.3	*58* *106.3*	*58* *99.2*	*58* *109.4*	57 138.9	57 177.9	57 225.4	xxx	xxx	xxx
22	72 x	72 x	72 x	72 x	72 x	71 x	71 x	71 x	xxx	xxx	xxx
39	xxx	xxx	xxx	xxx	xxx	xxx	xxx	xxx	317 x	317 x	316 x
40	xxx	xxx	xxx	xxx	xxx	xxx	xxx	xxx	331 x	331 x	330 x
41	xxx	xxx	xxx	xxx	xxx	xxx	xxx	xxx	345 x	345 x	344 x

Table 3.2.18: Float 80 and *Meteor* 39 leg 4

80-394	35	36	37	38	39	94	95	96	97	98	99
2	xxx	xxx	xxx	xxx	xxx	-257 x	-257 x	-257 x	-258 x	-258 x	-258 x
7	xxx	xxx	xxx	xxx	xxx	-187 x	-187 x	-187 x	-188 x	-188 x	-188 x
8	xxx	xxx	xxx	xxx	xxx	-173 x	-173 x	-173 x	-174 x	-174 x	-174 x
9	xxx	xxx	xxx	xxx	xxx	-159 x	-159 x	-159 x	-160 x	-160 x	-160 x
10	xxx	xxx	xxx	xxx	xxx	-145 x	-145 x	-145 x	-146 x	-146 x	-146 x
11	xxx	xxx	xxx	xxx	xxx	-131 x	-131 x	-131 x	-132 x	-132 x	-132 x
12	xxx	xxx	xxx	xxx	xxx	-117 x	-117 x	-117 x	-118 x	-118 x	-118 x
13	xxx	xxx	xxx	xxx	xxx	-103 x	-103 x	-103 x	-104 x	-104 x	-104 x
14	xxx	xxx	xxx	xxx	xxx	-89 x	-89 x	-89 x	-90 x	-90 x	-90 x
15	xxx	xxx	xxx	xxx	xxx	-75 x	-75 x	-75 x	-76 x	-76 x	-76 x
16	-48 120.2	*-48* *103.9*	*-48* *91.1*	*-48* *85.6*	*-48* *90.7*	xxx	xxx	xxx	xxx	xxx	xxx
17	*-34* *85.3*	*-34* *65.4*	*-34* *50.2*	*-34* *50.2*	*-34* *64.3*	xxx	xxx	xxx	xxx	xxx	xxx
19	xxx	xxx	xxx	xxx	xxx	-33 160.7	-33 116.4	*-33* *88.8*	*-34* *91.2*	-34 111.3	-34 136.1
20	xxx	xxx	xxx	xxx	xxx	-19 149.8	*-19* *92.3*	*-19* *38.1*	*-20* *15.4*	*-20* *55.7*	*-20* *89.2*
21	xxx	xxx	xxx	xxx	xxx	-5 208.9	-5 152.5	*-5* *98.8*	*-6* *46.6*	*-6* *15.1*	*-6* *32.4*
22	xxx	xxx	xxx	xxx	xxx	9 181.7	9 127.5	*9* *79.1*	*8* *44.9*	*8* *51.2*	*8* *73.9*
24	xxx	xxx	xxx	xxx	xxx	37 142.8	*37* *105.3*	*37* *90.3*	*36* *103.6*	36 128.5	36 153.4
25	xxx	xxx	xxx	xxx	xxx	51 120.4	*51* *108.8*	51 123.5	50 155.1	50 185.8	50 213.0

Table 3.2.18: Float 80 and *Meteor* 39 leg 4 continued

394 80	100	101	102	103
2	-258 x	-258 x	-259 x	-259 x
7	-188 x	-188 x	-189 x	-189 x
8	-174 x	-174 x	-175 x	-175 x
9	-160 x	-160 x	-161 x	-161 x
10	-146 x	-146 x	-147 x	-147 x
11	-132 x	-132 x	-133 x	-133 x
12	-118 x	-118 x	-119 x	-119 x
13	-104 x	-104 x	-105 x	-105 x
14	-90 x	-90 x	-91 x	-91 x
15	-76 x	-76 x	-77 x	-77 x
19	-34 160.7	-34 186.7	-35 214.4	-35 233.7
20	-20 120.1	-20 150.1	-21 180.9	-21 202.0
21	*-6* *61.9*	*-6* *91.4*	-7 122.0	-7 143.0
22	*8* *101.1*	8 129.0	7 158.4	7 178.9
24	36 179.6	36 206.2	35 234.4	35 254.2
25	50 240.2	50 267.3	49 295.7	49 315.6

Table 3.2.19: Float 80 and *Knorr* 154

154 80	75	76	77	78
38	168 x	168 x	167 x	168 x
39	182 x	182 x	181 x	182 x
40	196 x	196 x	195 x	196 x
41	210 x	210 x	209 x	210 x
42	224 x	224 x	223 x	224 x

Table 3.2.20: Profile matching for launch cruise (*Discovery* 223).

Float	Stations
77	12995-7
78	12995-6
79	13002
80	12997-9

Table 3.3: Results of calculating salinity offsets (sal.C = sal.F + offset) by comparing groups of float and ship profiles. In some cases, results of repeat calculations are shown where the matching group of ship CTD profiles was varied.

Float	Cycles	Cruise	Stations	Offset
77	1	223	12995-7	+0.015
77	20-23	230	82-87	+0.008
77	20-23	230	84-87	+0.010
77	20-21	151	100-103	+0.019
77	20-21	151	100-102	+0.021
77	19-23	394	98-103	+0.019
77	19-23	394	98-101	+0.015
78	1	223	12995-6	-0.028
78	15	151	84-85	-0.019
79	1	223	13002	-0.029
79	1-5	147	47-50	-0.028
79	1-5	147	47,49,50	-0.031
79	25-27	154	74-77	-0.035
80	1	223	12997-12999	+0.013
80	19-21	230	79-85	-0.018
80	16-21	151	103-108	-0.013
80	19-25	394	95-101	-0.011
80	16-17	394	35-39	-0.008

Tables 3.4: The following tables show all comparisons made between profile pairs from floats 77–80. The format is the same as that of Tables 3.2, except that the top left box contains two float numbers, the upper of which refers to the cycle numbers in the top row, the lower to the cycle number in the left column.

Table 3.4.1: Floats 77 and 78

78 77	02
03	*14* *126.6*

Table 3.4.2: Floats 77 and 80

80 77	01	03
02	*14* *43.8*	*-14* *28.6*
03	*28* *72.9*	*0* *71.1*
04	*42* *29.2*	*14* *42.1*

Table 3.4.3: Floats 78 and 79

79 78	30	31	32	33
28	*-28* *45.0*	*-42* *34.9*	*-56* *108.2*	-70 214.6
29	*-14* *56.6*	*-28* *9.8*	*-42* *85.2*	-56 203.1
33	*42* *123.0*	*28* *162.3*	*14* *78.2*	*0* *51.2*

Table 3.4.4: Floats 79 and 80

80 79	9	10	11
11	*28* *105.7*	*14* *58.6*	*0* *70.0*
12	*42* *58.9*	*28* *178.2*	*14* *193.2*
13	*56* *95.6*	*42* *80.5*	*28* *85.2*

Table 3.5: Float – float relative salinity offsets, calculated as Float.1 = Float.2 + Offset.

Float.1	Cycles.1	Float.2	Cycles.2	Offset
77	3	78	2	+0.051
77	2-4	80	1	+0.011
77	2-4	80	3	+0.032
78	28,29,33	79	30-32	+0.012
79	11-13	80	9-11	-0.029

Table 4.1: Average θ / S statistics for all four floats and three section segments

Data	potential temperature	number	mean salinity	standard error
Float 77	2.675	0		
	2.725	0		
	2.775	3	34.8588	0.0155
	2.825	35	34.8491	0.0012
	2.875	66	34.8528	0.0008
	2.925	45	34.8561	0.0008
	2.975	53	34.8592	0.0006
	3.025	49	34.8637	0.0007
	3.075	45	34.8654	0.001
Float 78	2.675	0		
	2.725	1		
	2.775	3	34.8486	0.0012
	2.825	22	34.8533	0.0015
	2.875	46	34.857	0.0008
	2.925	65	34.8607	0.0008
	2.975	57	34.8652	0.0008
	3.025	53	34.8696	0.0008
	3.075	54	34.8712	0.0009
Float 79	2.675	6	34.8268	0.0019
	2.725	7	34.8342	0.0031
	2.775	19	34.8434	0.0012
	2.825	60	34.8499	0.0009
	2.875	61	34.8552	0.0009
	2.925	68	34.8579	0.0009
	2.975	52	34.8614	0.0011
	3.025	47	34.8638	0.0014
	3.075	39	34.8621	0.0022
Float 80	2.675	0		
	2.725	0		
	2.775	1		
	2.825	28	34.8456	0.0009
	2.875	61	34.8505	0.0009
	2.925	72	34.8516	0.0007
	2.975	64	34.8501	0.0018
	3.025	66	34.8522	0.0022
	3.075	67	34.8513	0.0023

Table 4.1 continued

Data	potential temperature	number	mean salinity	standard error
D230 South-east Irminger Basin	2.675	0		
	2.725	0		
	2.775	0		
	2.825	0		
	2.875	41	34.8497	0.0002
	2.925	195	34.8524	0.0002
	2.975	207	34.8541	0.0003
	3.025	240	34.8586	0.0004
	3.075	243	34.8606	0.0005
D230 West Irminger Basin to Cape Farewell	2.675	0		
	2.725	0		
	2.775	1		
	2.825	246	34.8432	0.0002
	2.875	427	34.8466	0.0001
	2.925	379	34.8486	0.0001
	2.975	261	34.8539	0.0003
	3.025	248	34.8578	0.0003
	3.075	332	34.8612	0.0003
D230 North-west Irminger Basin	2.675	0		
	2.725	0		
	2.775	0		
	2.825	0		
	2.875	13	34.8617	0.0002
	2.925	149	34.8532	0.0004
	2.975	184	34.8538	0.0002
	3.025	155	34.8583	0.0002
	3.075	186	34.8627	0.0002

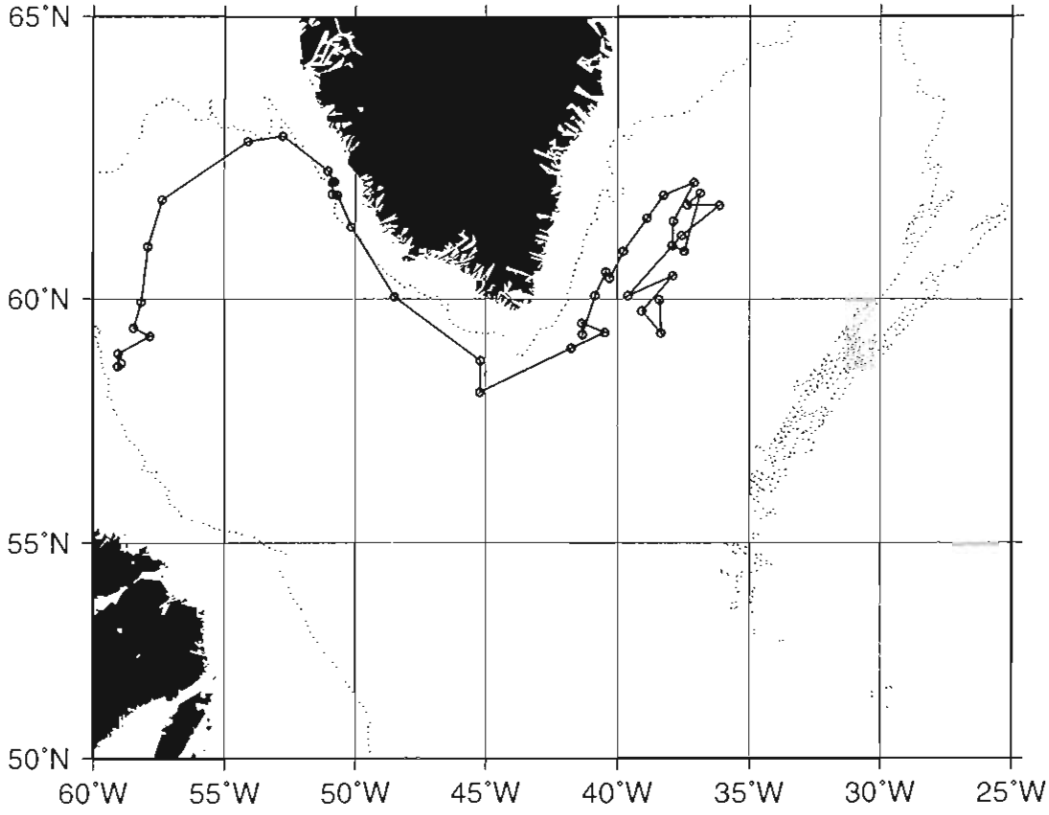

Figure 2.1: Float 77 trajectory. This and all subsequent charts show the 1500 m isobath.

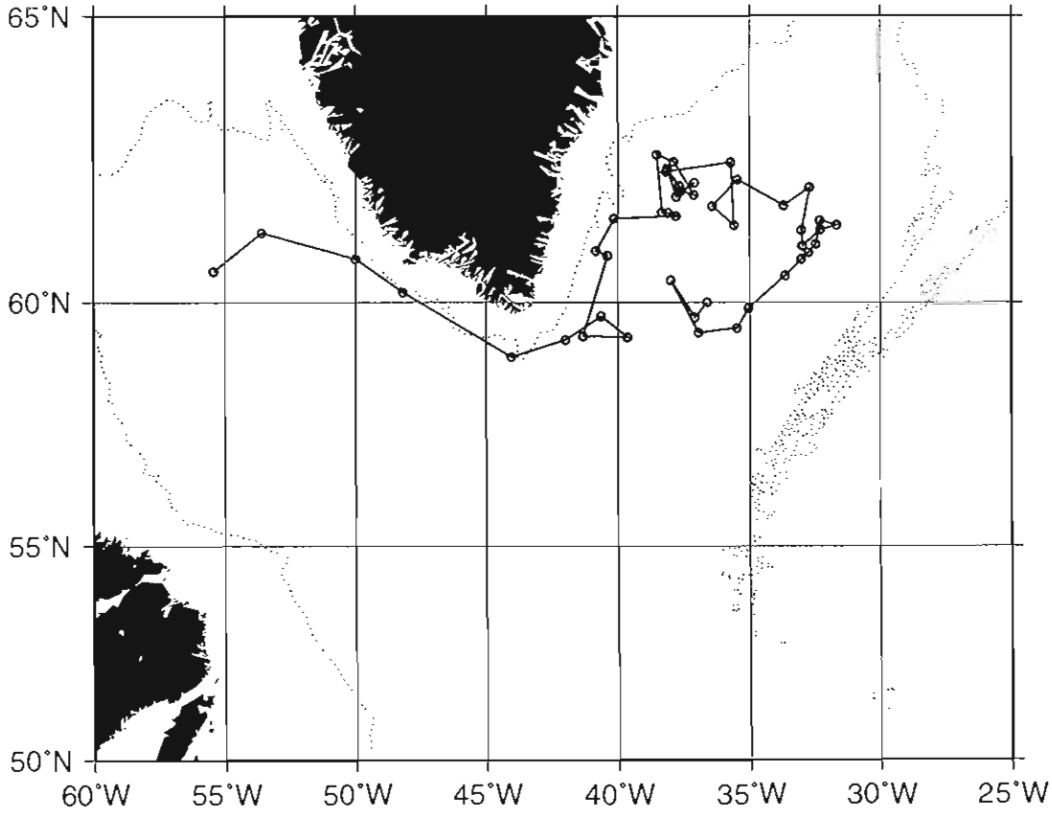

Figure 2.2: Float 78 trajectory

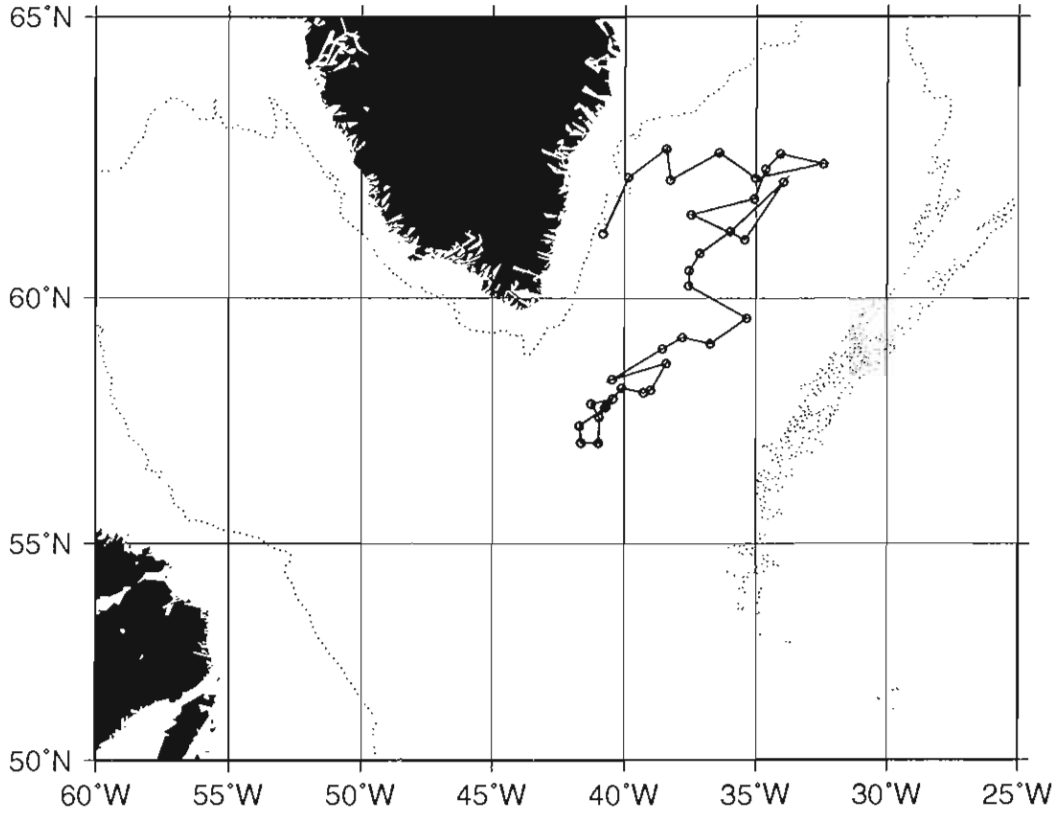

Figure 2.3: Float 79 trajectory

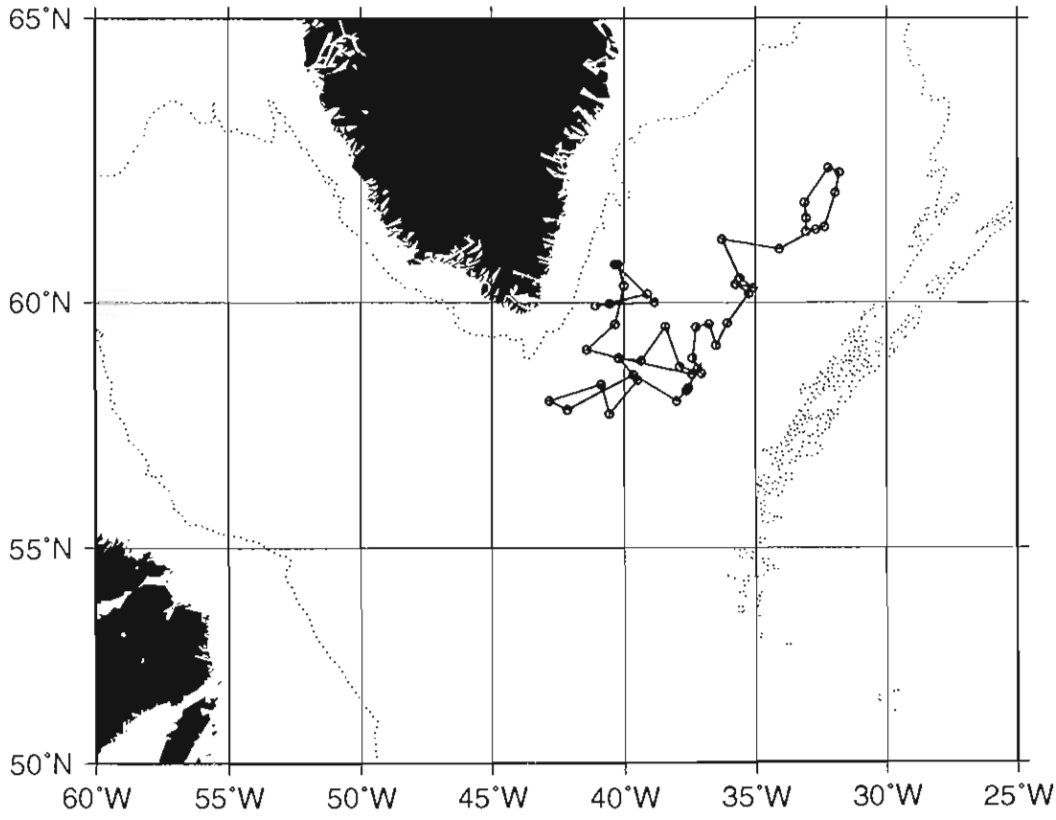

Figure 2.4: Float 80 trajectory

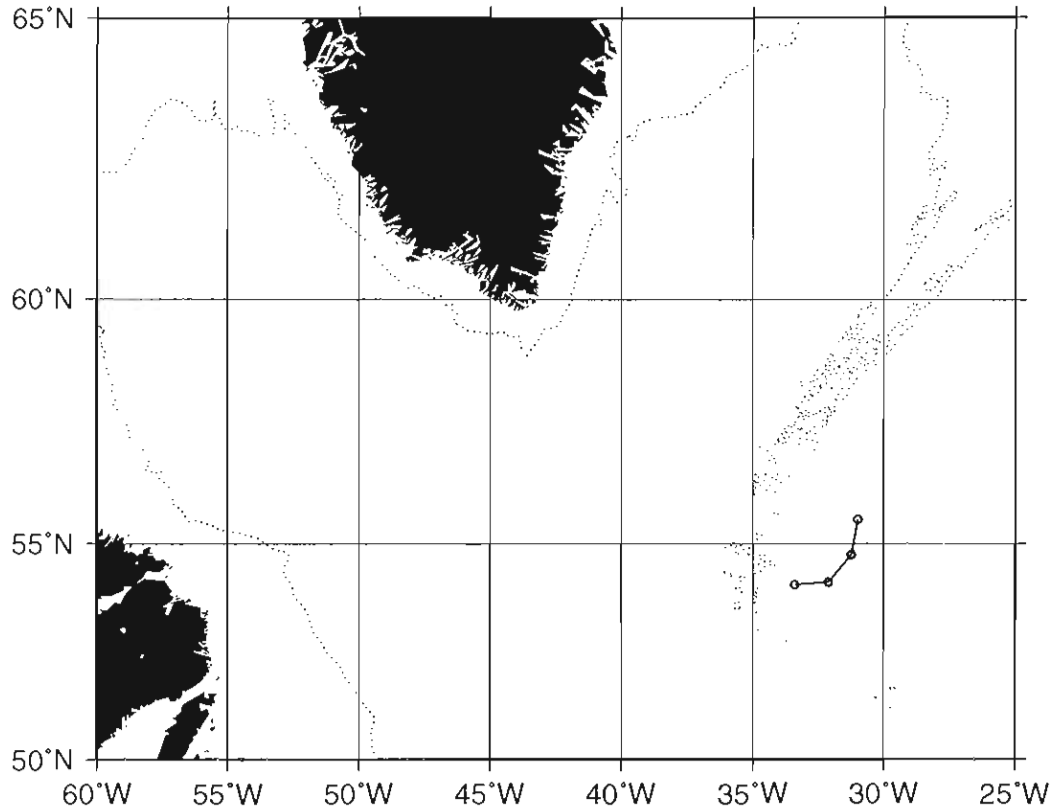

Figure 2.5: Float 81 trajectory

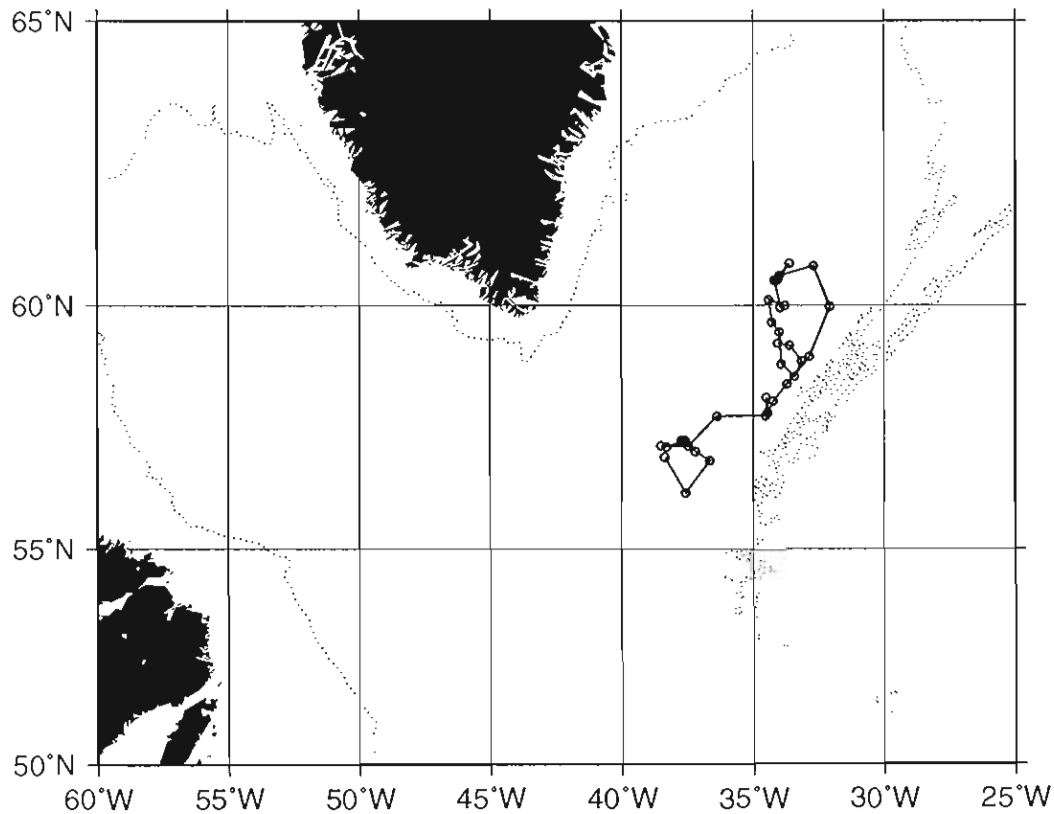

Figure 2.6: Float 82 trajectory

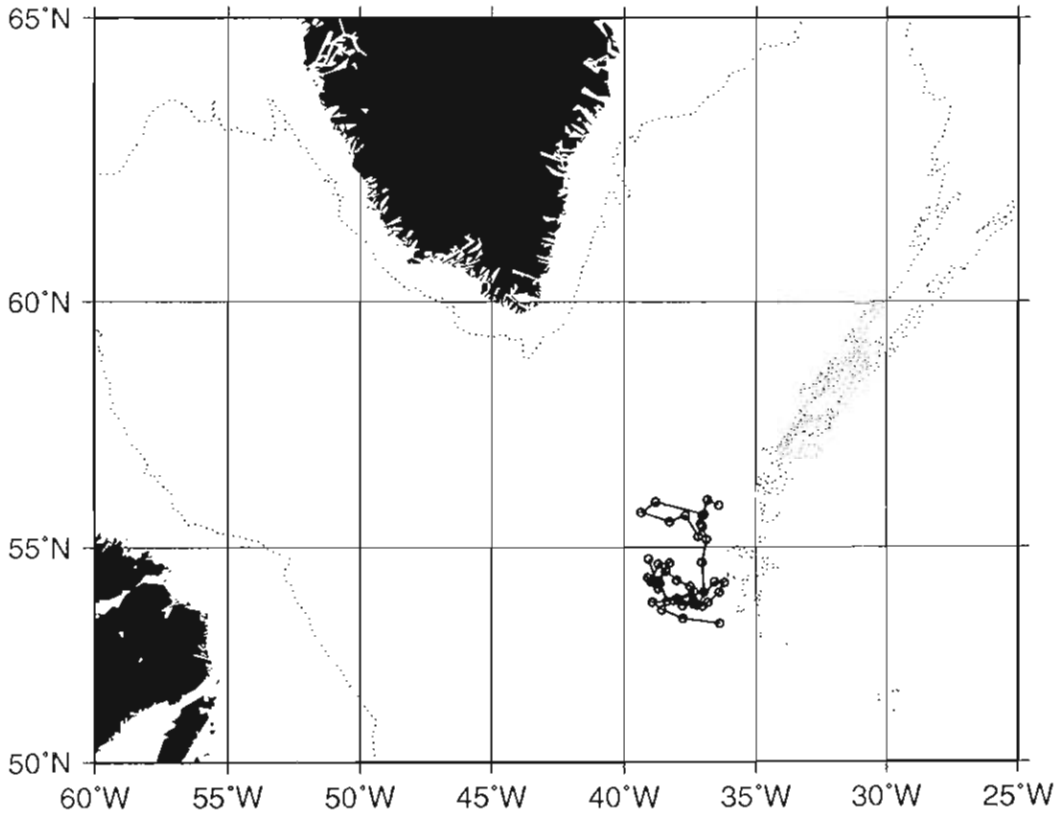

Figure 2.7: Float 83 trajectory

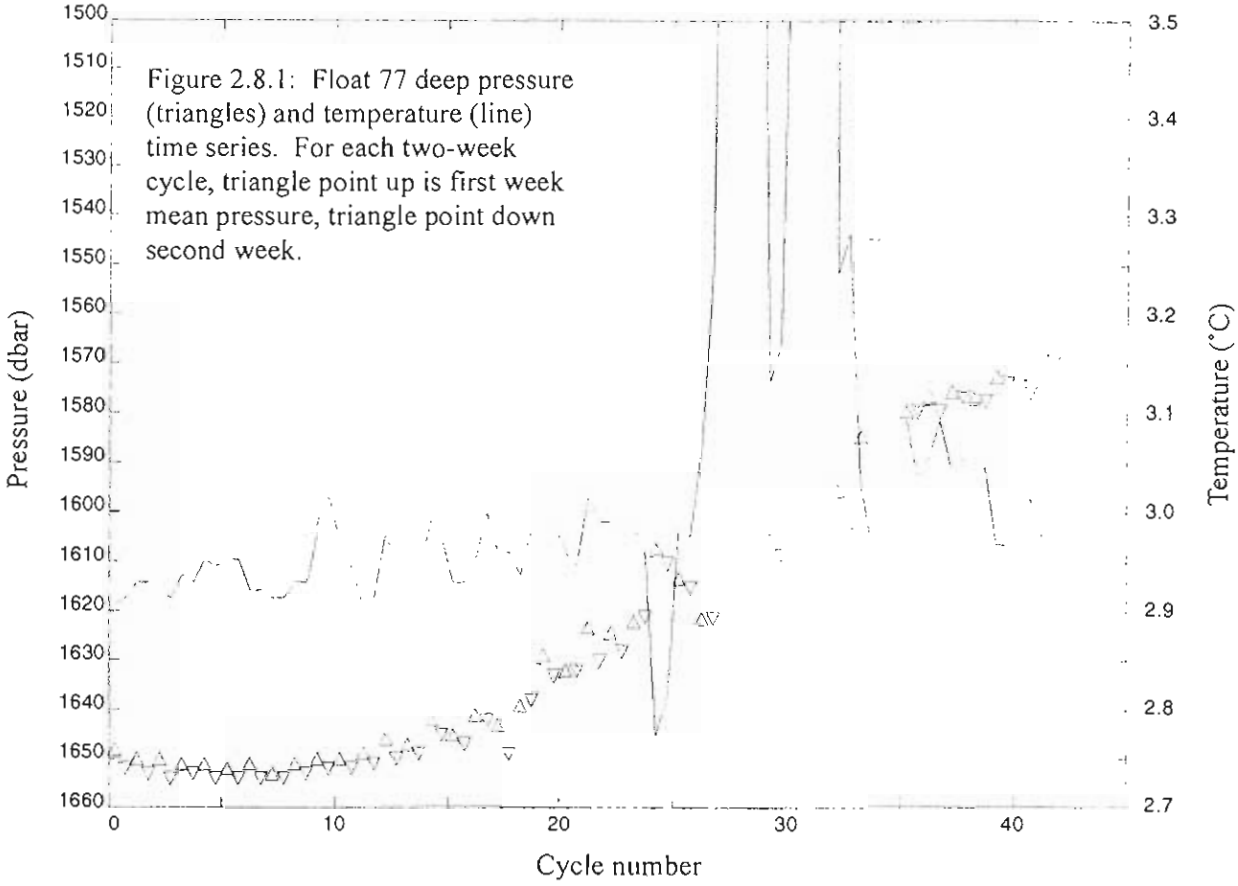

Figure 2.8.1: Float 77 deep pressure (triangles) and temperature (line) time series. For each two-week cycle, triangle point up is first week mean pressure, triangle point down second week.

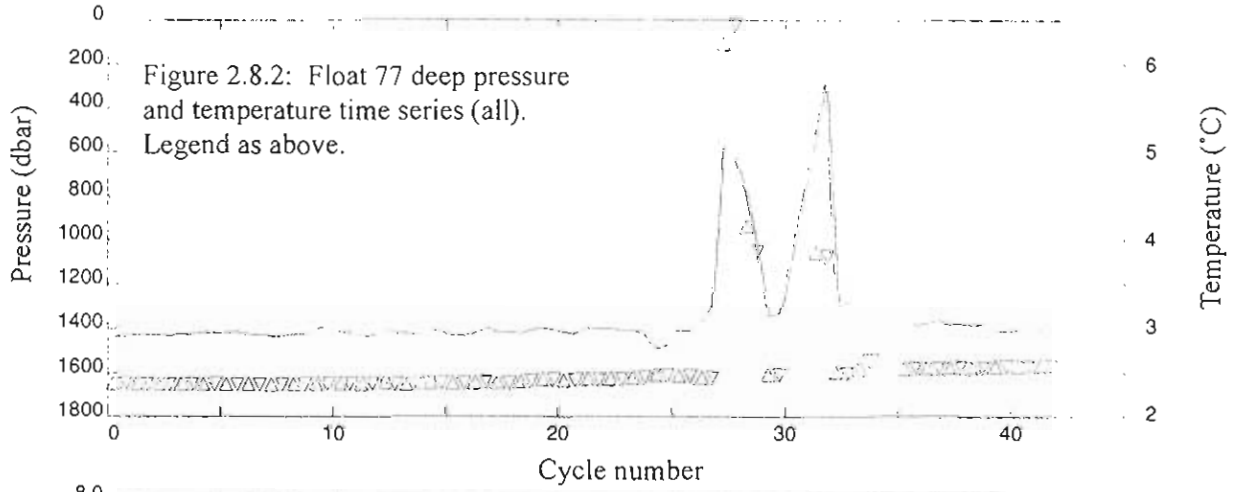

Figure 2.8.2: Float 77 deep pressure and temperature time series (all). Legend as above.

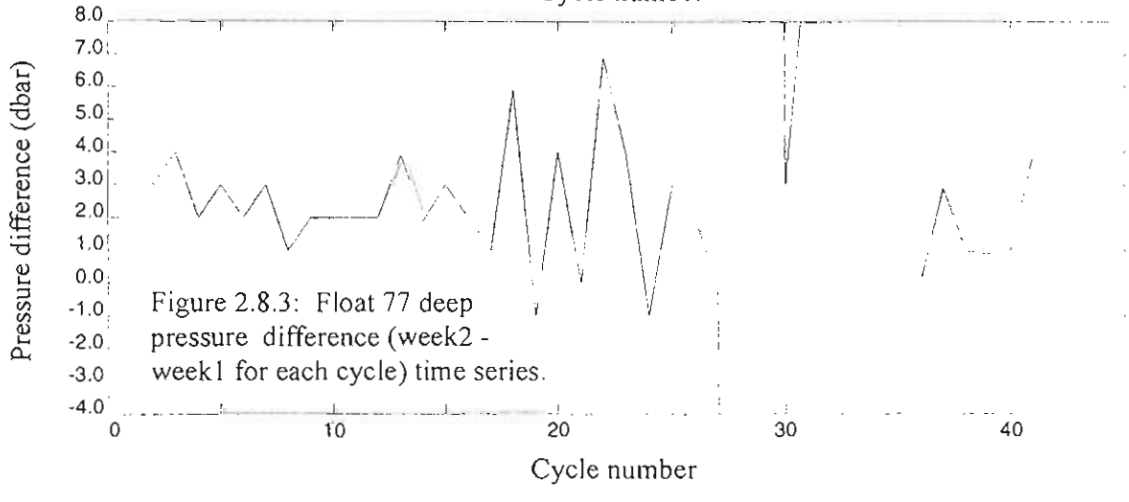

Figure 2.8.3: Float 77 deep pressure difference (week2 - week1 for each cycle) time series.

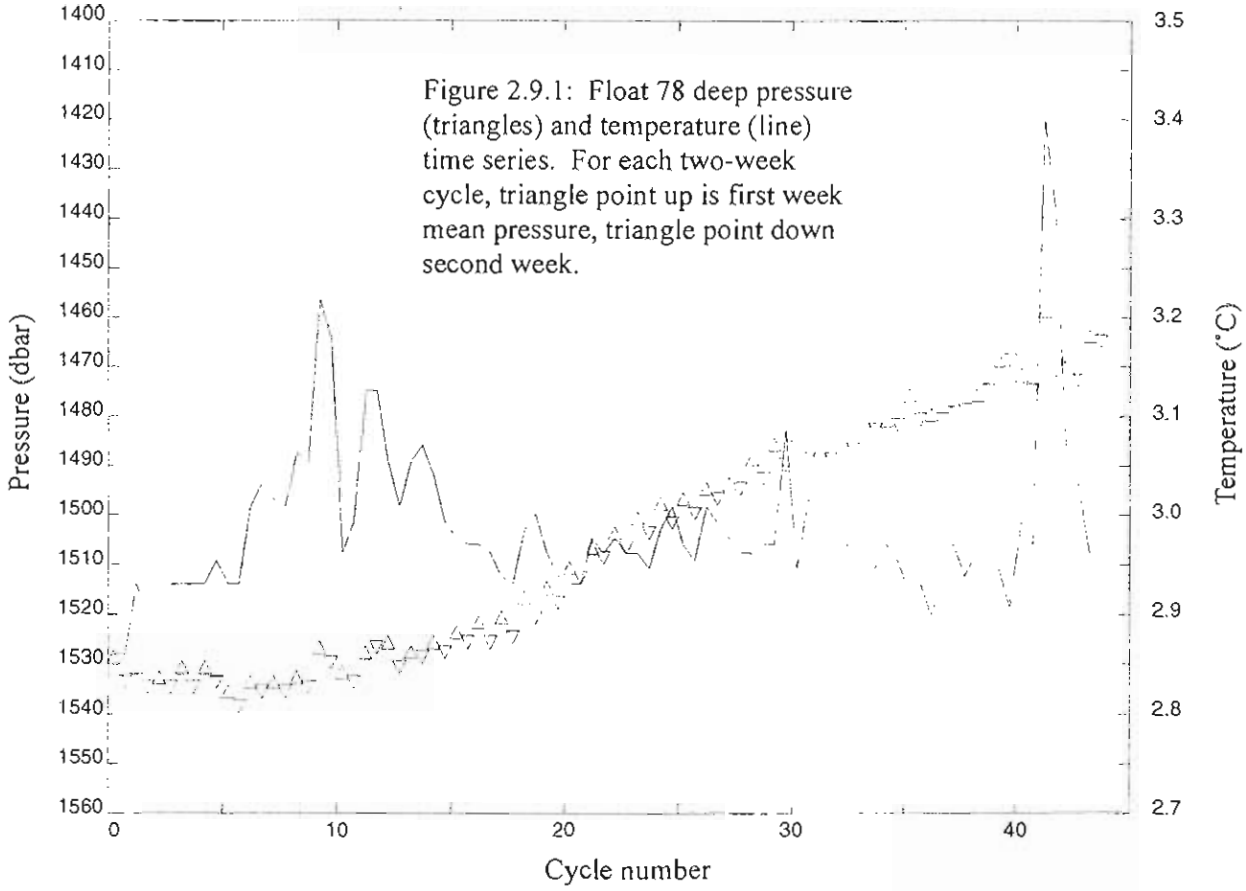

Figure 2.9.1: Float 78 deep pressure (triangles) and temperature (line) time series. For each two-week cycle, triangle point up is first week mean pressure, triangle point down second week.

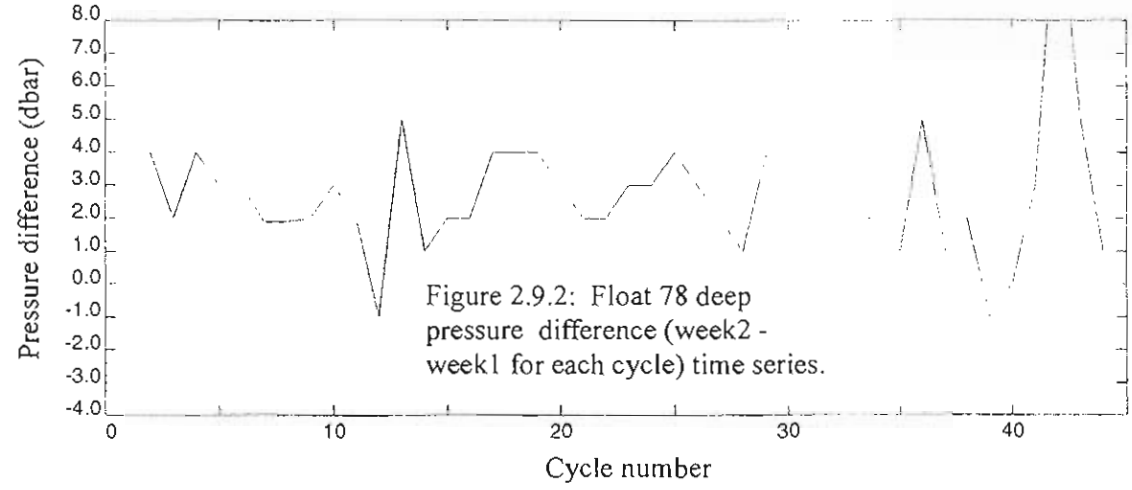

Figure 2.9.2: Float 78 deep pressure difference (week2 - week1 for each cycle) time series.

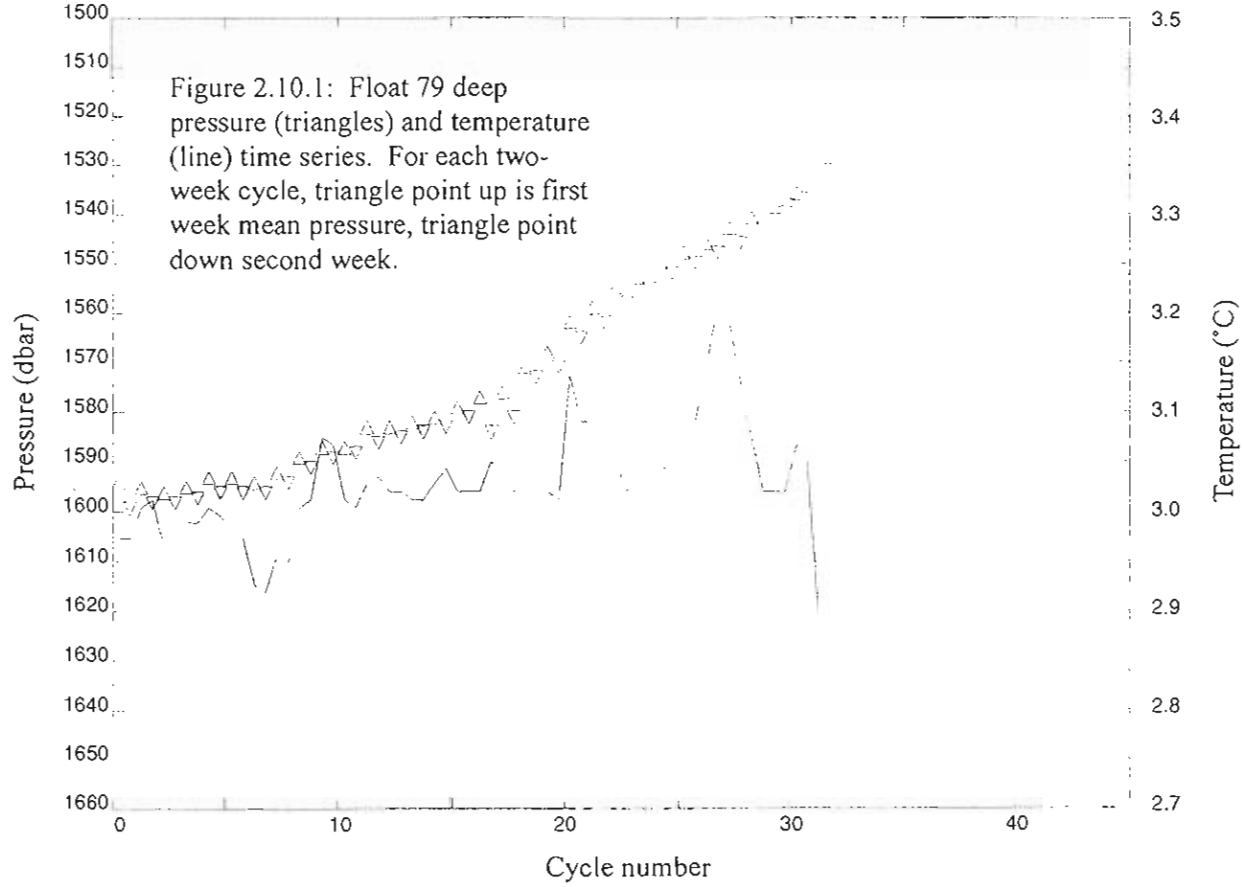

Figure 2.10.1: Float 79 deep pressure (triangles) and temperature (line) time series. For each two-week cycle, triangle point up is first week mean pressure, triangle point down second week.

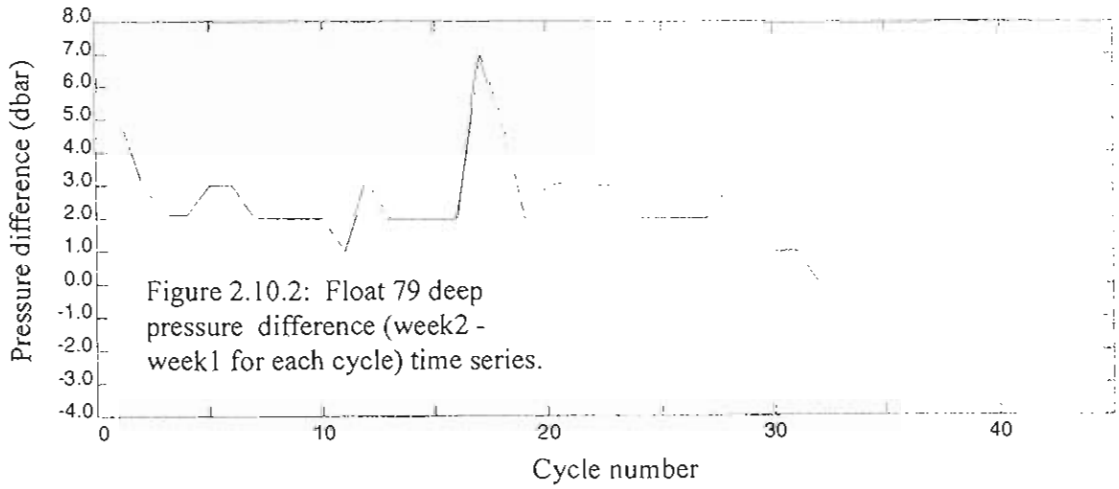

Figure 2.10.2: Float 79 deep pressure difference (week2 - week1 for each cycle) time series.

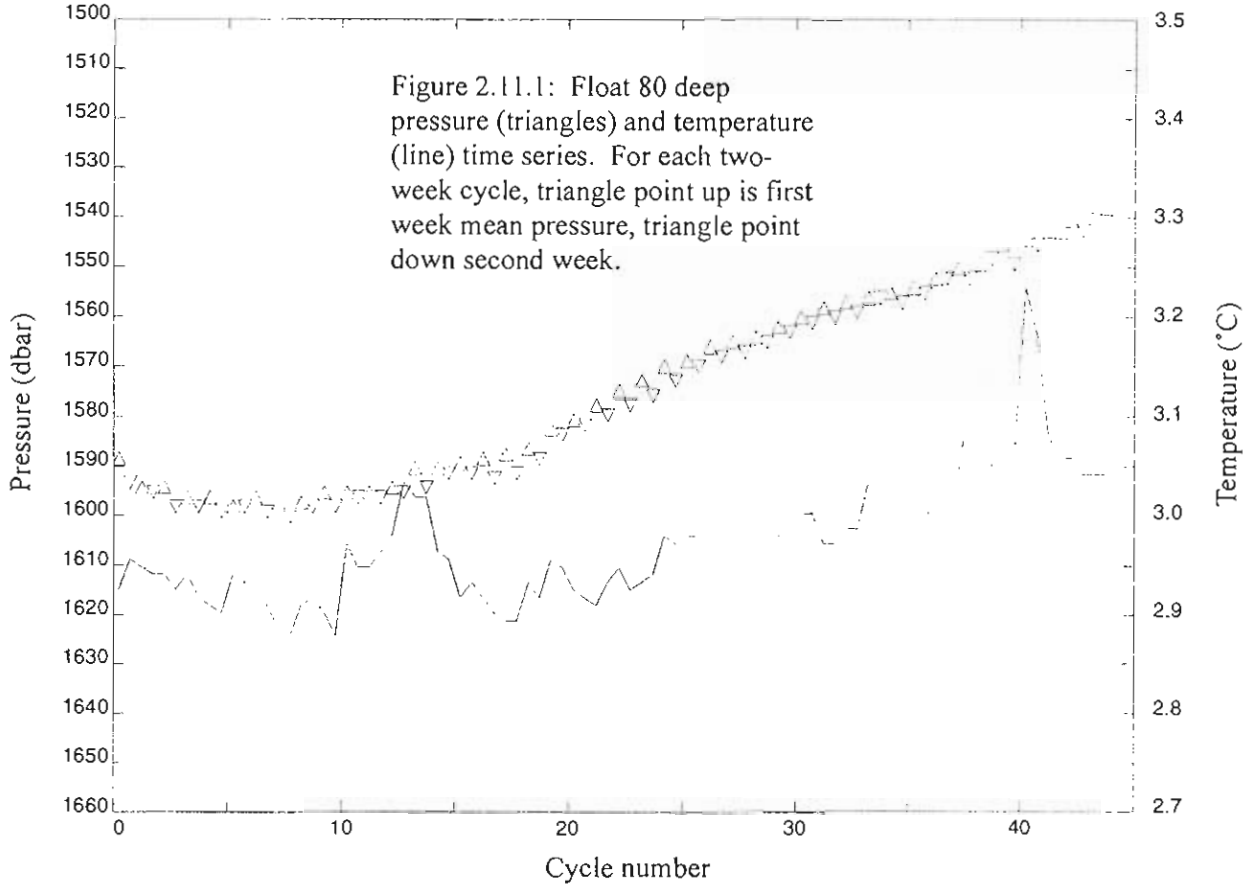

Figure 2.11.1: Float 80 deep pressure (triangles) and temperature (line) time series. For each two-week cycle, triangle point up is first week mean pressure, triangle point down second week.

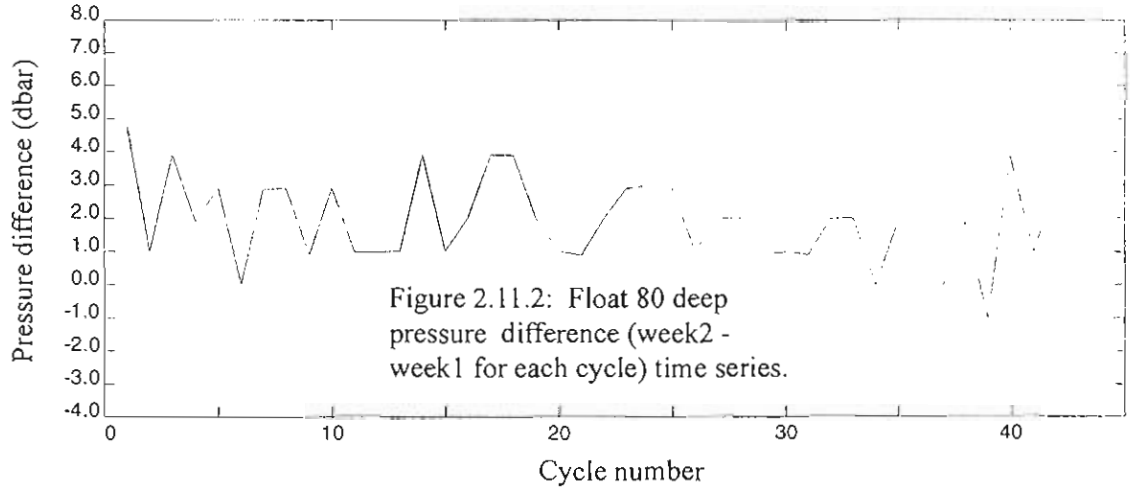

Figure 2.11.2: Float 80 deep pressure difference (week2 - week1 for each cycle) time series.

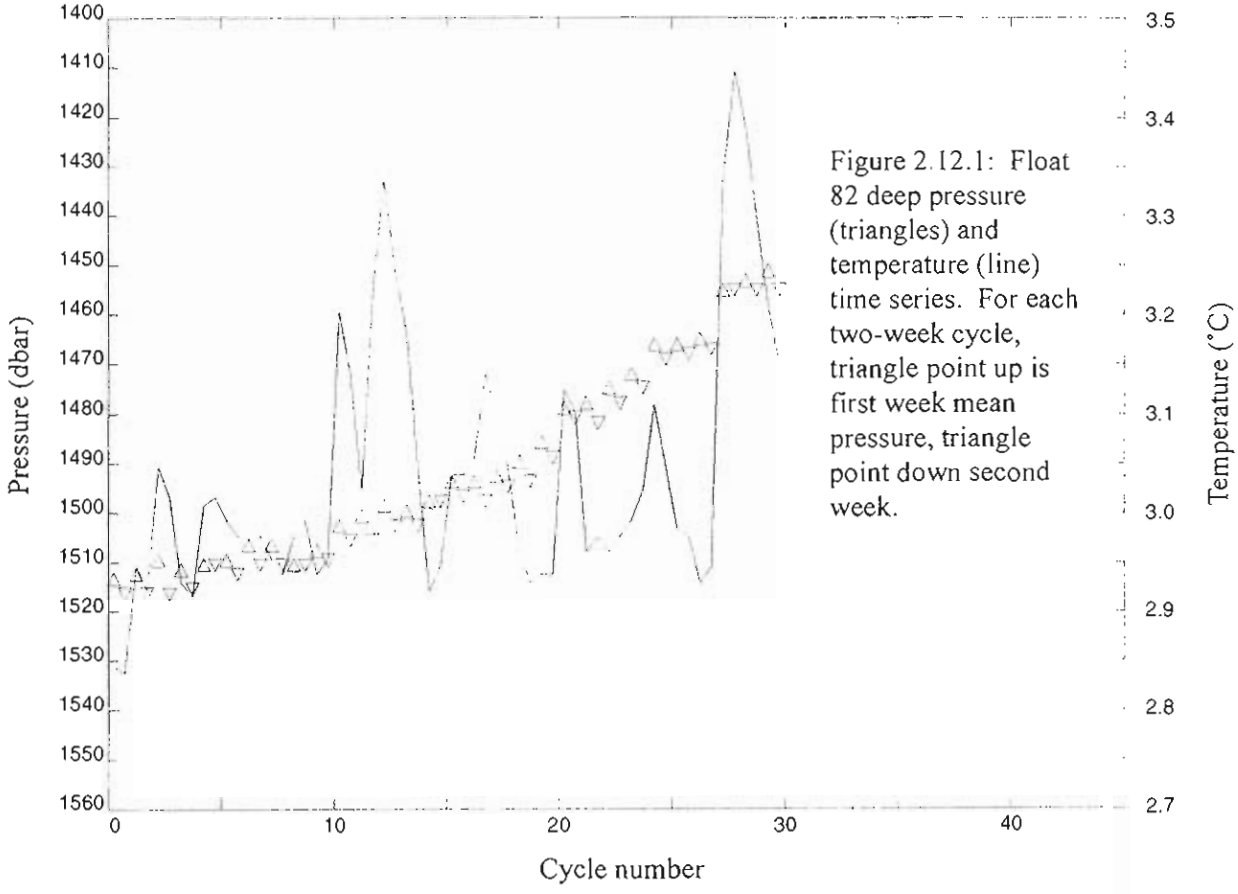

Figure 2.12.1: Float 82 deep pressure (triangles) and temperature (line) time series. For each two-week cycle, triangle point up is first week mean pressure, triangle point down second week.

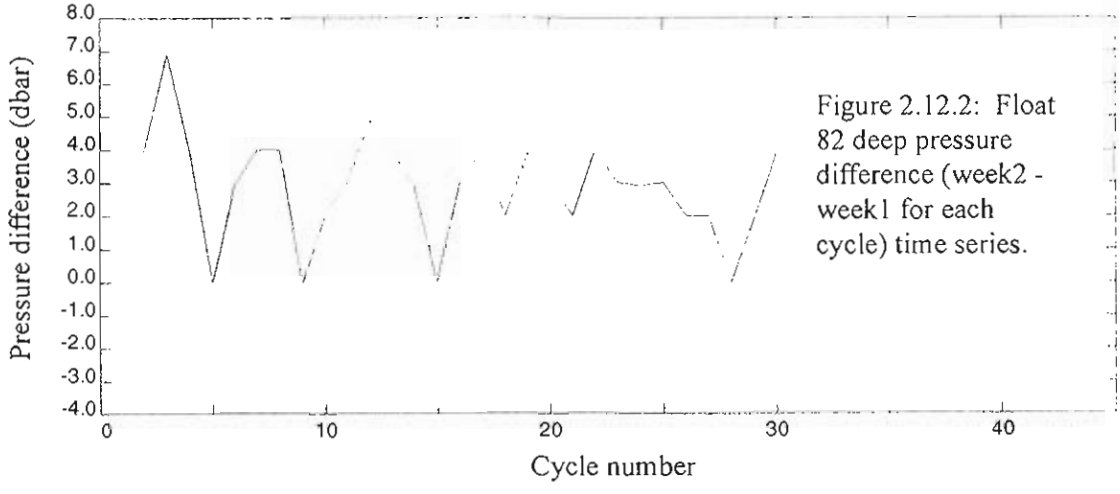

Figure 2.12.2: Float 82 deep pressure difference (week2 - week1 for each cycle) time series.

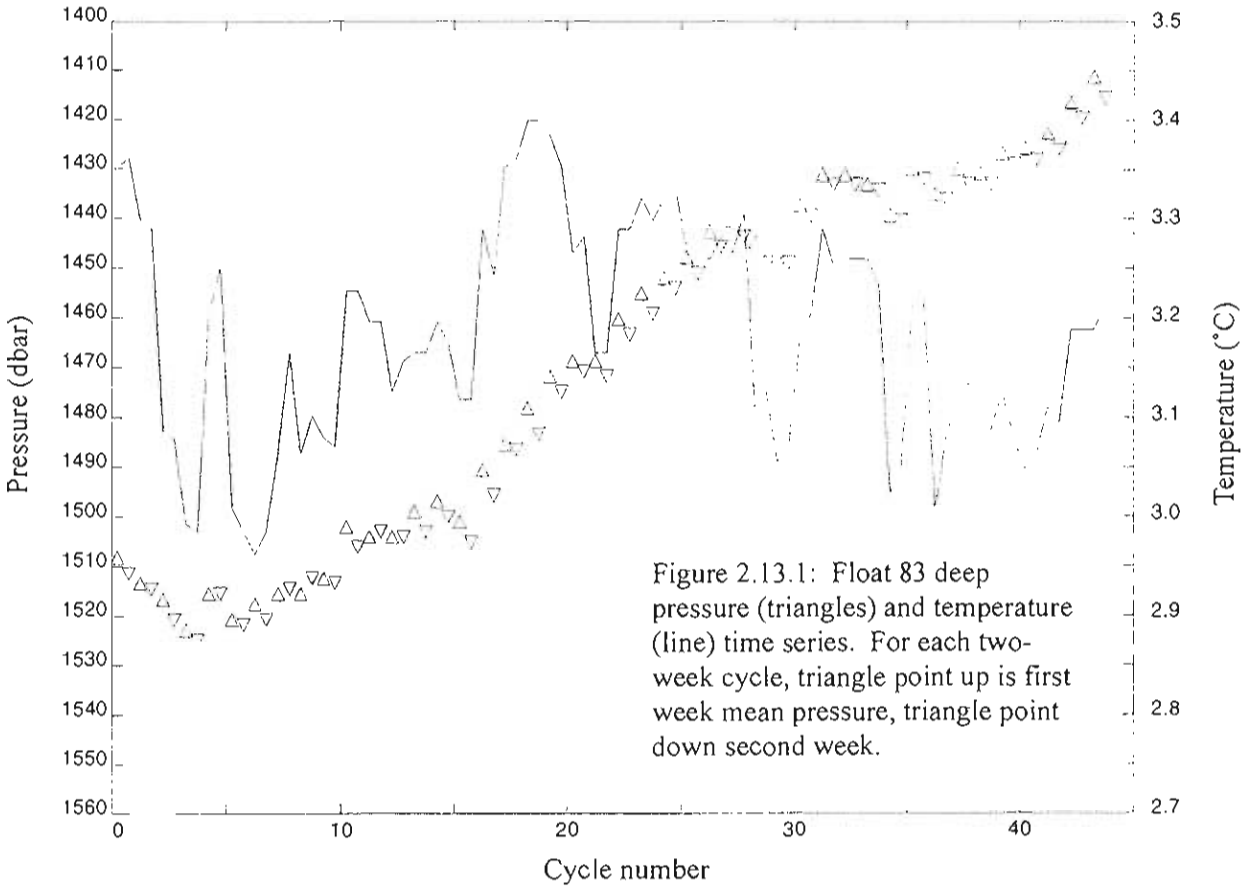

Figure 2.13.1: Float 83 deep pressure (triangles) and temperature (line) time series. For each two-week cycle, triangle point up is first week mean pressure, triangle point down second week.

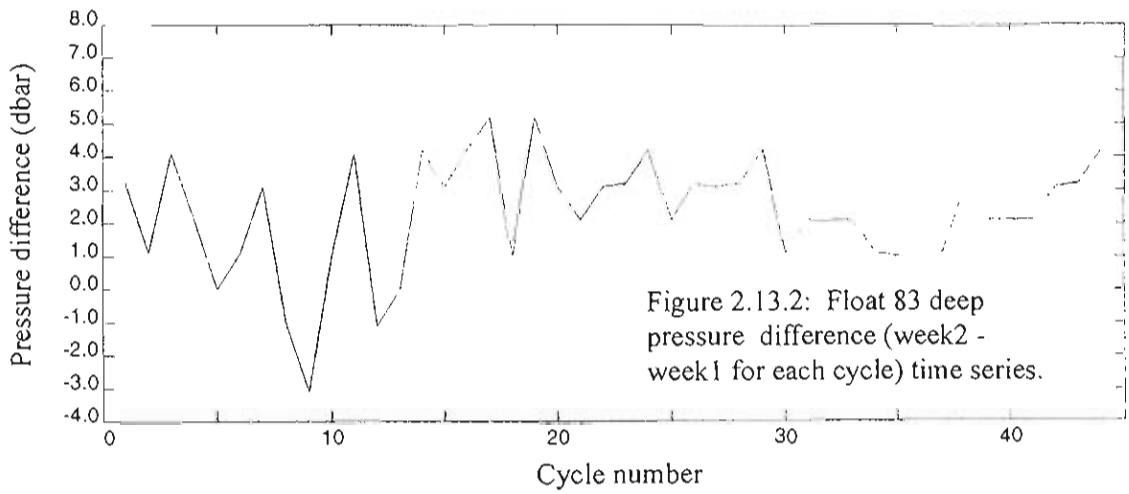

Figure 2.13.2: Float 83 deep pressure difference (week2 - week1 for each cycle) time series.

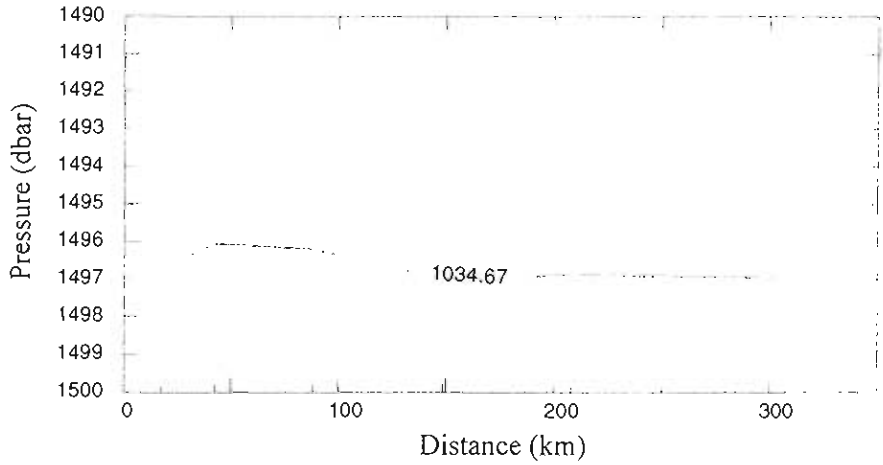

Figure 2.14: Depth of target density surface on deployment cruise (Discovery 223). Stations 12995 (right) to 13001(left) are used; see figure 3.1 for station positions.

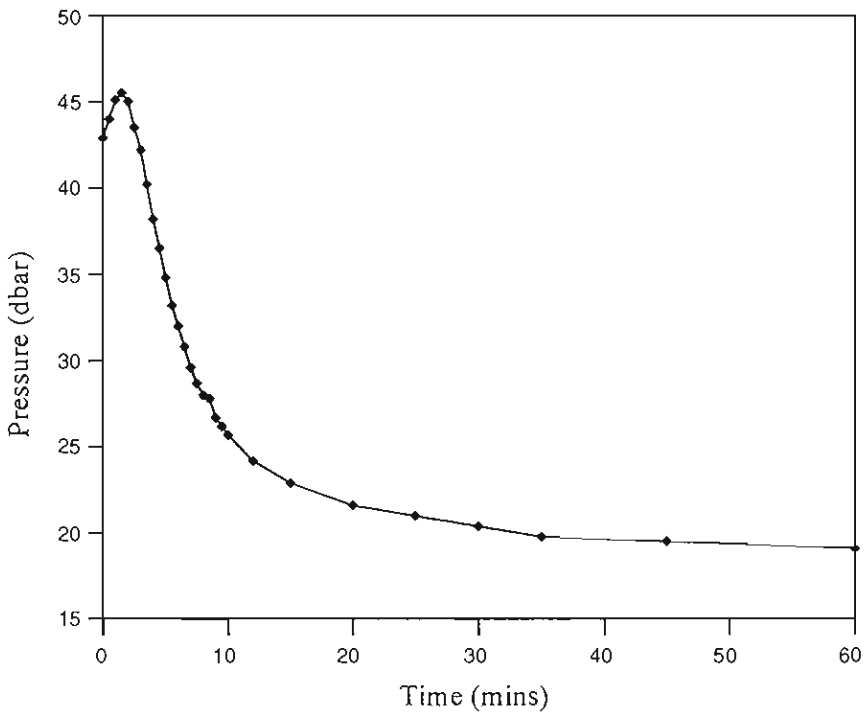

Figure 2.15: Example of measured thermal response of a pressure transducer.

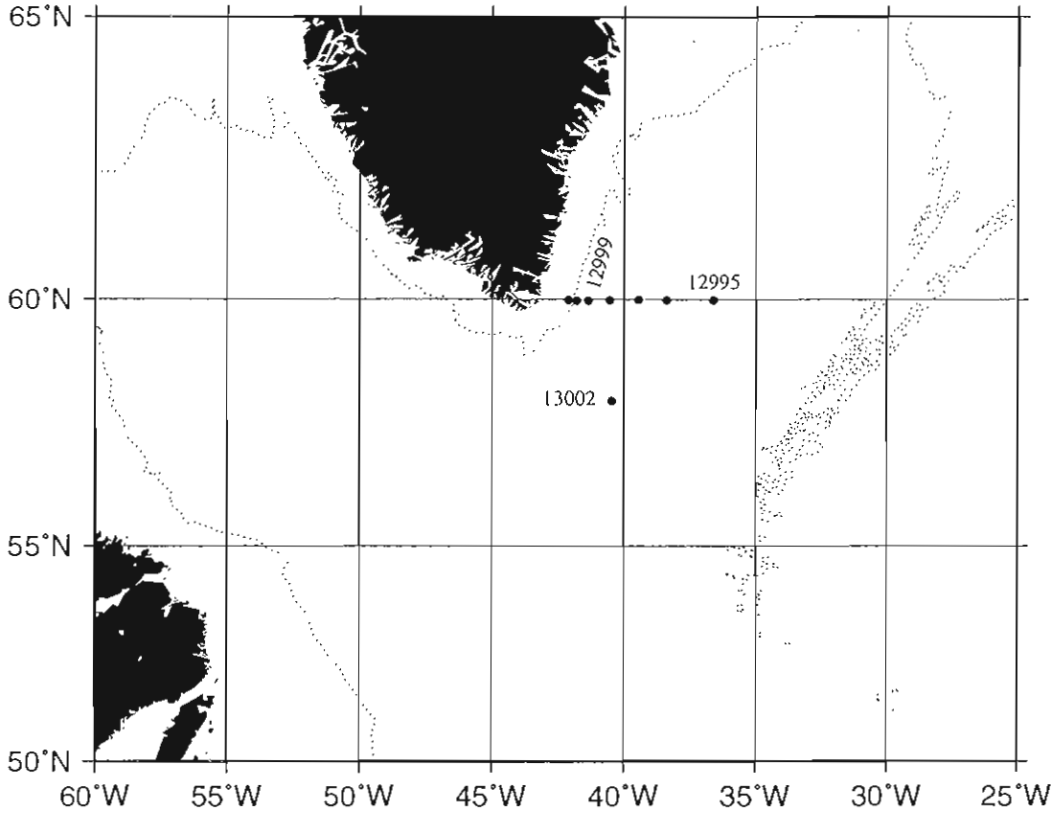

Figure 3.1: *Discovery* 223 station positions

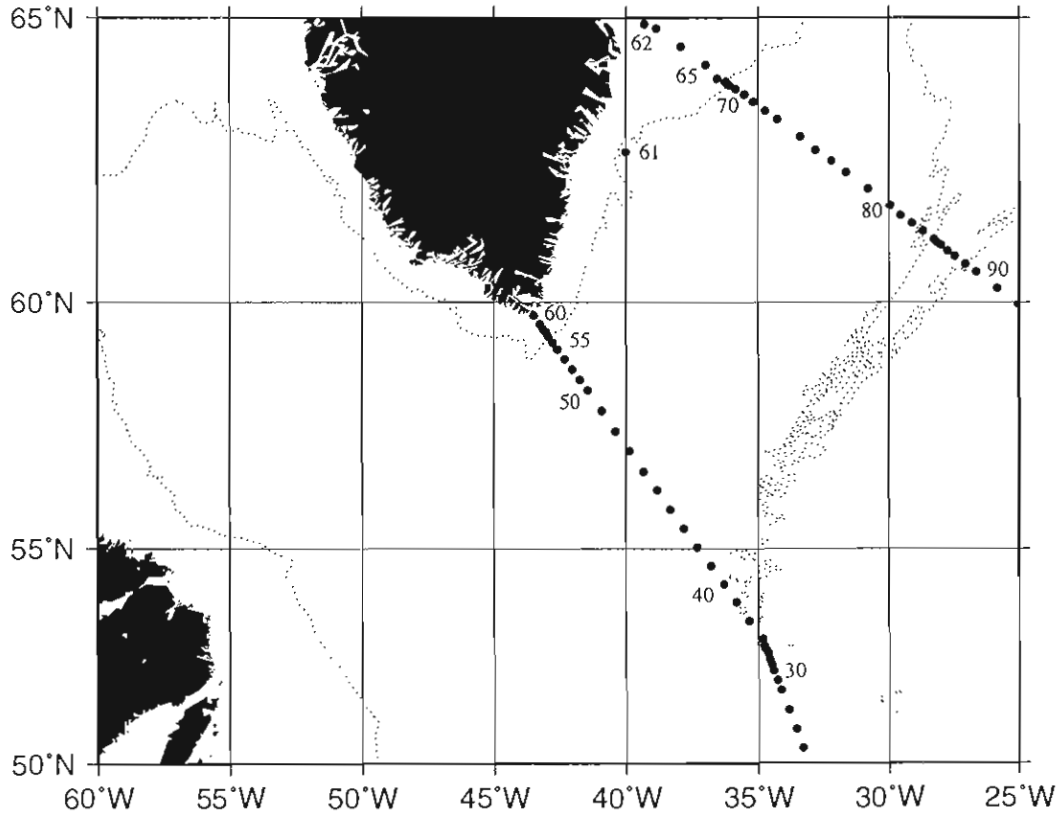

Figure 3.2: *Knorr* 147 station positions

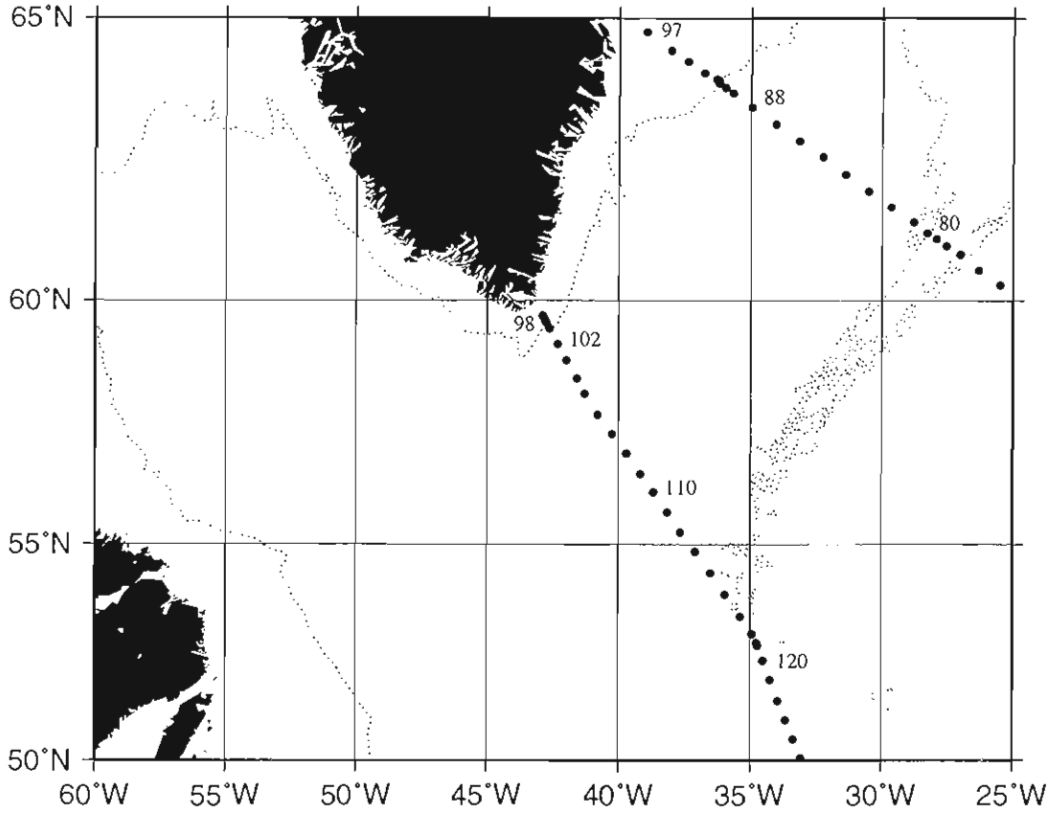

Figure 3.3: *Knorr* 151 station positions

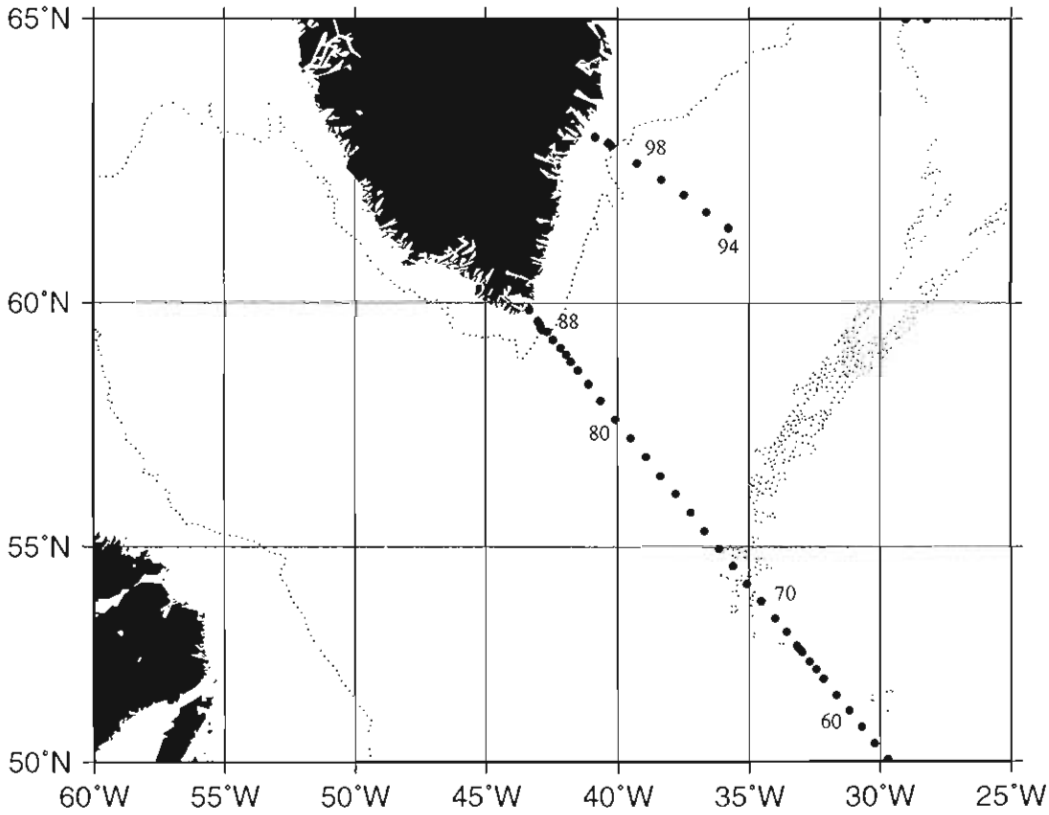

Figure 3.4: *Discovery* 230 station positions

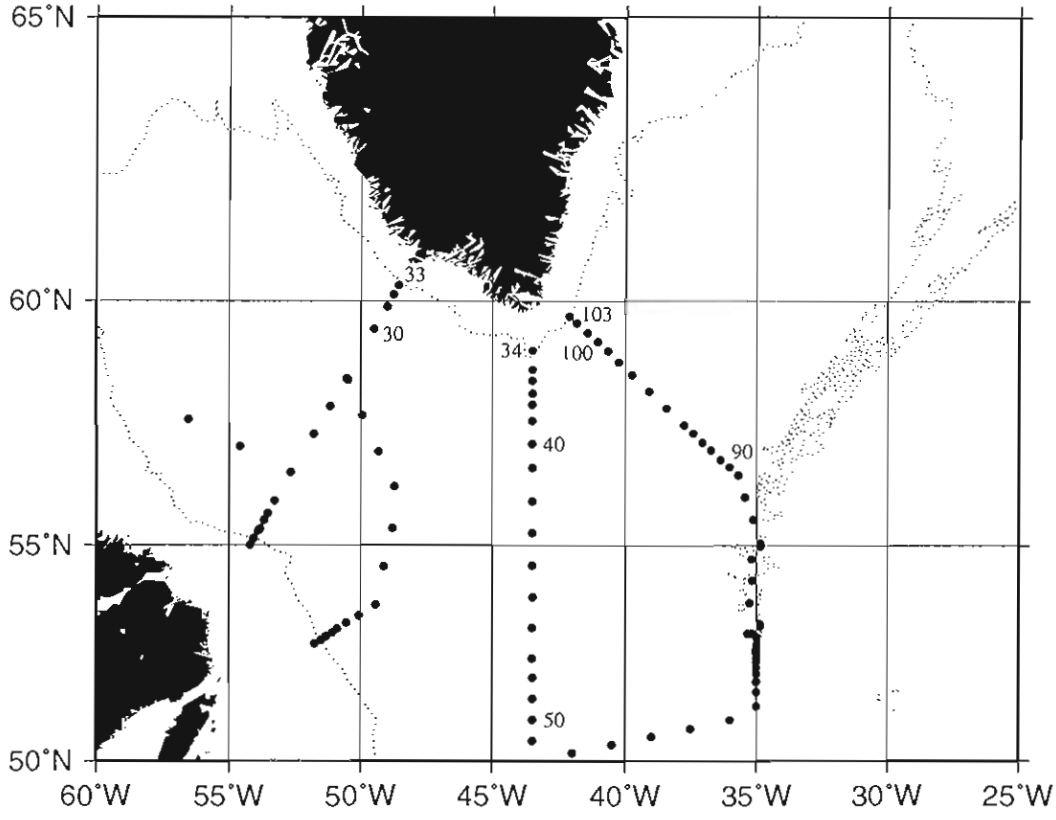

Figure 3.5: *Meteor* 39 leg 4 station positions

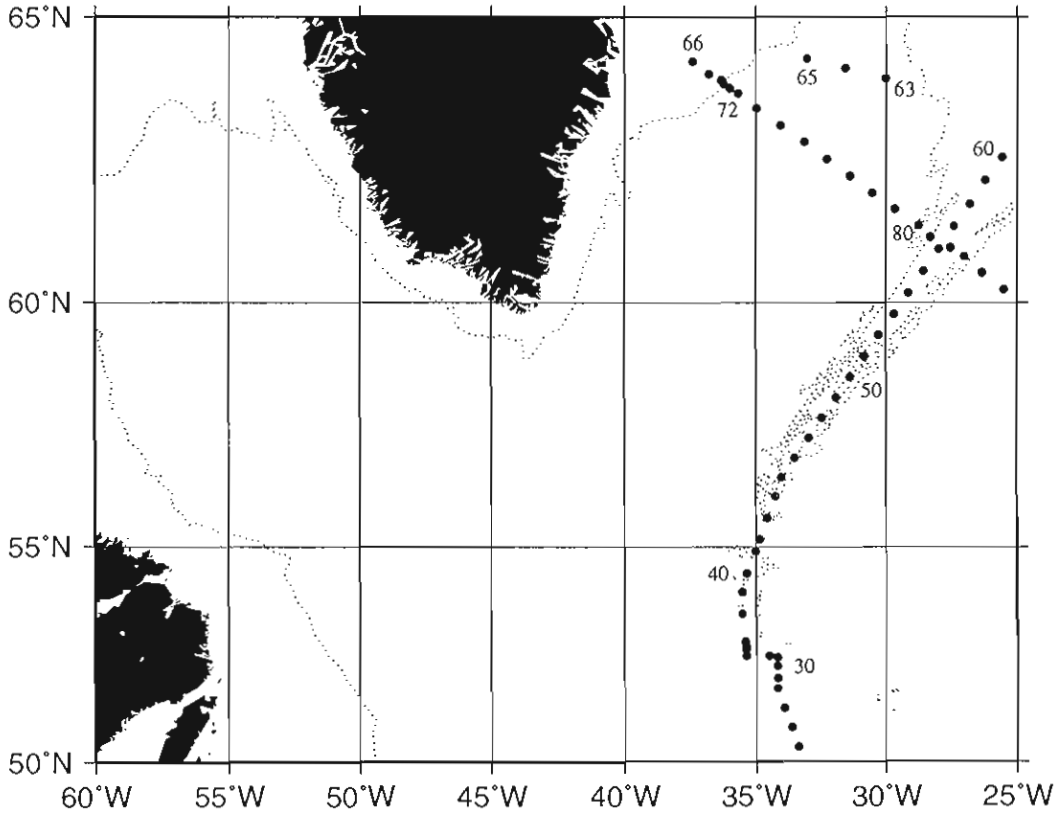

Figure 3.6: *Knorr* 154 station positions

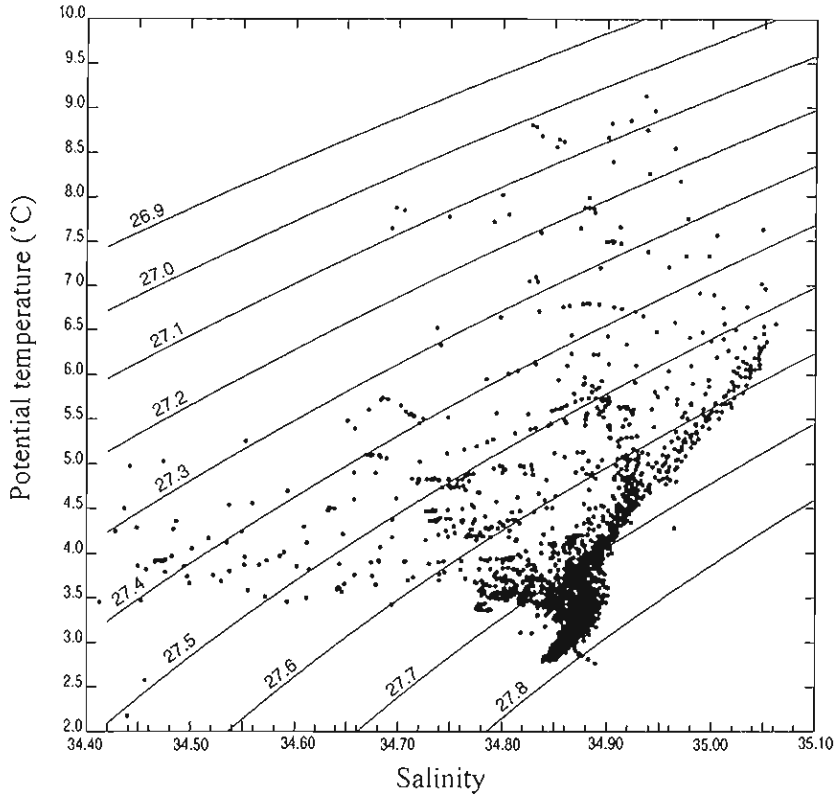

Figure 4.1.1:
Float 77
θ / S relationship,
all data.
Contours show σ_0.

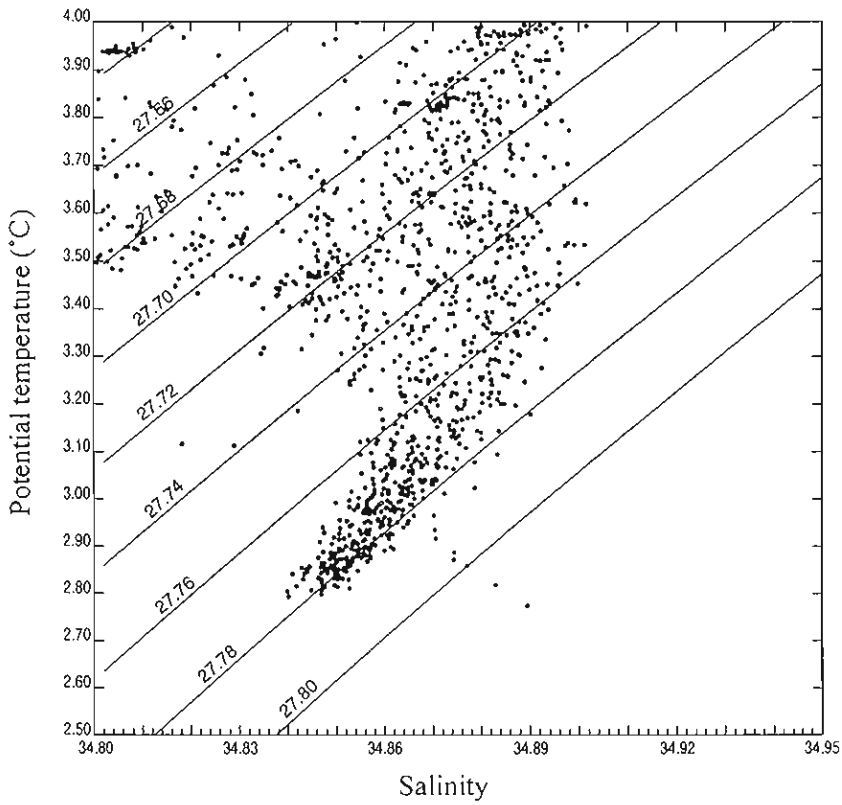

Figure 4.1.2:
Float 77
θ / S relationship,
deep data.
Contours show σ_0.

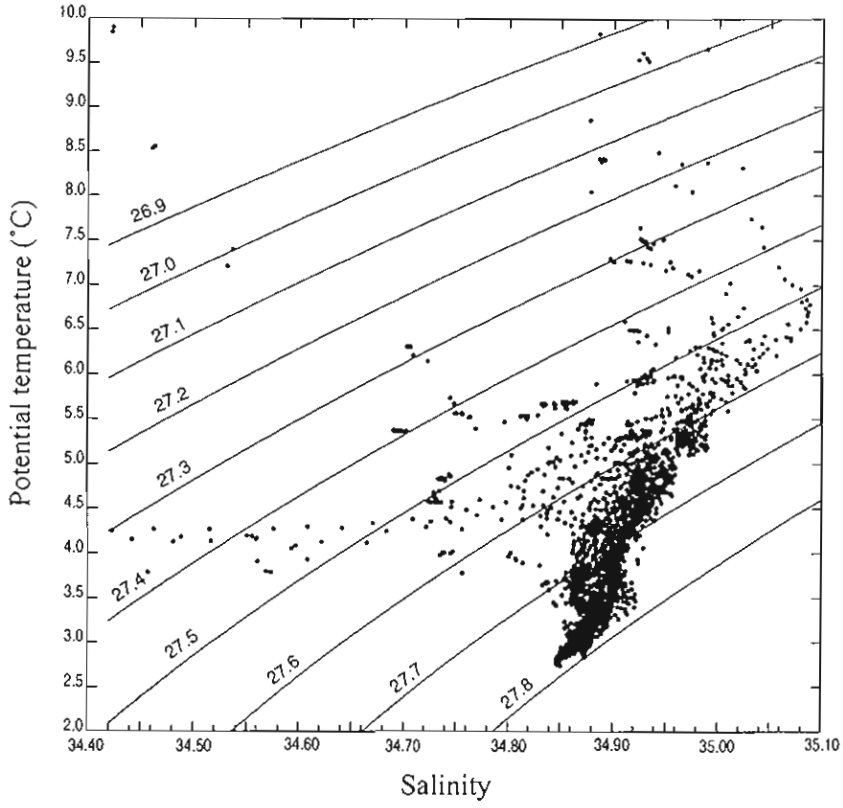

Figure 4.2.1:
Float 78
θ / S relationship,
all data.
Contours show σ_0.

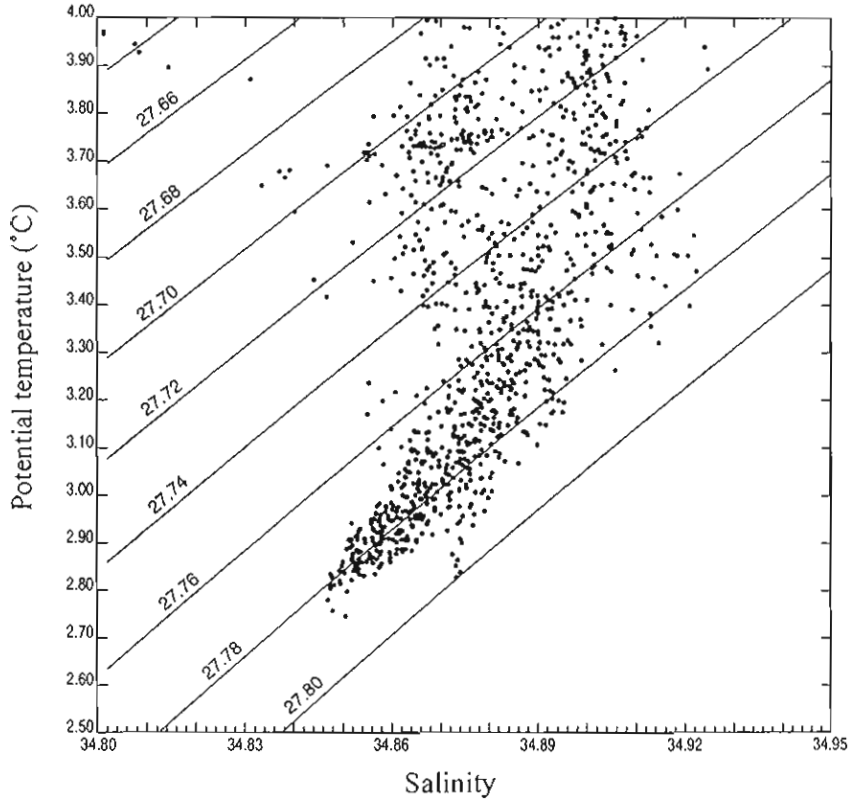

Figure 4.2.2:
Float 78
θ / S relationship,
deep data.
Contours show σ_0.

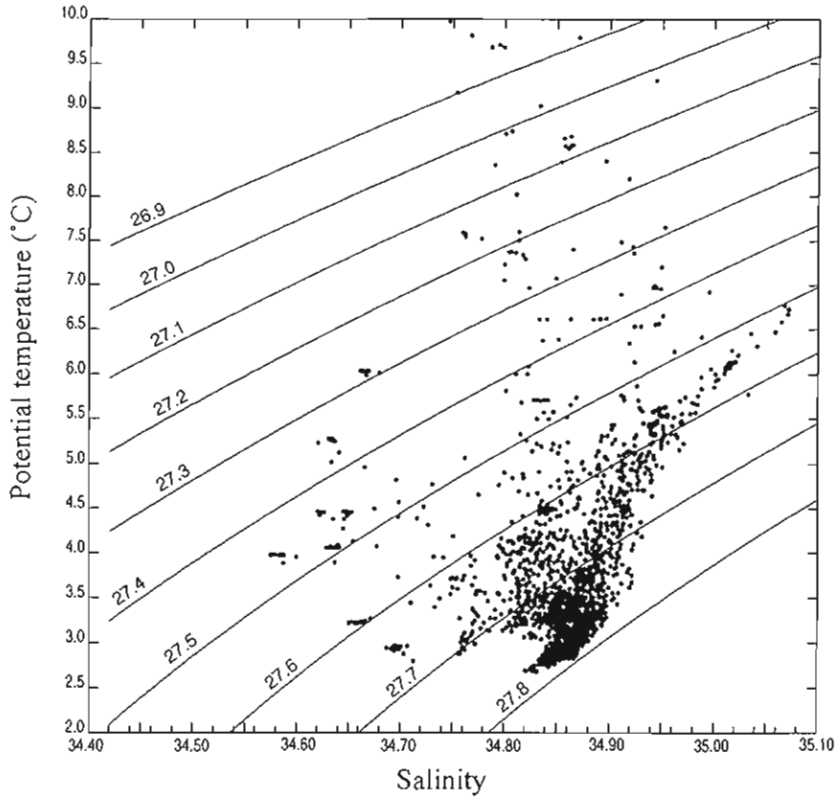

Figure 4.3.1:
Float 79
θ / S relationship,
all data.
Contours show σ_0.

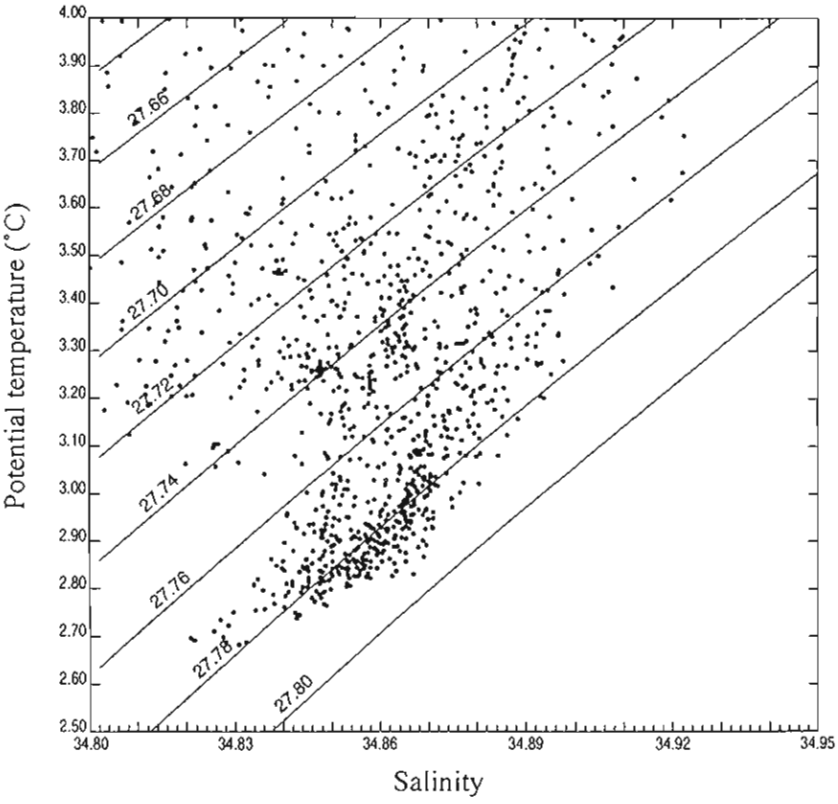

Figure 4.3.2:
Float 79
θ / S relationship,
deep data.
Contours show σ_0.

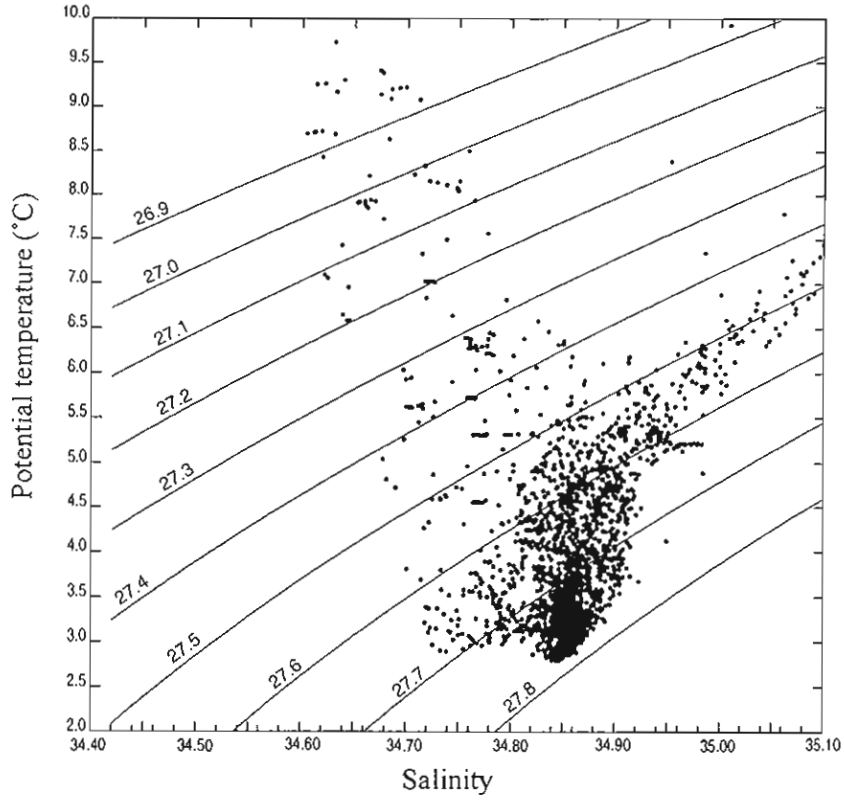

Figure 4.4.1:
Float 80
θ / S relationship,
all data.
Contours show σ_0.

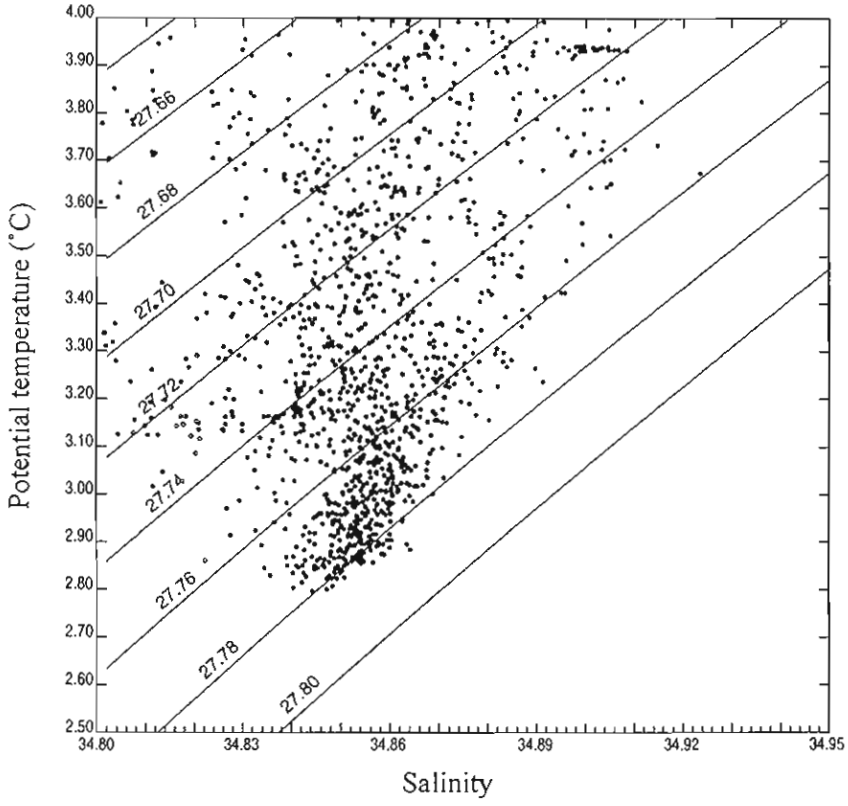

Figure 4.4.2:
Float 80
θ / S relationship,
deep data.
Contours show σ_0.

Figure 4.5.1: Float 77 salinity time series

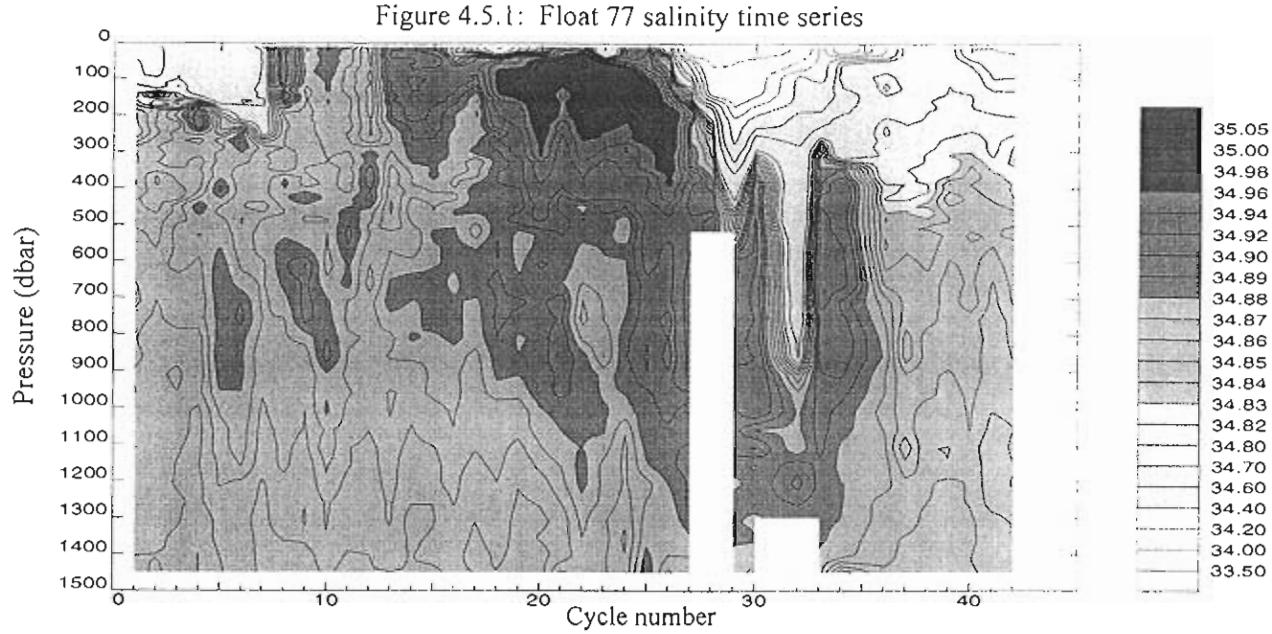

Figure 4.5.2: Float 77 potential temperature (°C) time series

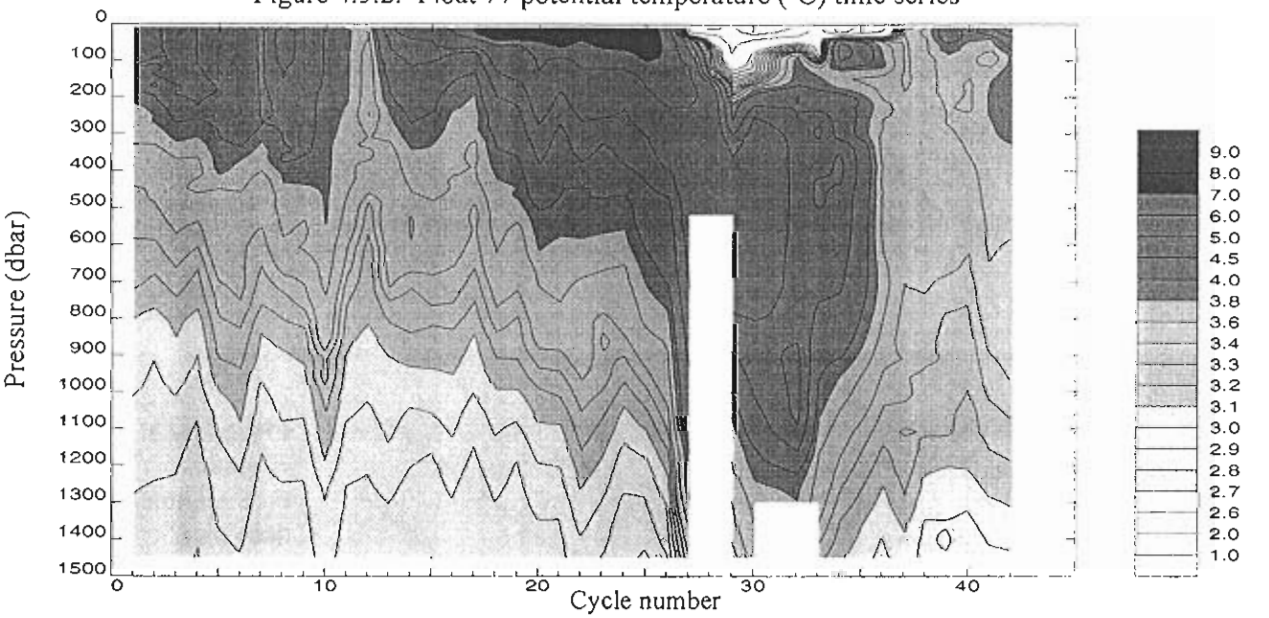

Figure 4.5.3: Float 77 density (σ_0) time series

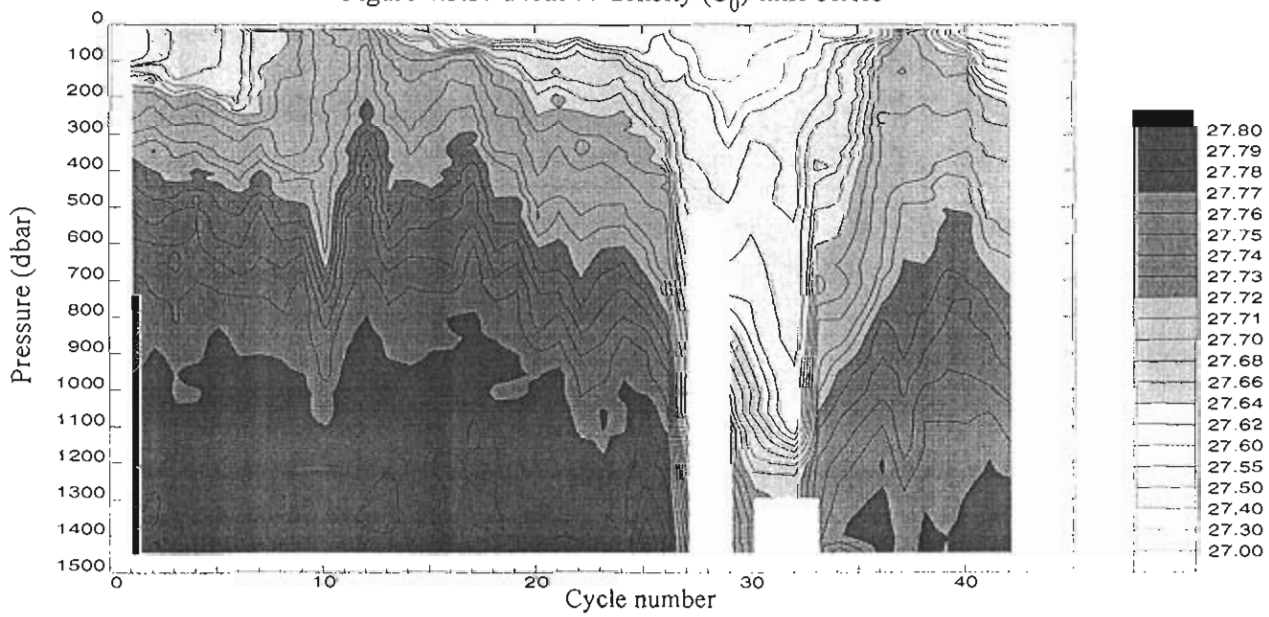

Figure 4.6.1: Float 78 salinity time series

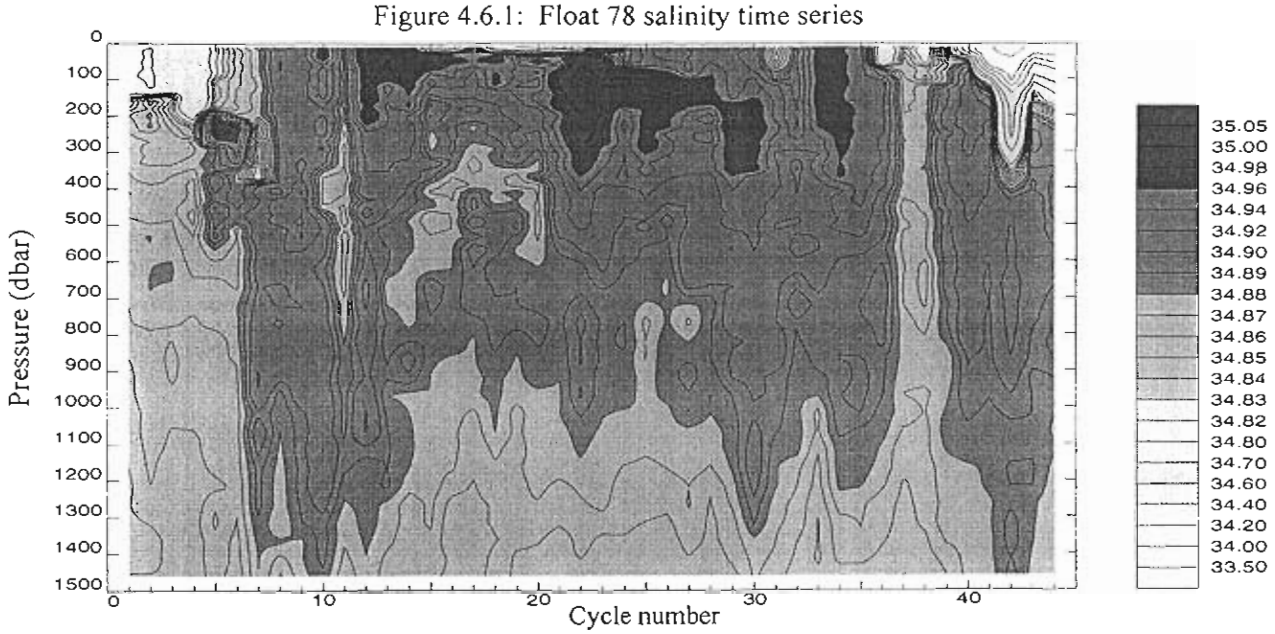

Figure 4.6.2: Float 78 potential temperature (°C) time series

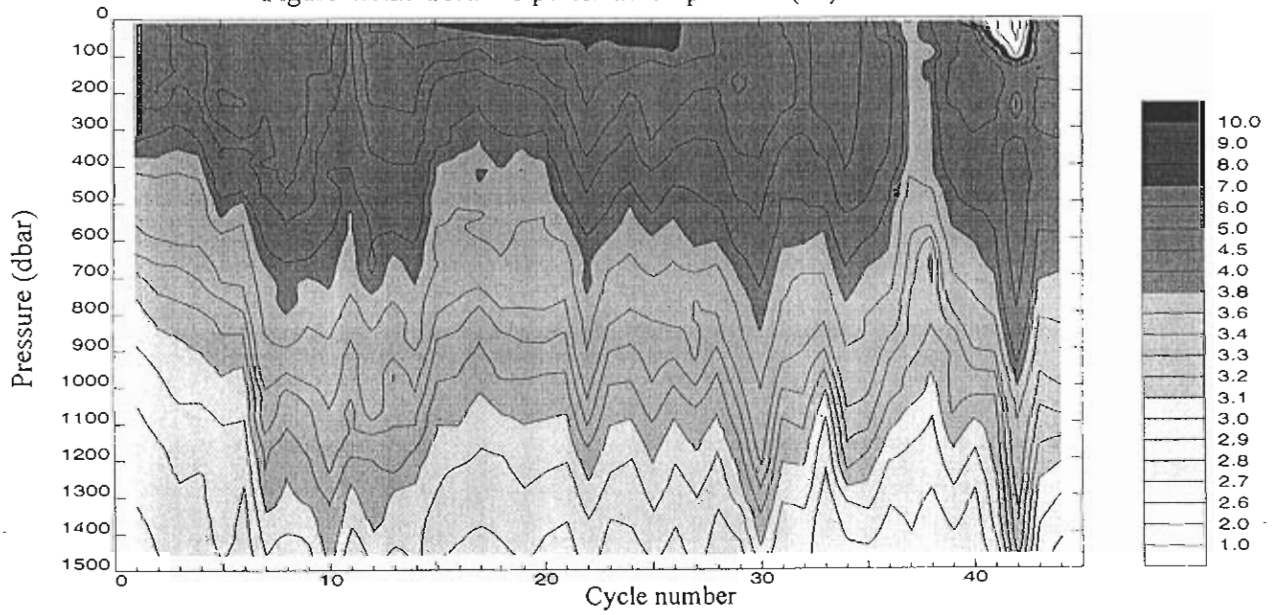

Figure 4.6.3: Float 78 density (σ_0) time series

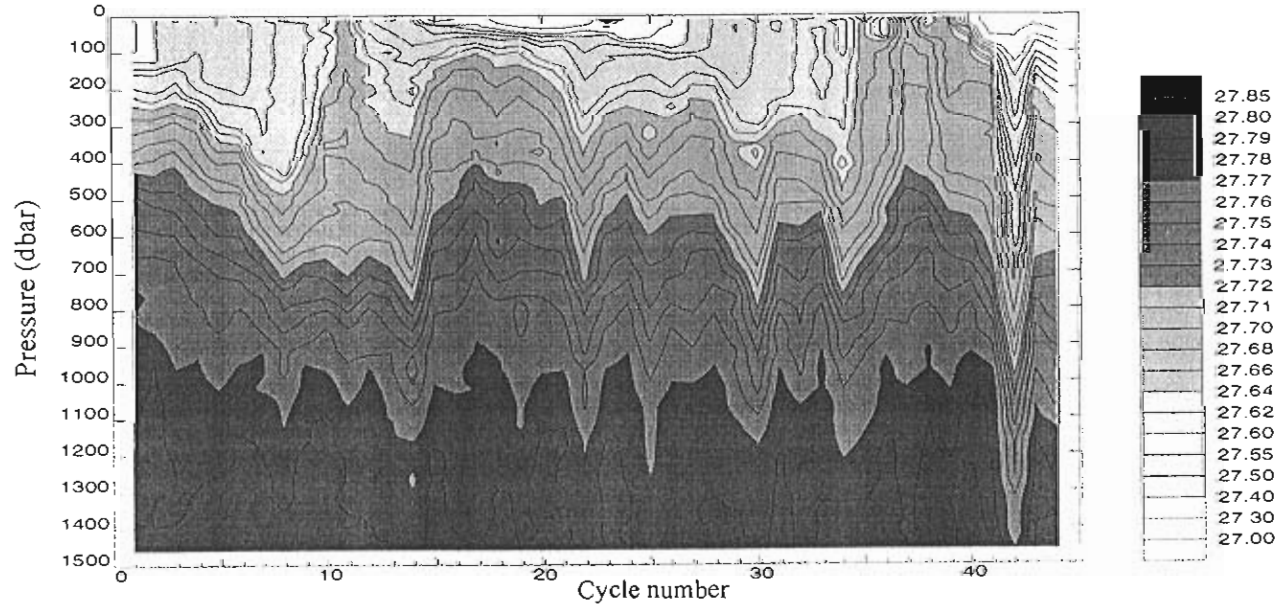

Figure 4.7.1: Float 79 salinity time series

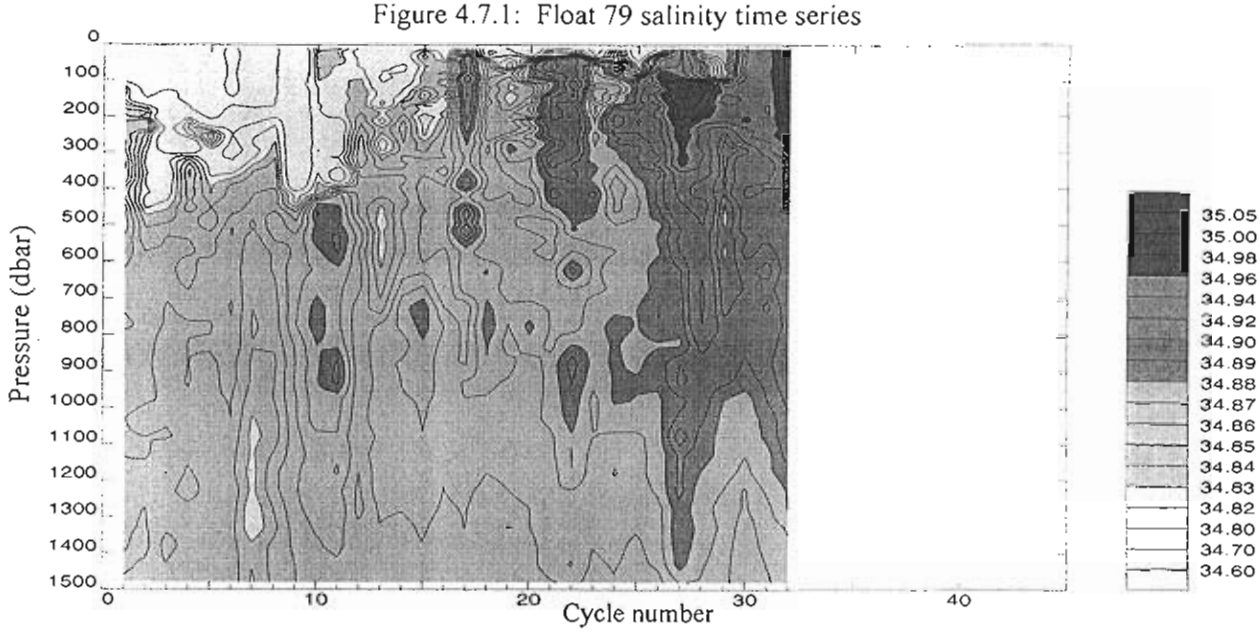

Figure 4.7.2: Float 79 potential temperature (°C) time series

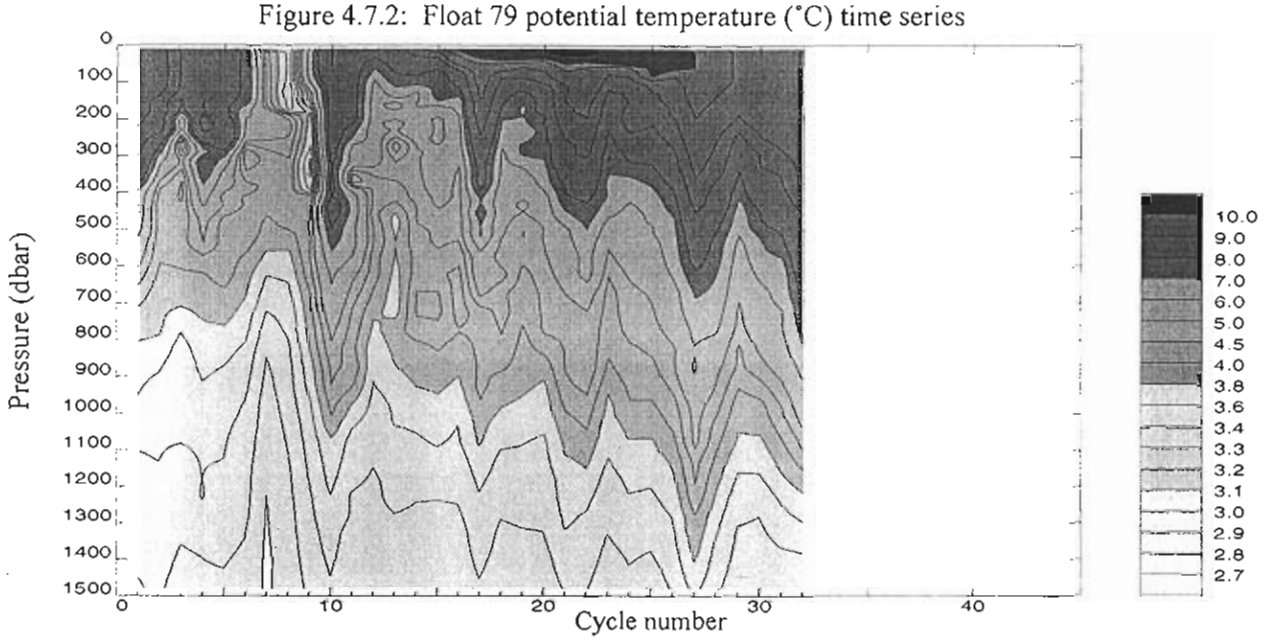

Figure 4.7.3: Float 79 density (σ_0) time series

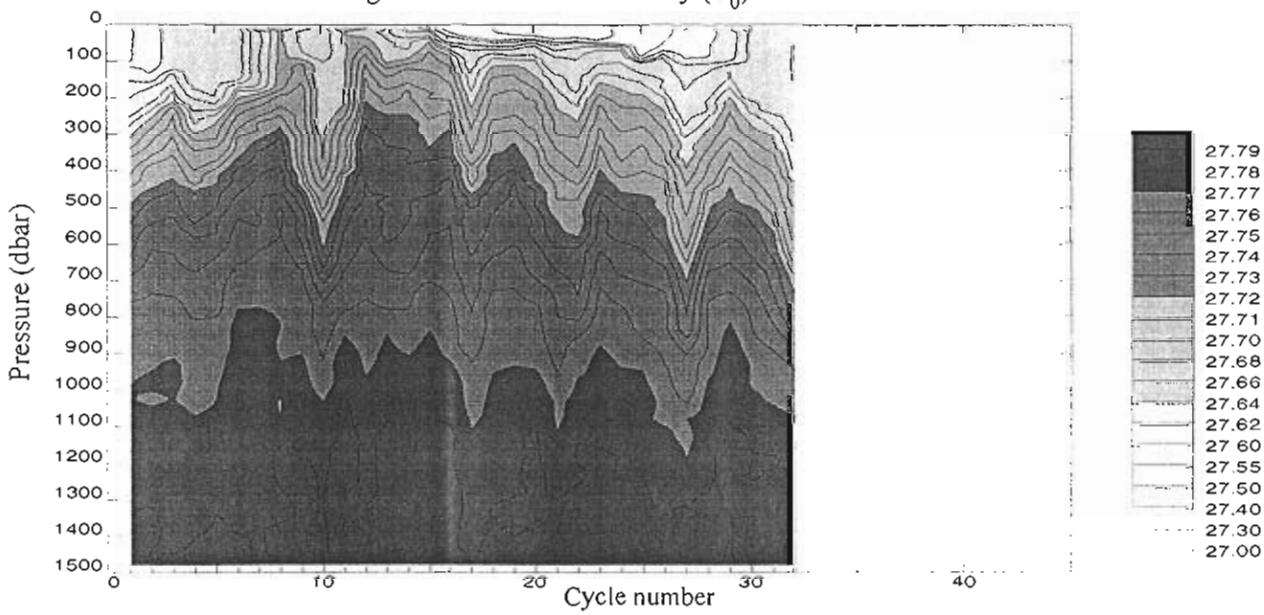

Figure 4.8.1: Float 80 salinity time series

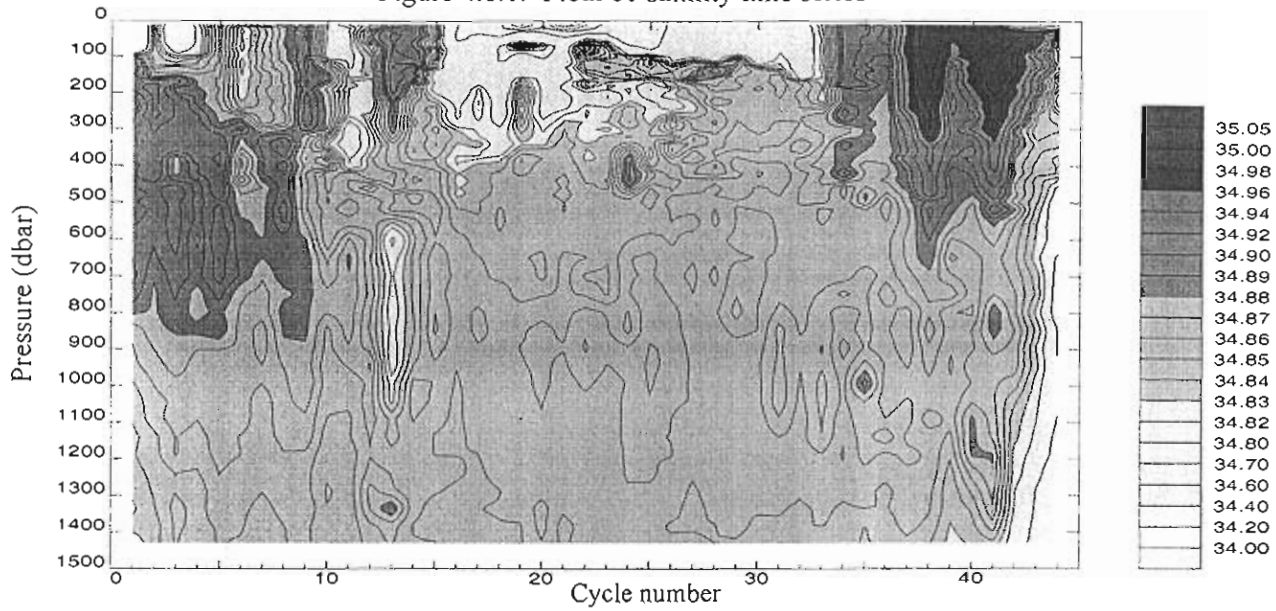

Figure 4.8.2: Float 80 potential temperature (°C) time series

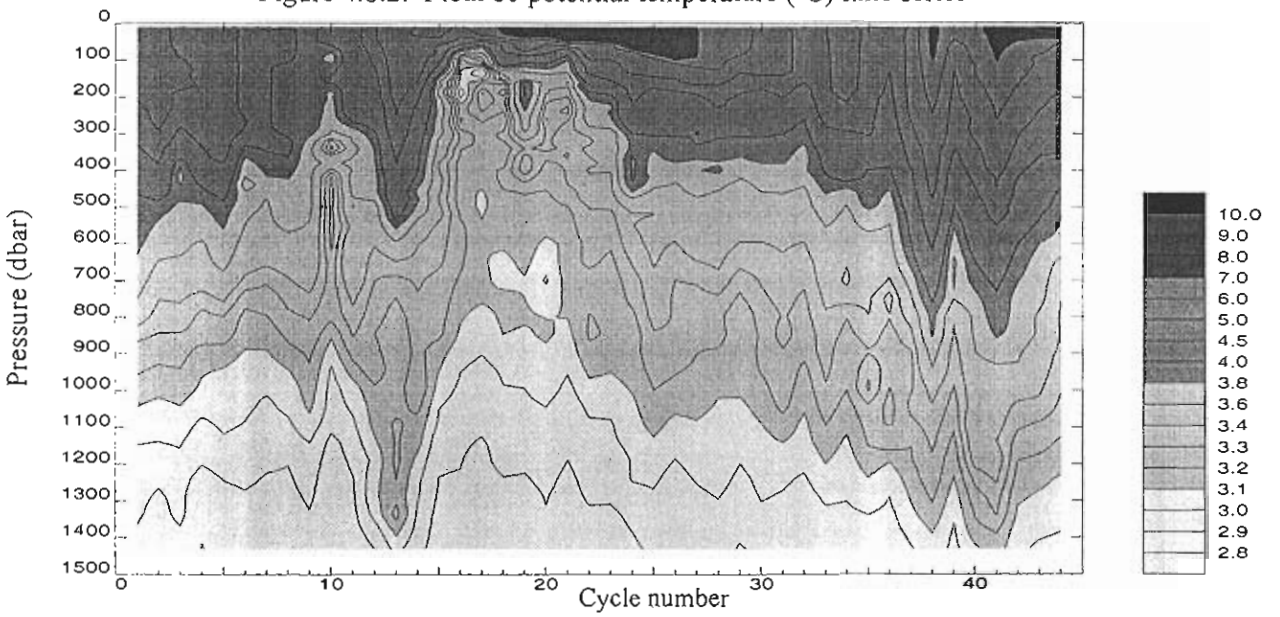

Figure 4.8.3: Float 80 density (σ_0) time series

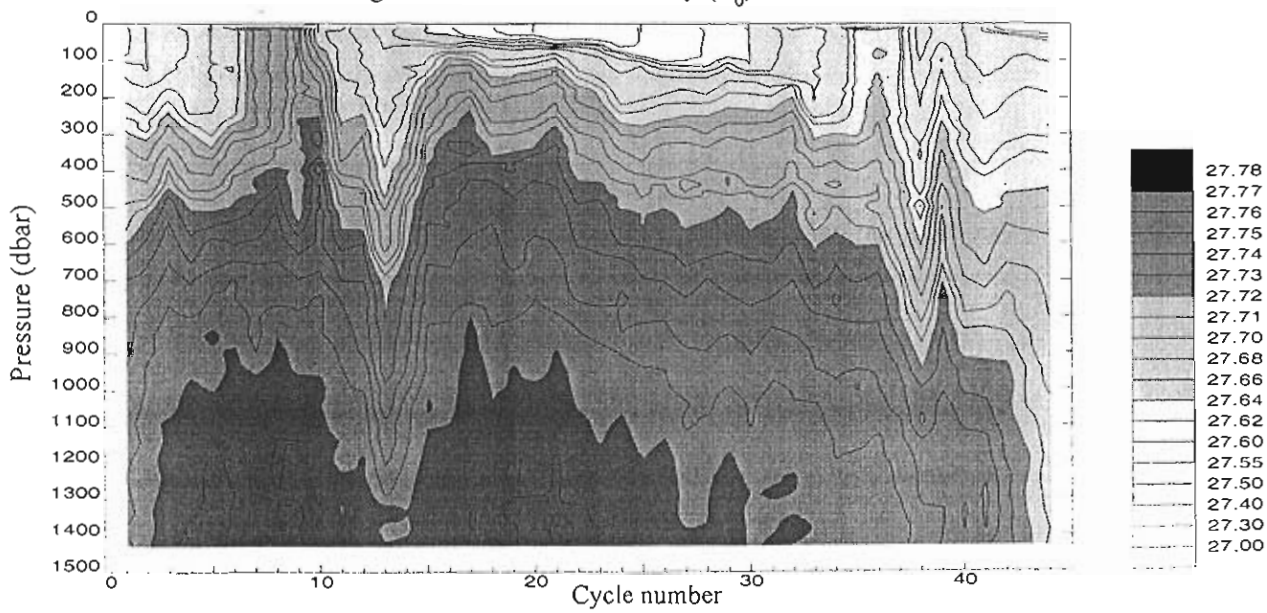

Figure 4.9: Float 82 temperature (°C) time series

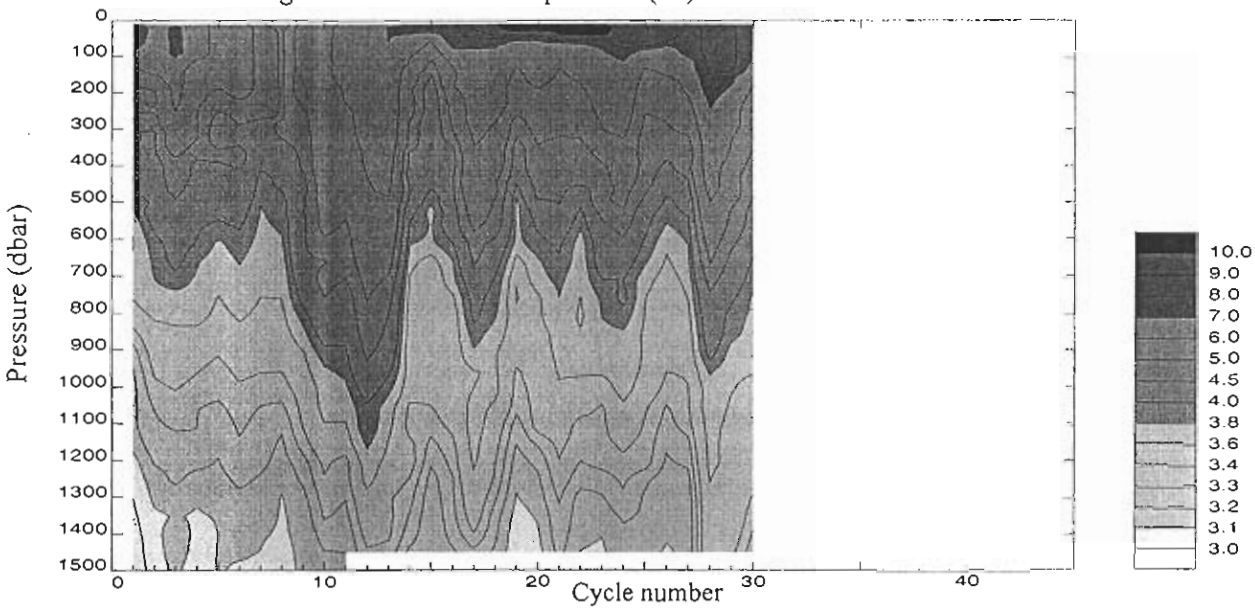

Figure 4.10: Float 83 temperature (°C) time series

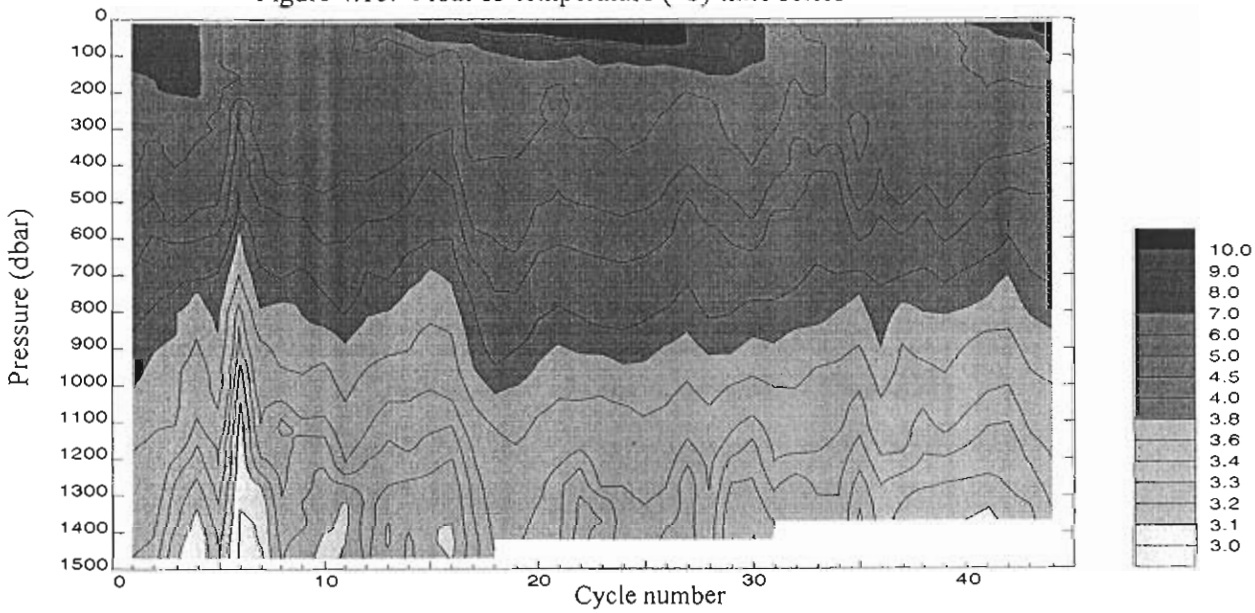

Figure 4.11: Float 77 salinity, potential temperature and σ_0 time series at 1400 dbar

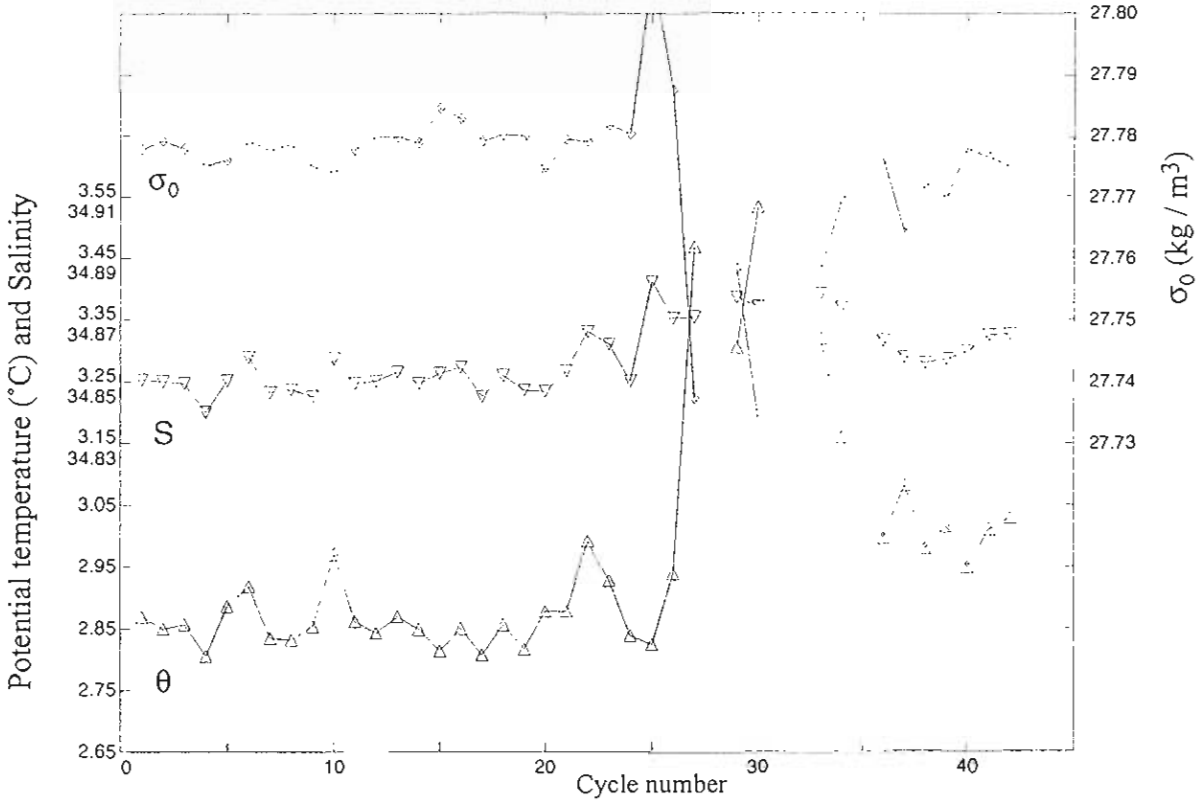

Figure 4.12: Float 78 salinity, potential temperature and σ_0 time series at 1400 dbar

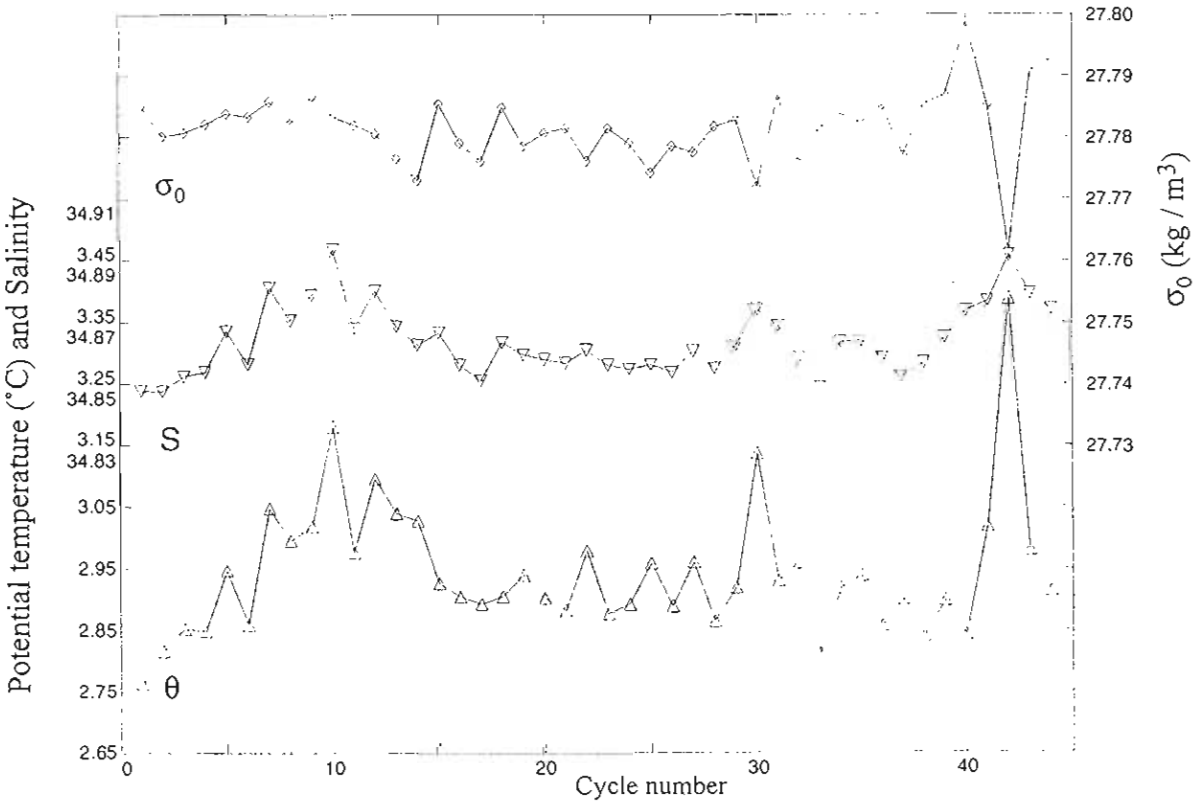

Figure 4.13: Float 79 salinity, potential temperature and σ_0 time series at 1400 dbar

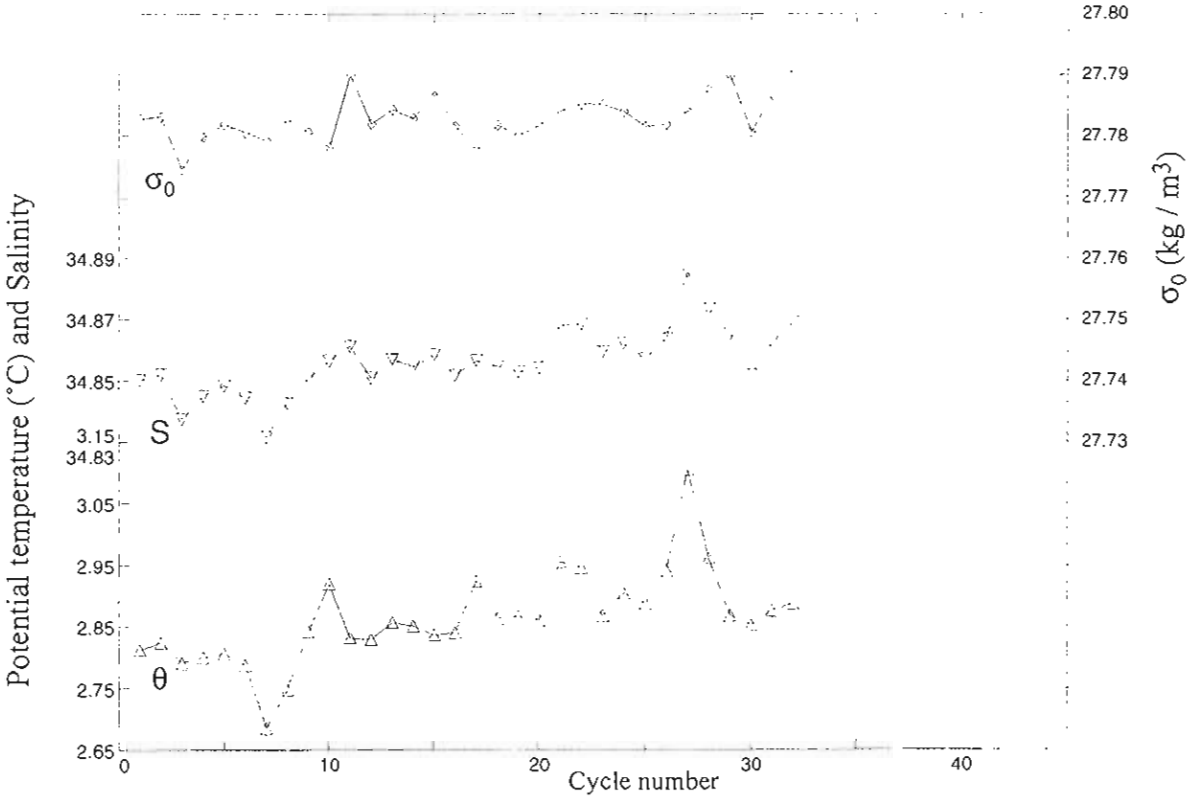

Figure 4.14: Float 80 salinity, potential temperature and σ_0 time series at 1400 dbar

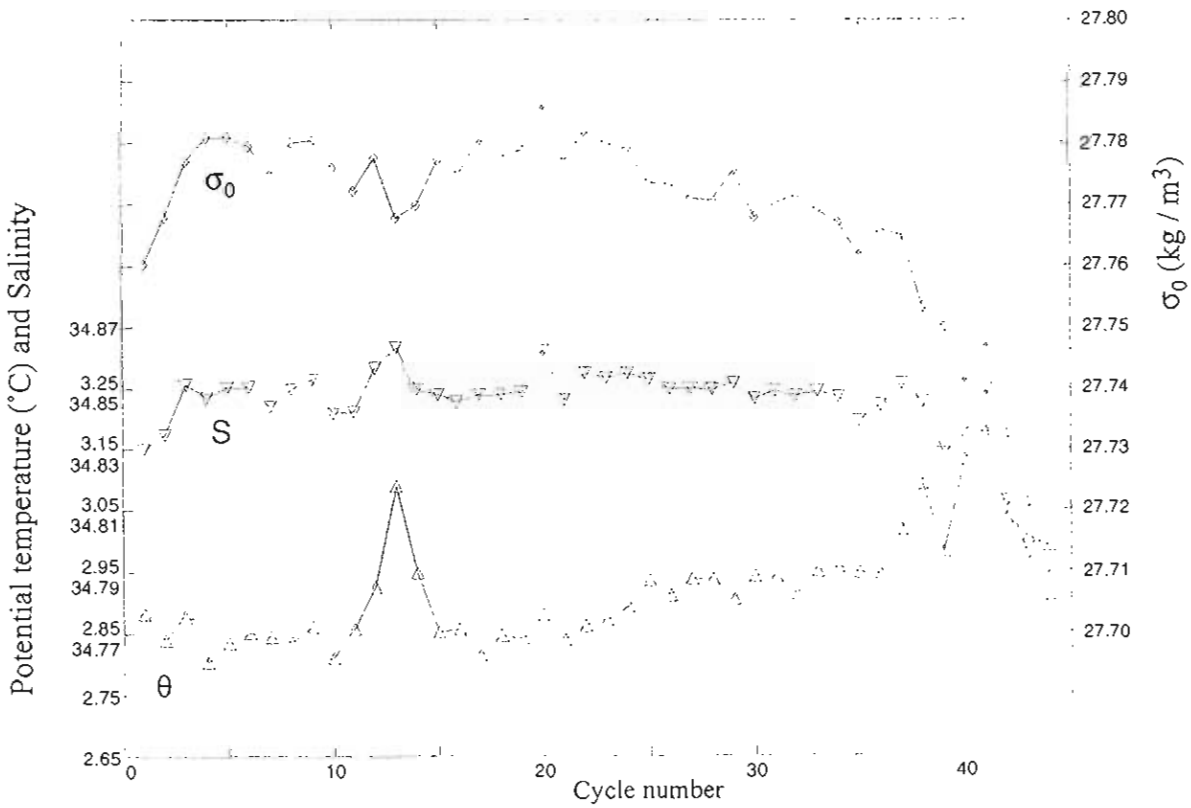

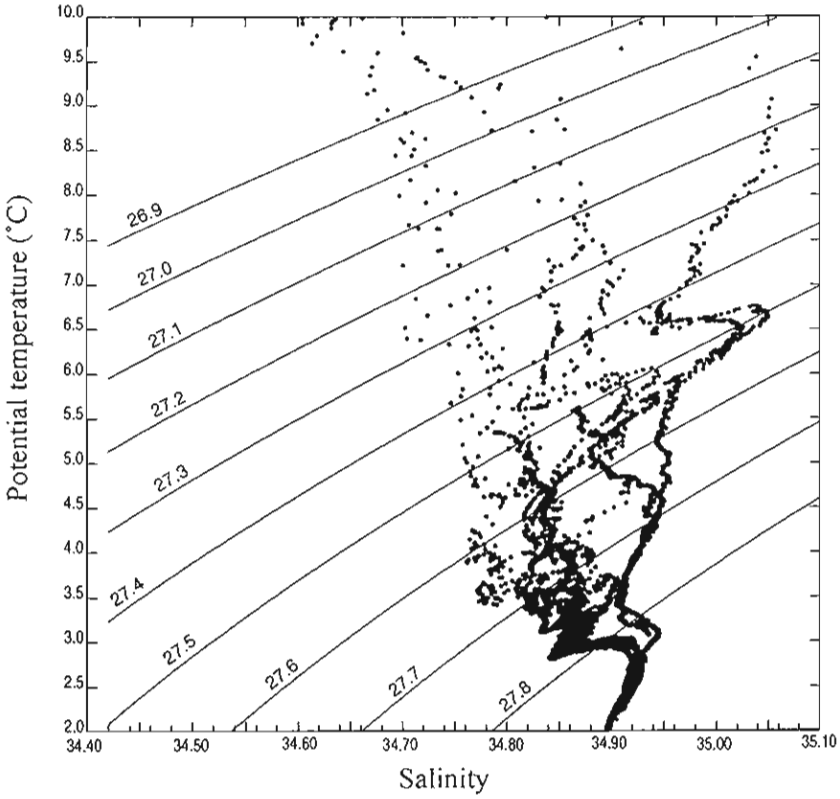

Figure 4.15.1:
Discovery 230 stations 73 to 80 in the south-east Irminger Basin (see fig. 3.4).
θ / S relationship, all data.
Contours show σ_0.

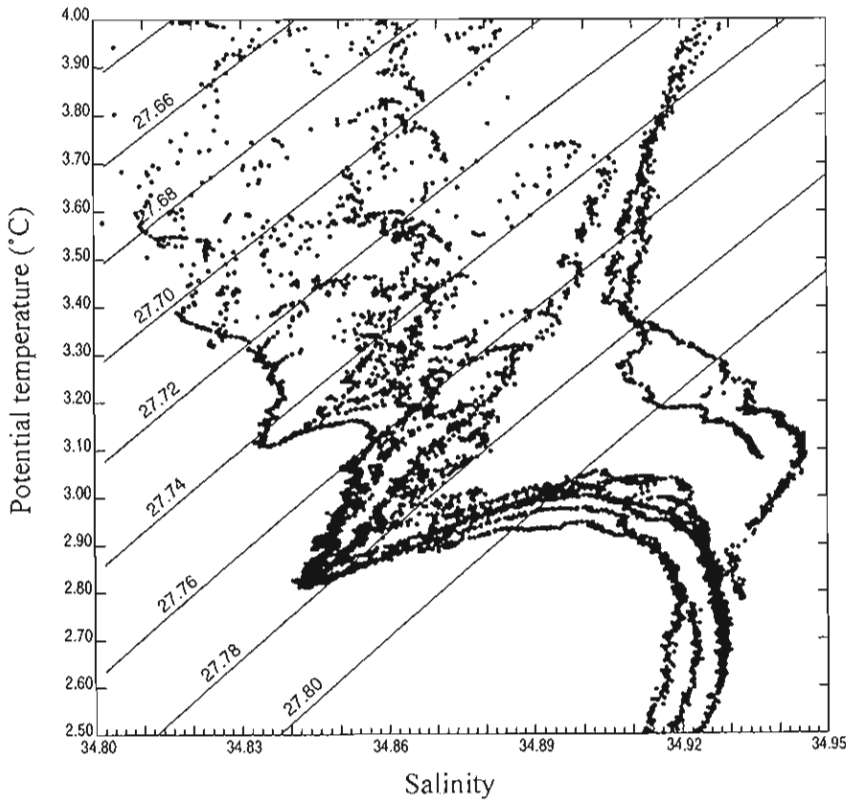

Figure 4.15.2:
Discovery 230 stations 73 to 80 in the south-east Irminger Basin (see fig. 3.4).
θ / S relationship, deep data.
Contours show σ_0.

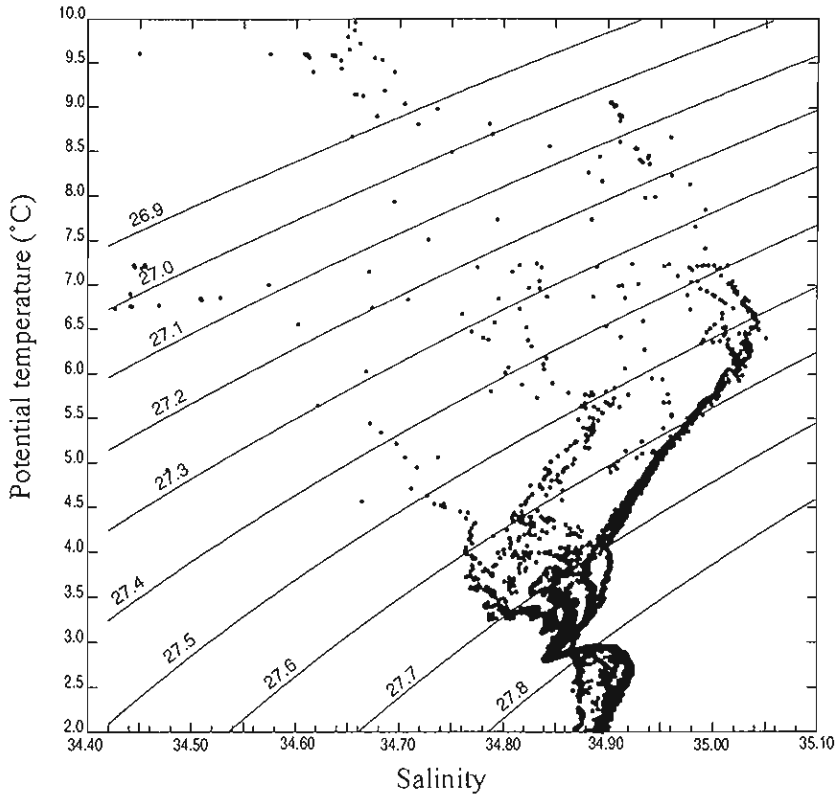

Figure 4.16.1:
Discovery 230 stations 81 to 88 in the western Irminger Basin (see fig. 3.4).
θ / S relationship, all data.
Contours show σ_0.

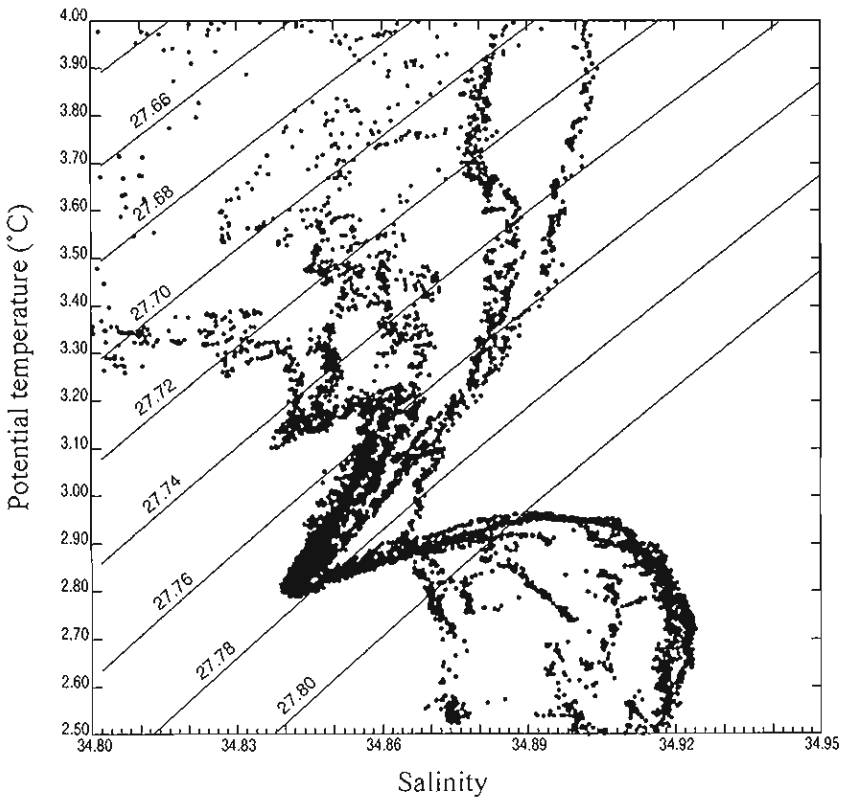

Figure 4.16.2:
Discovery 230 stations 81 to 88 in the western Irminger Basin (see fig. 3.4).
θ / S relationship, deep data.
Contours show σ_0.

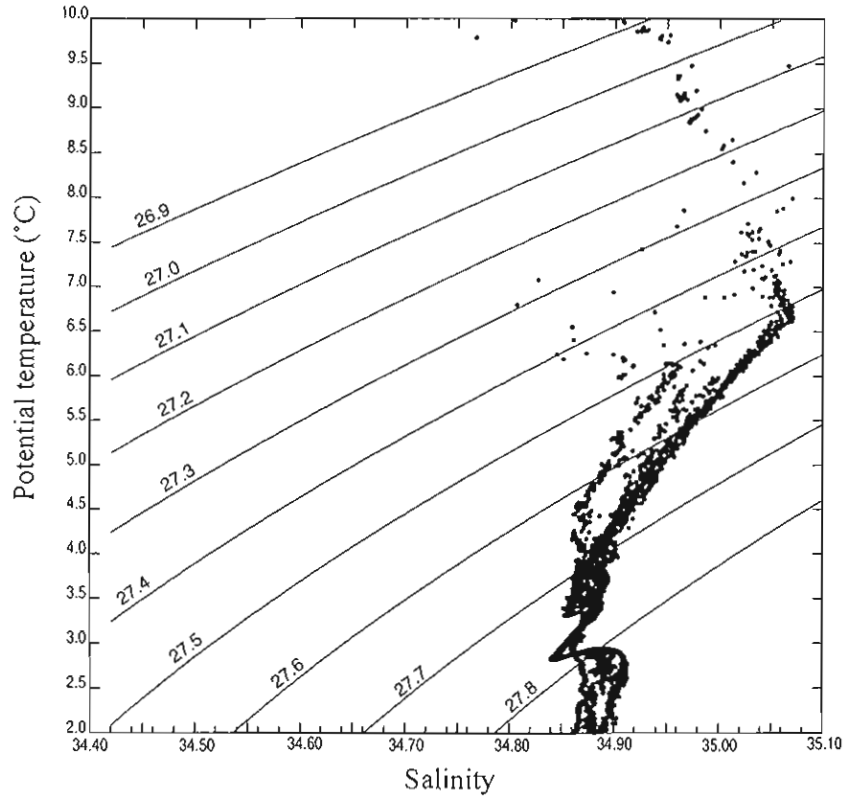

Figure 4.17.1:
Discovery 230 stations 94 to 98 in the north-west Irminger Basin (see fig. 3.4).
θ / S relationship, all data.
Contours show σ_0.

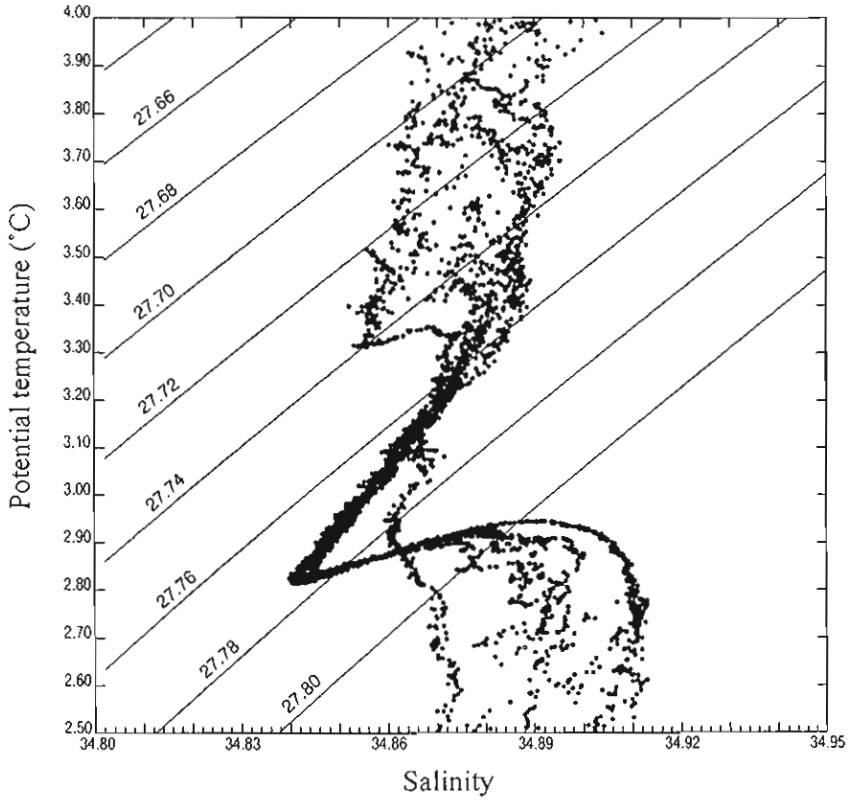

Figure 4.17.2:
Discovery 230 stations 94 to 98 in the north-west Irminger Basin (see fig. 3.4).
θ / S relationship, deep data.
Contours show σ_0.

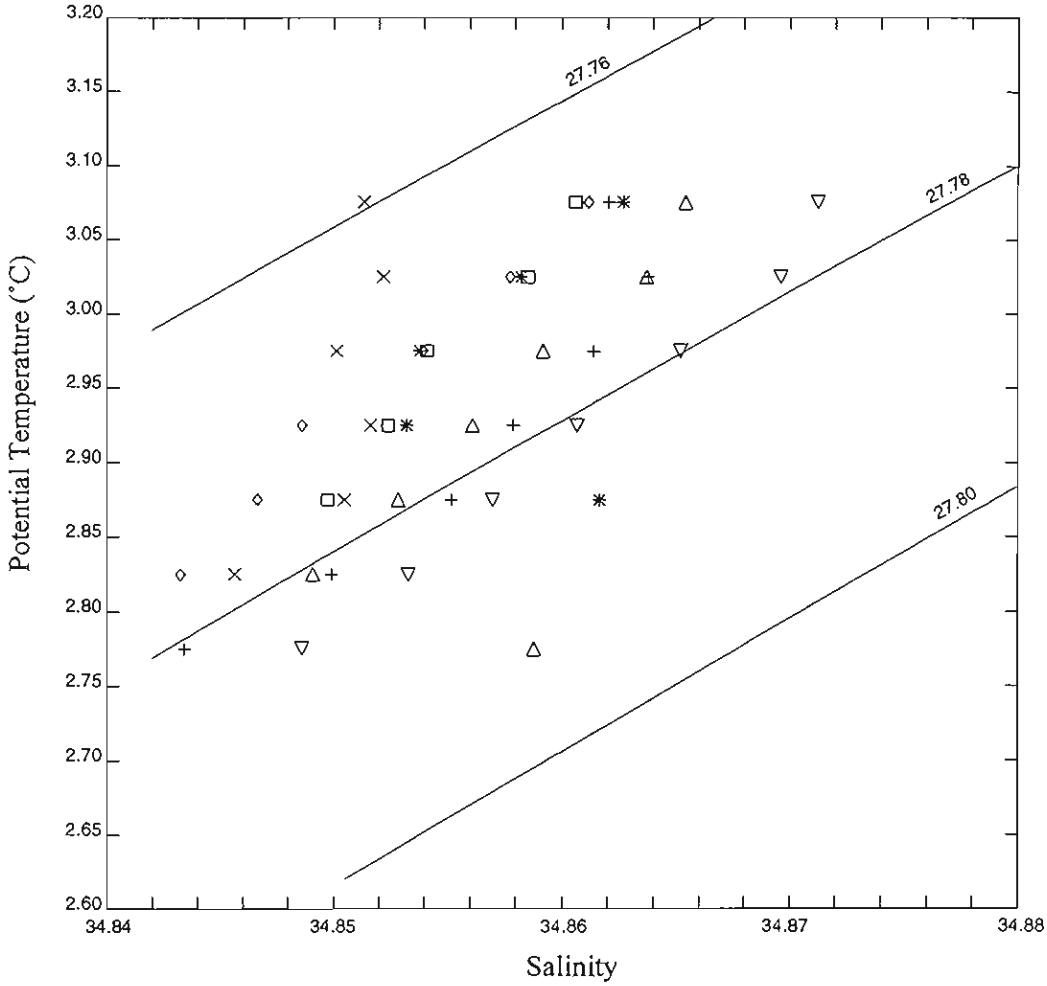

Figure 4.18: Averaged θ / S relationships for all four floats and three section segments. Selected σ_0 contours are superimposed.

Key:

▲ Float 77
▼ Float 78
✛ Float 79
× Float 80
■ South-east Irminger Basin
◆ Western Irminger Basin
✳ North-west Irminger Basin